Lawrence Berkeley Laboratory
UNIVERSITY OF CALIFORNIA

ENERGY & ENVIRONMENT DIVISION

ZINC CHLORIDE CATALYSIS IN COAL AND BIOMASS
LIQUEFACTION AT PREPYROLYSIS TEMPERATURES

Christopher O. Onu and Theodore Vermeulen
(Ph.D. thesis)

June 1980

DISCLAIMER

ZINC CHLORIDE CATALYSIS IN COAL AND BIOMASS LIQUEFACTION AT PREPYROLYSIS TEMPERATURES

Christopher O. Onu and Theodore Vermeulen
Ph.D. Thesis

Energy and Environment Division
Lawrence Berkeley Laboratory
University of California
and
Department of Chemical Engineering
University of California
Berkeley, CA 94720

June 1980

ZINC CHLORIDE CATALYSIS IN COAL AND BIOMASS LIQUEFACTION AT PREPYROLYSIS TEMPERATURES

Christopher O. Onu and Theodore Vermeulen
Energy and Environment Division, Lawrence Berkeley Laboratory
and Department of Chemical Engineering
University of California, Berkeley, California 94720

ABSTRACT

Coal liquefaction processes currently under development operate with thermal decomposition of coal. This step is non-selective, and wastefully forms light hydrocarbon gases and refractory char as byproducts. It requires severe operating conditions (over 400°C and 100 atm.), giving rise to high capital costs, and relatively low thermal efficiencies.

In the present study, coal liquefaction has been investigated under milder, more selective conditions, utilizing a zinc chloride-methanol melt as a liquid-phase catalyst. Operating at 275°C with 35-55 atm. of H_2, this catalytic medium has been found to give over 95% conversion of Wyodak sub-bituminous coal to solvent-extractible, but not yet truly liquid, products. The products are identified in a standard manner as oils, asphaltenes, and preasphaltenes, with hydrogen-to-carbon atomic ratios in the ranges of 1.2-1.4, 1.0-1.1, and 0.8-0.9 respectively.

Many co-catalytic systems, including finely powdered metals, inorganic salts, bifunctional complexants, and wetting agents, were studied as possible activators for zinc chloride

which would improve the yield of oils. The addition of finely powdered metallic zinc to the zinc chloride-methanol melt was most effective of the materials investigated, in increasing the yield of oils. It is not yet known whether the favorable behavior of zinc metal is exerted in a finely divided metallic form, or is due to its forming liquid-phase monovalent zinc ion.

Increasing the reaction temperature for coal conversion appears to accelerate some wanted reactions and decelerate others. Because of this, a progression of two or more reaction temperatures was investigated, and was found to increase overall conversion, while retaining a high yield of oils. First-stage treatment at 275°C proved preferable to pretreatment at either 250° or 300°C. For second-stage treatment, 325°C proved preferable to either 300° or 340°C and then brought about a substantial product improvement, including a 54% yield of oils.

Preasphaltenes (pyridine-soluble but toluene insoluble) were observed to vary greatly in their properties. Those obtained at 325°C are considerably different from those obtained at 275°-300°C. The higher-temperature preasphaltenes begin to melt at 200°C, and nearly 30% have melted by 400°C, whereas the lower-temperature preasphaltenes do not melt below 400°C. In gel-permeation chromatography studies, the higher-temperature preasphaltenes show a lower average molecular weight with fewer aromatic fused rings. Scanning electron microscopy (SEM) studies confirm a complete

structural change in the original coal taking place in the
325°C treatment, compared with the effects at 275° or 300°C.

Solubilization of wood, as chips or flour, and of wood-
derived lignin and cellulose has been examined in the zinc
chloride-methanol catalytic medium. Experiments show a
carbon recovery of 79% for cellulose and 90% for both wood
flour and chips. Under treatment, wood changes markedly in
form and oxygen content before solubilization begins, as
shown by both SEM examination and elemental analysis. At low
solubilization, the bulk of the wood is converted to pre-
asphaltenes, with asphaltenes and oils being formed and addi-
tional oxygen being removed as the reaction progresses.

* * *

TABLE OF CONTENTS

CHAPTER I

INTRODUCTION

NEED FOR COAL AND BIOMASS LIQUEFACTION

The projected U.S. energy flow diagram for 1980 (A1) is given in Figure 1, based on the energy demands of the early 1970's. However, the recent setting of an 8.2 million barrel/day limit on importation of crude oil and the growing opposition to the establishment of new nuclear plants, reducing the contribution of the nuclear sector to energy supply, has affected the accuracy of this diagram.

Imported crude oil represents 47% of the total crude oil requirement, and nearly 56% of the total requirement will be utilized in the transportation sector. It is clearly evident that if the dependence of the U.S. on imported crude oil is to be reduced, alternative sources of energy must be developed rapidly that can be utilized in the transportation sector.

The increasingly unfavorable political climate and the growing time lag for nuclear power plant construction drastically reduce the probably contribution of the nuclear sector to overall energy generation. For gas, there has been limited success in utilizing it at a level to drastically reduce the need for imported petroleum.

Fortunately, coal is abundant in the U.S. by almost any measure. The lower 48 states contain about one-third of the known economically recoverable coal reserves in the world (S1). In the unlikely event that all the energy consumed by the U.S. were to be supplied by coal, Parent (C1) notes "the lower figure of the estimated remaining recoverable quantity $(1036 \times 10^9$ tons) would suffice for over a century at zero
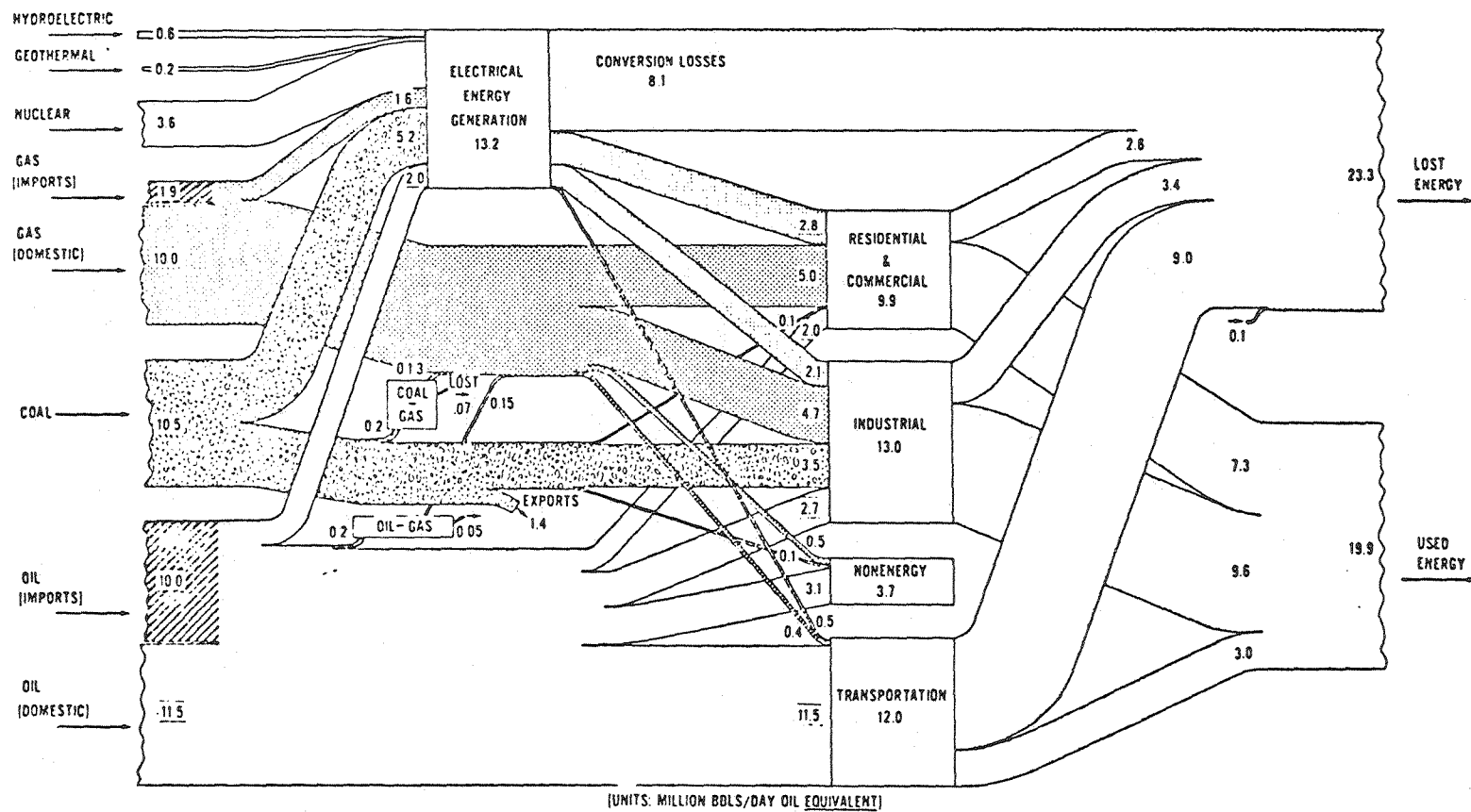
Figure 1. The United States energy flow diagram for 1980 (after Austin Al)

growth, and for 64 years at a growth rate of 4% per year." In addition, roughly half of the economically recoverable seams are located in areas of low population density and are surface mineable. In the short term, coal consumption is projected to be limited by demand rather than by supply, since most of the existing mines are operating below maximum capacity.

Thus coal appears destined to play an important role in the energy future of this country, especially through liquefaction for producing liquid products needed in the transportation sector.

Direct use of solar energy as a major energy source presents considerable technical difficulties, and may prove prohibitively expensive in the future. However, the indirect use of solar energy through its capture and storage by plant photosynthesis may become increasingly attractive. Biomass represents a large and long-term renewable resource of feedstock for energy conversion processes. The low pollution level associated with biomass utilization is another advantage of its conversion and use as liquid fuels.

It is estimated that crop, forestry, and manure residues amount to 430 million dry tons within the continental United States (A2): 280 million tons of crop wastes, 30 million tons of livestock and poultry manure, and 120 million tons of logging residues. Their seasonality, lack of guaranteed availability, and large storage volume per unit of heat release are offsetting disadvantages which indicate that individually biomass materials will have modest impacts, but in

the aggregate, they are likely to contribute substantially to the energy supply.

COAL CHEMISTRY AND STRUCTURE

The design of an optimum process for converting coal to a liquid fuel demands that the chemical and physical characteristics of coal be well understood. Coal is a complex matrix of very large nonvolatile insoluble organic molecules, with minor amounts of volatile or solvent-extractible compounds trapped within the matrix (L1, T1, E1). Both the matrix and the trapped compounds are products which originated from plants by way of the geological coalification process. The original plant material comprising well ordered polymers such as cellulose and lignin appears to have evolved to varying extents along a path defined by humic acid, peat, lignite, sub-bituminous coal, bituminous coal, and finally anthracite (W1, H1, R1, D1).

Coal contains a significant internal pore structure. Van Krevelen and Zwietering (Z7) applied Ritter and Drake's method of mercury penetration to the study of coal and suggested that coal contains two pore systems: a micropore system (size range below 12 $\overset{o}{A}$) and a macropore system (size range above 200 $\overset{o}{A}$). Medeiros (M13) using the adsorption of gases (CO_2, CF_4, N_2, and Ar) determined that the majority of the pores in Wyodak sub-bituminous coal are 4 $\overset{o}{A}$ in diameter. However, this demonstrates that the interior of the coal particles is relatively inaccessible for chemical conversion

methods.

Whitehurst (W2), by using ^{13}C NMR techniques, determined
that the carbon in Wyodak sub-bituminous coal is about 63%
aromatic. Various oxidative-degradation techniques have also
been utilized in determining the nature and abundance of aro-
matic units in coal (H1-2, I3-5, W14). Interpolation of such
data (S5) shows three-ring or more complex structures are re-
latively few.

Inverse degradative techniques, which destroy aromatic
units in coal and leave the aliphatic structures relatively
untouched, have been utilized in determining the nature of
the aliphatic network in coal (D2, 3). Applied to Wyodak
coal, this technique showed that about 23% of the hydrogen oc-
curs in aliphatic links and side chains.

Oxygen is relatively abundant in coal. Herskowitz (H10),
by chemical analysis of coal, determined the distribution of
hydroxyl and carbonyl oxygen, and calculated the remainder
(largely ether oxygen) by difference. For Wyodak sub-bitumin-
ous coal, with an oxygen content of about 20%, the distribu-
tion found was 3.26% hydroxyl, 1.00% carbonyl and 15.7% ether
oxygen.

The concentration of organic sulfur in Whydak coal is low,
about 1%. The distribution of sulfur groups in several coals
has recently been studied by Attar and Dupius (A3). They
estimated that about 25% of the organic sulfur in sub-bitumin-
ous coals occurs as aliphatic and alicyclic sulfides, about
20% as thiols, and the rest as thiophenes and condensed

thiophenic structures.

Systematic studies of nitrogen compounds in coal tar and in liquefaction products suggest that much of the nitrogen is bound in simple and condensed pyridines (S2-4). Also amines are believed to be present and to be the source of ammonia which coal releases during pyrolysis. The nitrogen content of Wyodak coal is also about 1%.

Metal oxides and salts constitute the mineral matter of coal. Some of the mineral matter is dispersed within the organic structure as organic-bound cations (M12).

Various chemical characterization techniques including chromatographic, wet-chemical, spectroscopic, and more recently solid-state cross polarization ^{13}C NMR technique (developed by Pines, P1) have been utilized by researchers to elucidate the structure of coal. Heredy and co-workers (H3-5) demonstrated that $-CH_2-$ and $-CH_2-CH_2-$ bridges connect aryl groups in coal, while recent work by Raaben (R2) on controlled oxidation of coal also suggests the presence of some longer aliphatic connecting chains, at least up to C_4. Numerous condensed aromatic structures have been isolated. Based on these results and many other coal structural studies, several investigators (W3, B2, K1, M1) have concluded that the coal molecule consists of aromatic and hydroaromatic structural units linked principally by relatively weak aliphatic bridges and other linkages.

A model of sub-bituminous coal constructed by Shinn (S5) based on studies by Farcasiu and others at Mobil Research and

Development Company (W1, I6) is shown in Figure 2.

COAL LIQUEFACTION PROCESSES

In order to liquefy coal, chemical reactions must not only rupture the aliphatic links connecting the aromatic moities, but also reduce the size of the polynuclear aromatic structures. The molecular structure must be transformed so that it contains very few three-ringed and almost no four-ringed or larger aromatic molecules. Perhaps the most significant parameter which marks the conversion of coal to liquid oil is the hydrogen content. Representative atomic H/C ratios for coal and other fuels are shown in Figure 3. The hydrogen content of the coal utilized in this study is 5%, whereas crude petroleum contains hydrogen to the extent of 11 to 14%. The need to protect the atmospheric environment makes the removal of heteroatoms--nitrogen and sulfur, generally as NH_3 and H_2S--not only desirable but imperative. This underscores the importance of hydrogenation in converting coal to liquid products. To improve the fluidity (or pumpability) and combustibility of the oil products from coal, the removal of ash from reaction products ia also essential.

The various coal liquefaction processes under development deal with these fundamental problems. All existing processes operate above coal-pyrolysis temperatures (above 400°C) at high pressures (over 1500 psig). Under these severe conditions, the reactions are not selective, and a wide range of products are formed including many undesirable ones. These
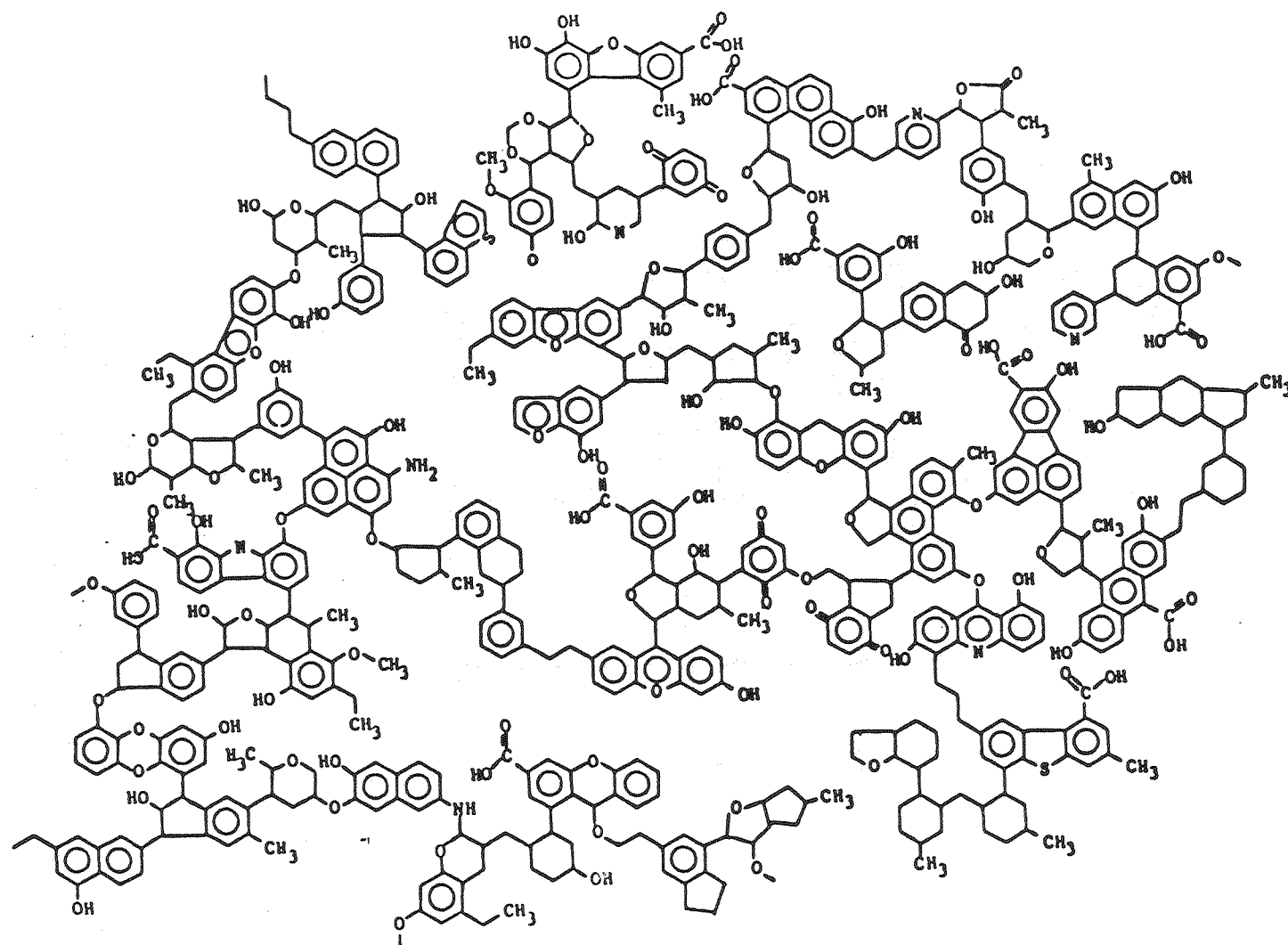
Figure 2. Model of sub-bituminous coal structure (after Shinn, S5)
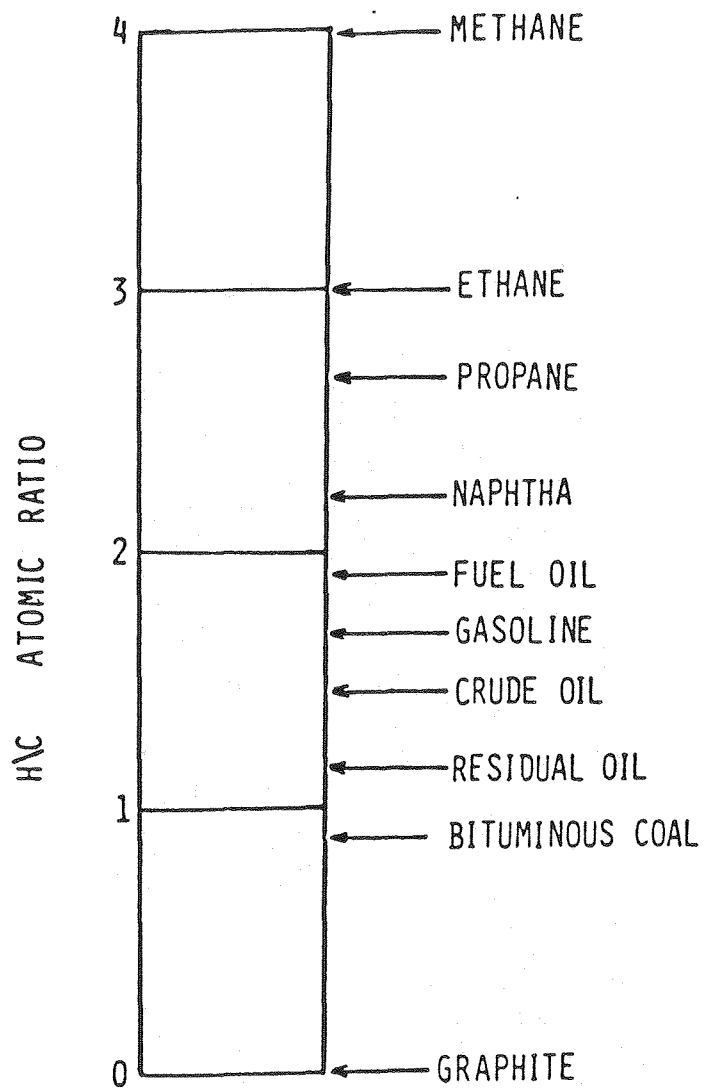
Figure 3. Representative atomic H/C ratios for coal and other fuels (after Wiser, W11).

undesirable products include light hydrocarbon gases which aggravate hydrogen consumption, and refractory char which requires special treatment to liquefy or burn. By virtue of the severe conditions of temperature and pressure utilized, these processes consume considerable energy and require expensive equipment.

The various liquefaction processes summarized in Table 1 utilize different approaches (I1). These include indirect liquefaction, pyrolysis, solvent extraction, and catalytic liquefaction.

Indirect liquefaction, an alternate process, starts with complete gasification to carbon monoxide and hydrogen as the first step, at 900°C in the presence of oxygen and steam. The carbon monoxide is then hydrogenated catalytically with yields of liquid hydrocarbons of the order of 1.8 barrels/ton of coal.

The simplest approach to production of liquids from coal is pyrolysis, which involves heating in the absence of external catalysts and hydrogen-donor solvents. Chemical bonds in coal are ruptured thermally, and the reactive fragments generated are stabilized with hydrogen from hydroaromatic structures in coal. The inadequate capping agents lead to considerable production of char and gaseous products. The Occidental pyrolysis process, through high-speed heating, involves a total residence time of less than thirty seconds, and achieves a higher conversion to liquid products than the COED process. The difficulty in locating a market for the char by-product, because of its impurities (high sulfur and ash content) and

Table 1

Operation Conditions and Yields of Major Processes for
Conversion of Coal to Clean-Burning, Liquid and Solid Fuels

Process	Temperature (^{O}C)	Pressure (psig)	Approx. Yield (%)			Comments
			Liquid	Gas	Char	
COED	315-455-535-870	–	20	17	60	Multistage fluisized-bed pyrolysis, with 4th-stage gas and char recycle.
Occidental Pyrolysis	500	15	35	7	58	Uses small particles, e.g., 25 μm. High-speed heating, preheating, reactor residence time less than 30 secs.
Solvent Refined Coal I	440	2000-3000	75	5	20	Product is solid at ambient temperature.
Solvent Refined Coal II	440	2000-3000	70	10	20	Ashless distillate fuel containing less than 0.4% sulfur is primary product.
Exxon Donor Solvent	440-480	1500-2500	50	15	35	Product is liquid at ambient temperature.
H-Coal	450	2700	75	20	5	Ebulated bed reactor with CoMoO catalyst.
Consol	425	4200	75	15	10	Conoco estimates $ZnCl_2$ processing will save 8 to 16% of cost over H-Coal process. $ZnCl_2$ recovery of 99.6% has been achieved.
Univ. of Utah	500-550	2000	60	10	30	Short contact time (10-20 sec) without solvent.

the difficulty in igniting and burning when compared with coal, threatens the prospects for commercializing any pyrolytic liquefaction process.

The use of hydrogen-donor solvents as a pyrolytic medium in coal liquefaction has been carefully investigated (G2, F1). The solvent not only helps stabilize thermally produced reactive fragments, but also prevents agglomeration and sticking of coal particles and facilitates pumping into high-pressure zones. The nature of the product is directly related to the amount of hydrogen added. By adding 1 to 2 wt-% hydrogen, as in the traditional solvent refined coal (SRC) process, a product which is solid at room temperature is produced; whereas addition of 3.5% to 4% hydrogen by weight results in a heavy product which is liquid at room temperature. The Exxon Donor Solvent (EDS) process, by employing catalytic hydrogenation in the solvent-recycle loop, produces a hydrogen-rich solvent which effectively hydrogenates coal and represents an improvement over the solvent refined coal process. The EDS process has already been demonstrated at a 1 ton/day pilot scale, and plans for a 250 t/d pilot plant are in progress.

In order to promote product hydrogenation and hetero-atom removal in coal liquefaction, certain commercial hydrodesulfurization catalysts such as cobalt molybdate or tungsten sulfide have been employed. Two processes have emerged. The H-Coal process (H6) involves an oil slurry of finely ground coal flowing together with hydrogen through an

ebullating (suspended) fluidized bed of particulate cobalt molybdate catalyst. The Synthoil process employs a fixed bed of cobalt molybdate catalyst pellets and proceeds by a rapid turbulent flow of coal, oil, and gas through the fixed bed. The H-Coal process has progressed through a 3 t/d process development unit, and construction is currently in progress to demonstrate the process at a 250 t/d scale.

Three processes: EDS, H-Coal, and SRC II, have been selected by the Department of Energy for full-scale development. The SRC II process evolved from the SRC I process, designed to convert coal into a low-melting clean-burning solid, low in sulfur and mineral matter, capable of being solubilized in simple organic solvents. The SRC II process yields an ashless distillate fuel containing less than 0.4% sulfur, and is presently being demonstrated at two 50 t/d pilot plants.

As a result of the inaccessibility of the internal pore structure of coal to conventional solid catalysts, there has been an extensive study of liquid catalysts that can penetrate the internal pores of coal. Molten salts, particularly $SnCl_2$, $AlCl_3$, and $ZnCl_2$, have been attractive as coal-conversion catalysts (C2,K2). Considerations of chemical stability, selectivity, cost, corrosiveness, and ease of recovery from reaction products resulted in the selection of $ZnCl_2$ as the molten salt catalyst for coal conversion. Workers at Shell Oil Company (L2, S8) found $ZnCl_2$ a good coal hydrocracking catalyst. Two major applications of $ZnCl_2$ in the

development of coal liquefaction processes have been carried
out by the Consolidation Coal Company (Consol), which has
been continued by Conoco Coal Development Company; and by
the University of Utah.

The work at Consol (R1, C3, P2, S10, Z1-5) involved the
application of massive amounts of $ZnCl_2$ to coal extracts and
to various coal substrates, leading to the production of
high yields (60%) of high-octane gasoline. High recovery of
$ZnCl_2$ (99.6%) from the spent melt has been achieved through
subliming and subsequent condensation of the $ZnCl_2$ vapor.
Major efforts are underway to develop a 1 t/d process devel-
opment unit for converting coal to distillate fuel.

The University of Utah process employs short contact time
(10-20 sec) and small amounts of $ZnCl_2$ (5 wt-%) with which
the coal is impregnated (W5, B3-4). The resulting liquids
were determined to be principally aromatic in nature. High
zinc recoveries (98.5 to 99.7%) have been achieved through a
combination of water, hydrochloric acid, and nitric acid
wash procedures. This process is still at the bench-scale
stage.

COAL LIQUEFACTION USING ZINC CHLORIDE

The coal conversion processes under development nation-
wide operate at post-pyrolysis temperatures. Liquefaction is
achieved in a hydrocarbon medium through thermal degradation
followed by hydrogenation of the initial pyrolysis products
from inside the coal, from hydrogen-donor solvent, and to

some extent from molecular H_2. The thermal degradation reactions, being nonselective, produce a wide range of products including light hydrocarbon gases and refractory char. Because of the high hydrogen content of the gases, their production aggravates the hydrogen consumption. Also, the refractory char requires special processing for its utilization.

To prevent these undesirable side reactions, operation at sub-pyrolysis temperatures would be highly desirable. The efficacy of mild reaction conditions for the liquefaction of coal depends upon the availability of effective catalytic systems. Hydrogenation, hydrodesulfurization, and hydrocracking catalysts used in the petroleum industry can be applied to hydrogenation of coal extracts. The problem is rather the conversion of solid coal to an extract form, which cannot be accomplished by catalysts in a solid state. Hence, the investigation of homogeneous catalytic systems that promote selective scission of certain bonds in the coal structure under these mild conditions is very necessary.

Molten salts have demonstrated catalytic activity for cracking hydrocarbons and removing heteroatoms (W9). In addition, they possess several unique characterisitics for coal liquefaction. Being molten at reaction conditions, they constitute a liquid reaction medium penetrable into the extensive interior pore surface of the coal, so as to achieve the necessary coal-catalyst contacting. There is constantly renewed liquid at the liquid-solid surface, so that any poisoning of active species does not deter further

catalysis (S11). They are efficient heat-transfer media, thus permitting thermal stabilization of the reacting coal at exactly their optimum reaction temperature. In addition, the composition of the salt mixture can be adjusted to promote the desired reactions.

Of many molten salts, the chemical stability, durability, ease of separation from reaction products, and relative cheapness of zinc chloride have made it the focus of the greatest attention (P3, B7, Z6). In addition, the zinc chloride catalyst is essentially inactive for hydrocracking single-ring aromatic hydrocarbons such as benzene, thereby enhancing its catalytic selectivity by limiting its production of hydrocarbons below the gasoline range. It has equally been shown that zinc chloride promotes the liquefaction of coal with moderate consumption of hydrogen (Z2, S10, W5). A remarkably high recovery (99.6%) of the catalyst has been reported (P2).

The potential of zinc chloride as a coal liquefaction catalyst under mild conditions led Derenscenyi (D4) to investigate the effectiveness of a zinc chloride-water melt in treating coal at 200°C, obtaining an improvement of benzene solubility from 1% for untreated coal to 3-4% with or without various inorganic additives. By operating at 250°C with 600 psig hydrogen, Holten (H9) found a product pyridine solubility of 20-25%. Adding tetralin to the reaction mixture gave about 70% conversion. Investigations of coal conversion in a two phase zinc chloride/tetralin system have been

carried out by Hershkowitz (H10); operating at 300°C with a 2-hour reaction time, he obtained as high as 56% conversion of the coal organics to oils.

Using methanol addition in the zinc chloride melt treatment, Shinn (S5) obtained product pyridine solutilities approaching 90% at 250°C, and 95% or better at 275°C. The action of methanol has been multifunctional. Like water, it depresses the melting point of zinc chloride, and the resulting melt gives better wetting and penetration into the coal compared with water as depressant. Methanol complexed with $ZnCl_2$ appears to serve as a stabilizing agent for the reactive fragments generated in the rupture of coal crosslinks. Finally it facilitates reaction product removal, thereby more rapidly exposing the unreacted regions of the coal particles to attack by the melt.

ZINC CHLORIDE STUDIES WITH MODEL COMPOUNDS

As a result of the complexity and heterogeneous molecular structure of coal, reaction-product identification and reaction-sequence interpretation are extremely difficult and inaccurate. Chemical studies of compounds that model the various structures in coal are therefore essential in elucidating the chemistry of liquefaction in general and the role of zinc chloride in particular.

Mobley (M5) studied zinc chloride catalysis of ether-linkage cleavage. Both cyclic and noncyclic ethers react readily in zinc chloride, provided the ether oxygen is adjacent

to at least one methylene group, or to an aromatic ring activated by nucleophilic substituents. Rupture of the ethers by zinc chloride activation forms fragments which rapidly alkylate aromatic centers. For dibenzyl and cycloaliphatic ethers, the oxygen atom is removed completely with formation of water. However, if the oxygen is bonded to a phenyl or naphthyl group, then a phenolic hydroxyl group is formed, which resists further attack. Notably, when cyclohexane is used as solvent for dibenzylether cleavage, the parent compound incorporates, and a polymer is formed; whereas when methanol is used as a solvent at $225^{O}C$, a single major product, methylbenzylether, is formed in 90% yield. This experiment explains the methanol incorporation observed in the present study and by Shinn (S5), which thus appears to result from the initial scissions, mainly of carbon-oxygen bonds.

Taylor (T2) studied the cleavage by zinc chloride of straight-chain aliphatic bridges between aromatic centers. Working at $300^{O}C$, he observed that zinc chloride fails to cleave aliphatic bridges or direct links between unsubstituted phenyl rings, yet it readily cleaves linkages between aromatic nuclei which contain ring-activating substituents. We judge that, since coal is known to be highly substituted with oxygen, nitrogen, and alkyl groups, zinc chloride is likely to catalyze the cleavage of many of the alkyl linkages between aromatic entities.

The reactions between zinc chloride and fused-ring structures in cyclohexane at $325^{O}C$ for one hour at 1500 psig of

hydrogen were studied by Salim and Bell (S12). They discovered that among the aromatics, naphthalene and phenanthrene are unreactive, while anthracene hydrogenates with minor cracking. For hydrogenation, the presence of a methyl group on naphthalene has a minor activating effect, whereas a hydroxyl group has a strong activating effect; in the latter case, the hydroxyl group is removed. They also studied the effect of molecular hydrogen on conversion of the aromatics to liquid products. These results, shown in Table 2, demonstrate that zinc chloride activates molecular hydrogen and that the resulting hydrides serve to stabilize the reactive fragments from bond scission. This stabilization reduces the production of refractory char and enhances the yield of liquid products.

BACKGROUND FOR BIOMASS STUDIES

Availability of Biomass as an Energy Feedstock

Biomass is defined as organic matter such as agricultural and forestry residues, municipal wastes, trees, grasses, and other plants including those that can be grown specifically for the production of fuels. The estimated recoverable wastes and residues available for biofuel production (A4, B8, U1, H11) are given in Table 3. Biomass resources currently available could contribute 5% of the U.S. energy consumption at present levels by the end of the century (E2).

The cultivation of biomass in large-scale farms for the specific purpose of fuel production, is currently the most

Table 2. Effect of hydrogen pressure on conversion of aromatics to liquid products. 325°C, 1500 psig; 2 mole % substrate in cyclohexane, $ZnCl_2$/Substrate = 1/2 molar (data of Salim, S12).
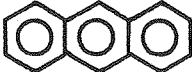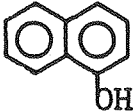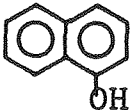
Substrate	Gas	Substrate Conversion, mole %		
		Liquid Products	Unreacted	Polymerized
(anthracene)	H_2	68	32	0
(anthracene)	N_2	0.1	5	95
(naphthol, OH)	H_2	26	74	0
(naphthol, OH)	N_2	4	20	76

Table 3.   Estimated recoverable wastes and residues
           available for biofuel production (A4, B8, Ul,
           Hll)

	Quantity, in 10^6 t/yr.	Total Higher Heating Value[1] (10^{15} Btu)
Municipal solid wastes	90	1.0
Municipal liquid wastes	11.5	0.2
Confined animal manures	23.5	0.4
Lumber and paper mill wastes[2]	23.5	0.4
Field crop residues	90	1.6
Forestry residues[3]	90	1.6
	329	5.2

[1]   Higher heating value is the heat of combustion of the
      dried biomass, assumed to be 9×10^6 Btu/t for MSW and
      14×10^6 Btu/t for all others.

[2]   Above present use of about 0.85×10^{15} Btu.

[3]   Includes noncommercial forest resources.

significant issue in bioconversion. Several general systems studies (A5, I2-3, M6) have examined the cultivation of trees (silviculture) for fuel production. Equal attention (L3-4, B9) has been given to the cultivation of such conventional crops as corn, sugarcane, and grasses for conversion to fuels.

Competition with food, feed, and fiber production; higher uses for land; water availability, uncertainty about yields; potential social and environmental impacts; and marginal economics all will limit energy farms in the near future. Considerations of collection and transportation costs, seasonality, lack of a market system or guaranteed availability, a relatively small local resource scale, and storage requirements will pose limitations on the size of biomass utilization and conversion facilities.

Chemical Structures of Biomass Components

The chemical composition of the various biomass materials is always similar to that of wood, with respect to major constituents. Wood is heterogeneous in its anatomical makeup, nonuniform in structure and exceedingly difficult to define chemically. It consists essentially of inter-penetrating components, largely of high molecular weight. The principal components generally are classified as lignin, cellulose, hemicellulose, and solvent-soluble substances (extractives); the amounts present are in the range of 15 to 35%, 40 to 50%, 20 to 35% and 3 to 10% respectively. These chemical components cannot be separated quantitatively without alteration

and degradation of their structure, due to their high molecular weight, close similarity, physical (and possibly chemical) bonding between components, and the high molecular order of the wood system, which reduces the accessibility of some components. Nevertheless, the chemistry of wood can for the most part be described by the chemistry of its constituents (B10).

Cellulose

This is the major component of cell walls of wood fibers, making it about 50% of the wood and therefore the most abundant organic chemical in the world. Cellulose is a high-molecular-weight polymer of D-glucose units joined by β-1, 4-glucosidic bonds having the structure shown in Figure 4. The average degree of polymerization, as deduced from the least degraded cellulose preparations, is 7,000 to 10,000. The influence of the crystallite regions of cellulose on the liquefaction rate tends to explain the faster rate of alkaline hydrolysis, the alkalies being more reactive and thus more able to swell the structure.

Hemicellulose

These materials, closely associated in plant tissues with cellulose, are mixtures of low-molecular-weight polysaccharides condensed from the following major saccharide units: D-glucose, D-xylose, D-mannose, L-arabinose, D-galactose, D-glucuronic acid, and D-galacturonic acid. Because D-glucose polymers are also found in hemicellulose, its
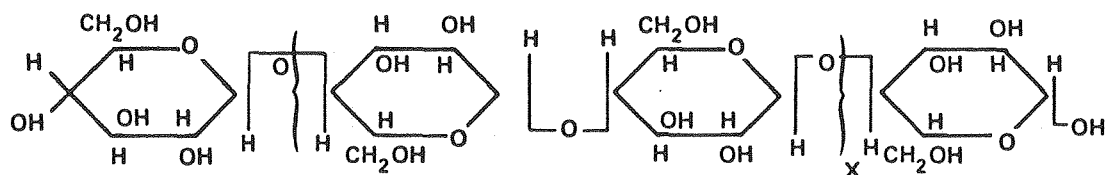
Figure 4 . Structure of cellulose.
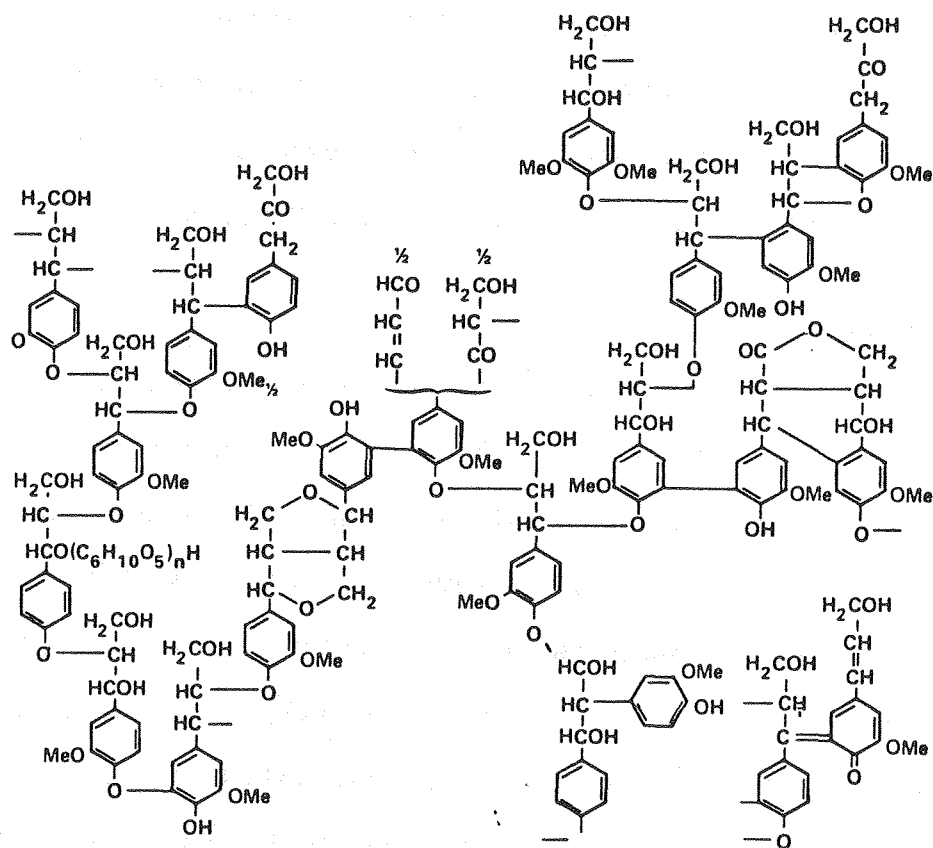
Figure 5 . Structure of lignin (F2).

XBL 795-1648A

difference from cellulose is not great. Primarily, hemi-
cellulose unlike cellulose is generally noncrystalline in
its natural state. This is consistent with its chemical
heterogeneity, a presence of short side groupings and in
some cases, branching in contrast to the highly uniform and
linear structure of cellulose. Although quantitative separa-
tion of hemicellulose and cellulose is impossible, hemicellu-
lose is more easily hydrolysed by acids, and reacts faster
due to its amorphous nature. Softwood hemicelluloses are
rich in galactoglucomannan polymers and contain as well,
significant quantities of xylan polymers.

Lignin

This is the polymeric noncarbohydrate fraction of wood,
extremely complex and difficult to characterize. It com-
prises 20 to 40% of wood by weight, does not occur alone in
nature, and cannot be removed selectively from the wood
structure. Lignin is noncrystalline, and thermoplastic in
nature. It acts as a capillary gel, which can be swelled
and appears very reactive in the solid phase. Lignin gives
wood its structural rigidity through its crosslinked
structure.

In wood, the lignin network is concentrated between and
in the outer layers of the fibers. Several chemical models
have been proposed for the structure of lignin. One such
model, due to Freudenberg (F2), is shown in Figure 5.
Lignins are essentially substituted three-dimensional

phenylpropane polymers, with the phenylpropane units connected by etheric and aliphatic bonds. Molecular-weight values for isolated lignins are in the range of 1,000 to 12,000 (a degree of polymerization of 5 to 65) depending on the extent of chemical degradation or condensation during isolation.

Extraneous Components

These are all non-cell-wall components of wood. Some of these components can be extracted with water of neutral organic solvents, or are volatilized by steam. These extractives include low-molecular-weight carbohydrates, terpenes, aromatic and aliphatic acids, alcohols, tannins, color substances, proteins, phlobaphenes, lignans, alkaloids, and soluble lignins. Other extraneous components include inorganic salts, and pectins which are generally nonextractible. These extraneous components are the source of many wood by-products, lend wood its resistance to insects and decay, inhibit pulping and bleaching in some instances, and give wood its odor, taste and color. The softwoods usually contain 5 to 8% extractives, whereas the hardwoods contain 2 to 4%.

Chemical Liquefaction of Wood and Wood Components

Wood conversion to liquid products has been pursued through many routes, among which hydrogenation and hydrogenolysis have been significant. Early hydrogenation experiments were carried out using noncatalytic methods. Doree

and Hall (D5) treated lignin sulfonic acid with zinc in both
dilute acetic and hydrochloric acid until hydrogen sulfide
formation ceased, producing very little lignin degradation
under these mild conditions. Willstatter and Kalb (W10)
treated spruce lignins, recovered by hydrogenation in hydro-
chloric acid, with red phosphorus and hydriodic acid and ob-
tained a yield of 60 to 80% of a complex mixture of hydrocar-
bons. Neither of these procedures showed much promise for
making commercially useful materials.

Catalytic hydrogenation is more interesting and has been
investigated more thoroughly. Lindblad (L5) was the first to
try to convert lignin into useful oils by catalytic hydrogen-
ation of wood, testing many different catalysts such as nick-
el and cobalt hydroxides, nickel, zinc, copper and manganese
sulfides, zinc chloride, cupric hydroxide, and molybdic acid.
He also treated wood with ferric hydroxide, then suspended it
in sulfite-spent liquor, and hydrogenated this suspension at
$350^{\circ}C$ to produce heavy oils containing saturated hydrocarbons;
he believed that the ferrous sulfide formed catalysed the
hydrogenation.

Drawing on the German work in coal liquefaction done in
World War II, the Noguchi Institute of Japan began to study
lignin liquefaction. Goheen (G3) reported that by 1952,
using a hydrogenation catalyst, a substantial portion of the
lignin was converted into relatively few monophenols and
substantially suppressed additional hydrogenation of the
phenols. Their work has been extended by the Crown-

Zellerbach Corporation (G3).

Seth (S13) and co-workers have recently conducted further exploratory research on wood liquefaction by various routes. The first involved solvolytic depolymerization of wood followed by hydrogenation of the resulting slurry or solution. Under operating conditions of 250°C and one hour reaction time, catachol, phenol, and ethylene glycol were most effective in solubilizing wood leaving acetone insoluble residues of 2, 9, and 18 wt-% of dry wood respectively. The second route involved wood hydrolysis followed by hydrogenation of the hydrolyzed slurry. Acid-catalyzed transfer of hydrogen from solvent molecules was tested for the hydrogenation step. Cyclohexadiene as the hydrogen donor solvent gave a conversion of 30% of the wood to acetone-soluble products.

Biomass Conversion Processes

Several routes, just discussed, have been investigated for conversion of biomass materials into liquid products. Such processes are principally involved in molecular-weight reduction, hydrogen addition, and deoxygenation of biomass. These processes can simply be divided into two major categories--thermochemical and biochemical processes. Thermochemical conversion includes pyrolysis, and direct and indirect liquefaction processes.

In order to liquefy biomass pyrolytically, operating temperatures of 480 to 930°C have been employed. The decomposition reactions are fairly uncontrolled, and result in

low yields of liquids with the dominant yields of undesirable gases and char. The Occidental Flash Pyrolysis process uses wood and municipal solid wastes as the feedstock (K3, B12). Operating at a relatively low temperature of $510^{\circ}C$ and short residence time, liquid yield is maximized producing 40 Kg oil per 100 Kg of organics on a dry basis. The Tech-Air Pyrolysis process (R4) utilizes peanut hulls, wood, or municipal wastes, and operates at a higher temperature of $593^{\circ}C$ with an oil yield of 25% of the biomass organics. Oxidation of char in the bottom of the reactor produces the heat needed for the pyrolysis reaction.

In order to have a better control over the decomposition reactions, a direct waste-to-oil liquefaction process (R4) employed lower temperatures (316 to $371^{\circ}C$) in the presence of sodium carbonate catalyst and high hydrogen pressure (2,000 to 4,000 psig). This enhanced the yield of oils, producing 400 to 500 Kg per 1,000 Kg of dry biomass material.

Indirect biomass liquefaction involves first gasifying the biomass material to a synthesis gas (a mixture of carbon monoxide and hydrogen); liquid fuels can then be obtained by subsequent conversion of the synthesis gas to methanol or Fischer-Tropsch hydrocarbons. Methanol can be converted to gasoline by the Mobil process, which involves reacting methanol over a metal catalyst deposited in a shape-selective zeolite; this limits the size of the molecules that can be formed.

Thermochemical conversion processes become economically

prohibitive as the moisture content of the feed rises. These high-moisture feeds are suitable for microbiological processing (fermentation). Biomass materials are hydrolyzed to fermentable sugars which are in turn converted to ethanol by fermentation. Ethanol is a clean fuel, yielding 30% more energy per unit mass than methanol.

OBJECTIVES AND SCOPE OF THIS RESEARCH

The thermal cleavage of chemical linkages in coal liquefaction processes now under development is reminiscent of the thermal cracking of crude oil employed by refineries in the 1920's. The severity of the operating conditions (over 400°C and 1500 psig) gives rise to high capital expenditures for equipment, and low thermal efficiencies. The need is very great to investigate coal liquefaction under milder conditions that will be more selective, reducing gas and char production and thereby improving the process economics.

Liquid-phase catalysts have proved effective in coal conversion under such mild conditions (below 325°C and 1000 psig). Previous work in this laboratory, using a liquid-phase catalyst, led to nearly complete solubilization of coal. However, the bulk of the product was asphaltenes and preasphaltenes. These are high molecular-weight components, rich in heteroatoms and deficient in hydrogen. The oil fraction, which comprises low molecular-weight components soluble in aliphatic hydrocarbon solvents, rich in hydrogen

and low in heteroatom content, is the desired product in coal liquefaction.

This study has focused on the increased solubilization of coal with a more favorable product distribution leading to increased oil production. In order to make more oils, additional activation of zinc chloride is necessary so as to boost its catalytic action.

The co-catalytic effect of several powdered metals was studied with the aim of increased activation of molecular hydrogen and consequent improvement in coal hydrogenation. These metals, Fe, Co, Ni, Zn, Sn, Al, and Mo are known to improve hydrogenation (H7-8, B5, M2-4, R3, V1, W6-8, Y1). In particular, addition of zinc metal to the zinc chloride melt was studied in some detail.

Inorganic salts were added to the zinc chloride melt in other runs. Their higher solubility in the melt, relative to metals, provides transport to reactive sites inside the coal particles. Co-catalysis by different metallic ions with different hydrocracking functions could be beneficial.

Further activation of zinc chloride was investigated by use of organic complexants. Bifunctional complexants potentially capable of complexing with zinc and other metallic ions and subsequently make them available at reactive sites in coal were sought.

As implied above, the reaction between solid coal and a liquid catalyst depends to a large extent on achieving penetration of the solid by the liquid. SEM studies (S5) have

demonstrated that an effective catalyst reacts throughout each particle, not just at the solid surface. Wetting agents potentially capable of reducing the liquid-solid interfacial tension and of increasing the mobility of product molecules within the coal, were also studied.

The comparative ability of other liquid-catalyst systems to liquefy coal was examined briefly using antimony chloride and phosphoric acid. Catalyst corrosivity and the ease of catalyst recovery and re-use were also considered.

The effect of reaction variables in product upgrading was particularly studied. As temperature is known to affect the rates of depolymerization and hydrogenation and the solubility of conversion products, reaction temperature was varied from 250 to 340°C. The upper limit was set by char production, when the rate of bond cleavage surpasses that of reactive-fragment stabilization. The effect of reaction time and methanol loading on product distribution was also determined.

Several analytical techniques were utilized to provide more fundamental information on the mechanisms of coal liquefaction. To elucidate the physical factors that affect the activity of zinc chloride in coal solubilization, several samples of treated coal were examined using a scanning electron microscope. The effect of various reaction variables on molecular-weight distribution of the different extracts was investigated with gel-permeation chromatography. The distribution of aliphatic and aromatic carbon was studied

using the solid CP-^{13}C NMR technique. Gas samples from se-
lected runs were analyzed by combined gas chromatography and
mass spectrometry. In order to characterize reaction pro-
ducts more fully, their elemental contents and melting points
were determined.

The effect of the zinc chloride-methanol catalytic sys-
tem on wood solubilization was likewise investigated. Reac-
tion variables--temperature, time,hydrogen pressure, particle
size, and methanol loading--were studied. This study is
aimed at furnishing more fundamental information about wood
solubilization. Since coal originated from wood, understand-
ing the mechanism of wood solubilization will shed more light
on coal-conversion mechanisms.

CHAPTER II

EXPERIMENTAL PROGRAM

MATERIALS

Coal Studies

A subbituminous coal, supplied by the Wyodak Resources Development Corporation, from the Roland top seam of its Gillette, Wyoming, mine was used as the feed material for this study. The coal was received, ground to minus 3/4 inch, in 55-gallon drums.

This material was crushed in a jaw and roller crusher, to reduce the particle size to minus 1/6 inch, and subsequently stored under carbon dioxide in polyethylene bags. It was later milled and screened, the bulk of it into a -30 +60 Tyler-mesh fraction and the remainder into a -60 +100 Tyler mesh fraction. They were later stored under nitrogen, in 500 gm portions, in 1-quart cans.

The proximate and ultimate analyses of the coal are shown in Table 4.

Reagents and Solvents

Table 5 shows the sources and purities of all the inorganic materials (including cylinder gases) and organic reagents and solvents utilized in this study.

Biomass Studies

Cellulose

Ashless filter papers manufactured by Whatman Limited, England, were used as cellulose for this study. The filter papers were supplied as thin 11.0-cm-diameter circles. They were later shredded into narrow 1-cm^2 strips, and stored

Table 4. Analysis of Wyodak Sub-bituminous Coal

Proximate Analysis, %[+]

Moisture	22.50
Ash	10.92
Volatile	37.14
Fixed Carbon	29.44
	100.00

*Ultimate Analysis   % Moisture-Free Coal

Carbon	60.05
Hydrogen	4.92
Nitrogen	0.95
Sulfur	0.52
Ash	13.70
Oxygen (Difference)	19.86
	100.00
H/C (Atomic)	0.98

[+]Analysis performed by Commercial Testing and Engineering Inc. (Denver, Co.)

*Analysis performed by University of California Microchemical Analysis Laboratory.

Table 5. Sources and Purities of Reagents and
Solvents Used

Material	Source	Grade	Min. Purity (%)
Acetonitrile	J. T. Baker	Reagent	99+
Acetophenone	Eastman Kodak		
Adiponitrile	Matheson/C/B		
Aluminium metal	Ventron		
Ammonium chloride	Mallinckrodt	Reagent	
Ammonium molybdate	Mallinckrodt	Reagent	
Antimony chloride	Mallinckrodt	Reagent	99.00
Benzene	Mallinckrodt	Reagent	
Bipyridyl	Mallinckrodt	Reagent	
Calcium chloride	Mallinckrodt	Reagent	
Chromium metal	Ventron		
Cobalt metal	Ventron		
Cyclohexane	Matheson/C/B		
Decalin	Aldrich		
Dodecyl p-toluene sulfonate	Eastman Kodak		
Ethanol	Mallinckrodt	Absolute	
Ferric chloride	Mallinckrodt	Reagent	
Ferrous chloride	Mallinckrodt	Reagent	
Gallium chloride	Ventron		99.99
Hexyl mercaptan	Eastman Kodak		98.00
Hydrochloric acid	Mallinckrodt		36.5-38.0
Malonic acid	Aldrich		99.00
Manganese metal	Ventron		
Methanol	Mallinckrodt	Reagent	
Molybdenum metal	Ventron		
Nickel chloride	Mallinckrodt	Reagent	
Oleic acid	Braun/K/H		
Phosphoric acid	Mallinckrodt	Reagent	85.00
Pyridine	Mallinckrodt	Reagent	
Silver nitrate	Mallinckrodt	Reagent	
Sodium ferrocyanide	Matheson/C/B	Reagent	99.00
Tin metal	Mallinckrodt	Reagent	
Toluene	Mallinckrodt	Reagent	
Urea	Aldrich	Reagent	99+
Zinc chloride	Matheson/C/B	Reagent	97.00
Zinc cyanide			
Zinc iodide	Ventron	Technical	
Zinc metal	Mallinckrodt	Reagent	95.00
Zinc oxide	Mallinckrodt	Reagent	
Zinc sulfide	Ventron		99.9

Cylinder Gases

Carbon monoxide	Matheson Gas		99.50
Hydrogen	Liquid Carbonic		99.99
Nitrogen	Pacific Oxygen		99.99

under nitrogen in polyethylene bags. This material was used in this form.

The moisture content of the cellulose was determined by drying 10 gm of the sample to constant weight at $110^{\circ}C$ under 50 millibars of nitrogen. After removal of the sample from the vacuum oven, it was cooled in a vacuum desiccator prior to weighing. A small sample of the dried cellulose was analyzed by the University Microchemical Analysis Laboratory. The ultimate analysis is shown in Table 6.

Lignin

The lignin used in this study was derived from the Kraft pulping of pine wood and supplied by the Chemical Division of Westvaco Corporation, South Carolina, with a purity level of more than 99%.

Wood Flour and Chips

Douglas fir softwood from Oregon was selected for this study. The wood flour had already been ground and, both it and the 3/4" chips were dried to a moisture content of 8 wt-% by Rust Engineering Company at the DOE experimental facility in Albany, Oregon. They were shipped in polyethylene bags within a cardboard container. These materials were charged into the reactor as received.

Their moisture content and ultimate analysis, as shown in Table 6, were determined in a manner similar to those described for both cellulose and lignin above.

Table 6. Ultimate Analysis of Wood and Wood-Related
materials. (wt-%, moisture-free basis)

	Cellulose	Lignin	Wood Flour	Wood Chips
Carbon	43.68	62.00	48.81	49.55
Hydrogen	6.16	5.46	5.95	6.27
Nitrogen	0.03	0.99	0.08	0.06
Sulfur	0.00	0.92	0.08	0.04
Ash	0.00	3.40	0.90	0.20
Oxygen (by difference)	50.13	27.23	44.18	43.88
	100.00	100.00	100.00	100.00
H/C (atomic)	1.68	1.05	1.45	1.51
Moisture, %	4.5	6.7	8.5	10.7

EQUIPMENT

All the experiments reported were performed in a 600 ml autoclave supplied by Parr Instrument Co., Moline, Illinois. The schematic diagram of the autoclave and associated apparatus is shown in Figure 6.

The autoclave was fabricated from Hastelloy B. Glass liners of 300 ml. capacity, that fit into the body of the reactor, were used in all experiments.

The autoclave is operable to 350°C. Controlled heating was provided by a 780-watt quartz-fabric covered mantle, responding to automatic control by a solid-state potentiometric system actuated by an iron-constantan thermocouple which monitored the temperature inside the autoclave. Circulating water through an internal cooling loop connected to an external pump actuated by the temperature controller enabled the reactor to be maintained with $\pm3^{\circ}$C of the desired reaction temperature.

Agitation of the reactor contents was achieved by use of a direct-drive stirrer using a self-sealing packing gland. The pressure in the reactor vessel was measured by a 2000 psig pressure gauge attached to a side-arm of the gas outlet port. The autoclave was also equipped with a gold-coated Inconel rupture disc rated at 2000 psig.

EXPERIMENTAL PROCEDURE

In many of the coal reactions, 250 gm of $ZnCl_2$ and 35 gm of methanol were weighed into a glass-liner vessel. This
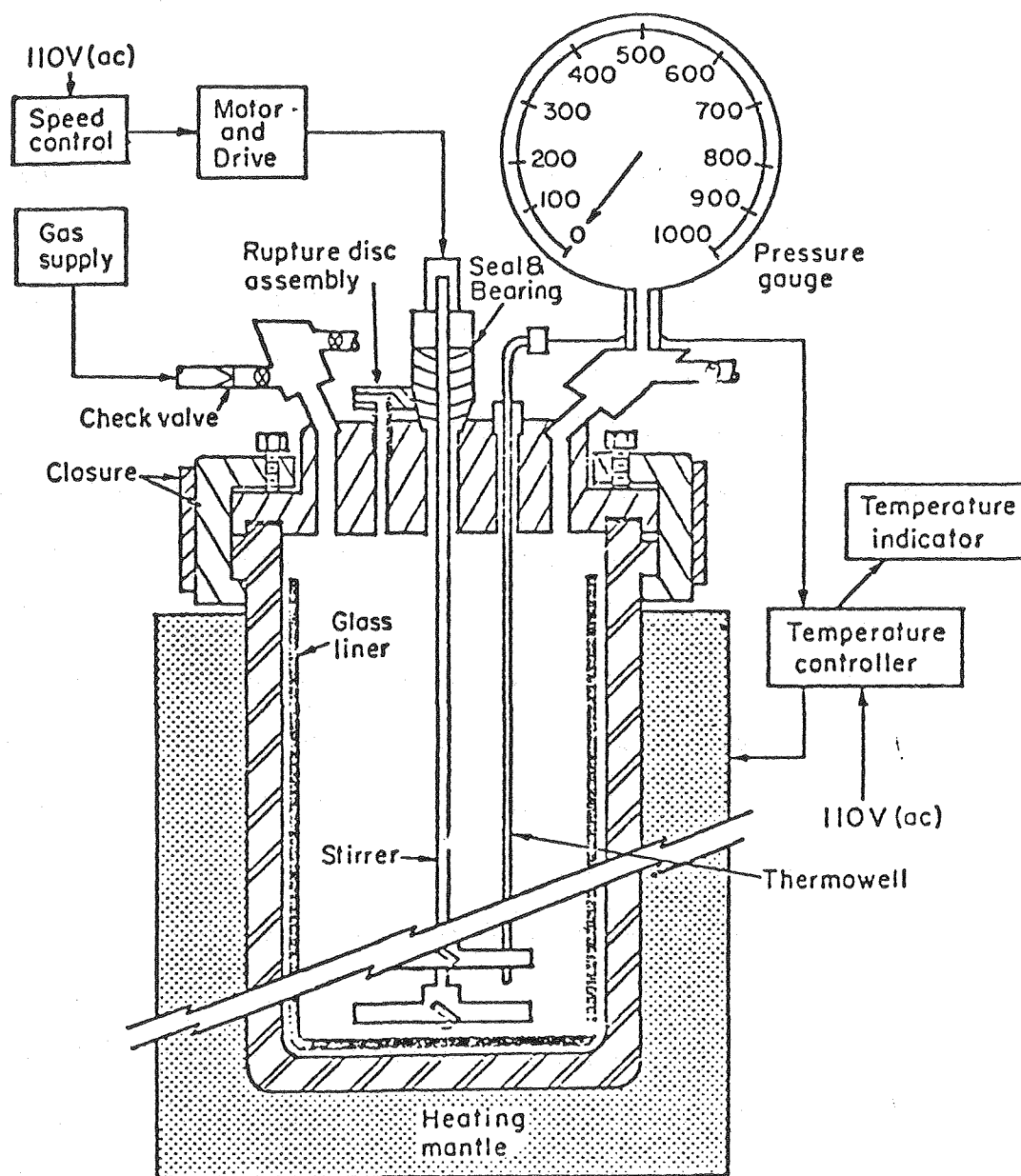
XBL7711-4006

Figure 6 . Parr autoclave.

mixture was heated to 150°C, reweighed, and additional methanol added to replace any evaporated solvent. 50 gm of undried coal, and any additional solvent and/or reagent were then introduced into the mixture. The glass liner was then inserted into the autoclave, and the latter was sealed.

The sealed autoclave was purged with hydrogen to remove air and subsequently checked for leaks; it was then pressurized with hydrogen so as to achieve the desired pressure at the reaction temperature. The reactor contents were then heated at a rate of approximately 10°C/minute, with constant stirring, until the desired temperature, usually 275°C, was reached. The reaction was maintained at this temperature for the desired reaction time. During both heat-up and reaction, temperature and pressure readings were recorded. After reaction had occurred for the desired time, the reactor was cooled by immersion in a cold water bath to approximately 200°C and depressurized. It was then repressurized so as to achieve the desired pressure at the second reaction temperature. The reactor contents were then heated, with constant stirring, usually to 300°C. The reaction was maintained at this temperature for the desired time, at the end of which the autoclave was rapidly cooled to 200°C by immersion in a cold water bath and then depressurized. In some cases, this cycle was repeated with heating to 325°C. After holding for the desired reaction period, the reactor was immersed in a cold water bath, depressurized, and opened.

The reaction products were dumped into acidified cold

distilled water (20 ml. concentrated HCl in 1 liter of water).
This was subsequently filtered in a Buchner funnel while
being washed with approximately six liters of hot distilled
water usually at 90°C. The filtered cake was dried to con-
stant weight in a vacuum oven at 110°C under 50 millibars of
nitrogen.

The dried product is referred to as melt-treated coal
(MTC). A small quantity of MTC was pulverized in a glass
vial and sent in a bigger vial containing $CaSO_4$ desiccants of
the Microlab for analysis. Small portions, representative of
the MTC, were stored under nitrogen for examination under the
scanning electron microscope. Approximately 2 gm of the MTC
was weighed into a predried single-weight Whatman 25x100 mm
cellulose extraction thimble for subsequent solubility de-
termination. The remaining melt-treated coal was stored in a
vacuum desiccator for any additional future use.

The solubility determination involves exhaustive se-
quential extraction in cyclohexane, toluene, and pyridine at
their normal boiling points using a standard Soxhlet appara-
tus yielding oils, asphaltenes, and preasphaltenes respec-
tively. Oils are characterized by low heteroatom content,
low molecular weight, a melting point range of 50° to 100°C,
and a high H/C ratio of 1.21 to 1.31. Asphaltenes have more
heteroatoms, higher molecular weight, a melting point range
of 120° to 260°C, and an H/C ratio of 0.98 to 1.10. Preas-
phaltenes are the richest in heteroatoms, highest molecular
weight, and an H/C ratio of 0.84 to 0.95. Extraction times

of 5 hours for cyclohexane, 5 hours for toluene, and 18 hours
for pyridine extraction have given complete extraction as ev-
idenced by a colorless solution in the Soxhlet siphon arm.
Overflow of insolubles from the thimble, which may occur
during pyridine extraction, is prevented by performing room-
temperature extraction in pyridine after toluene extraction
and prior to the pyridine extraction in the Soxhlet apparatus.

At the end of the extraction, the liquid extracts were
dried in predried and weighed crystallizing dishes by evapor-
ating to near dryness in the fume hood. These extracts and
the residues were further dried in a vacuum oven at $110^{\circ}C$
under 50 millibars of nitrogen. The samples removed from the
vacuum oven were cooled in a vacuum desiccator prior to
weighing. These extracts were sent to the Microlaboratory
for elemental analysis. Additional analytical investigations
were carried out to further characterize them.

A list of the experiments conducted is given in Table 7.
The effect of different additives on the catalytic activity
of zinc chloride was studied.

The procedure for the biomass study was similar, ex-
cept that it was conducted at a single temperature. $ZnCl_2$
and methanol were initially heated to $100^{\circ}C$ (as against
$150^{\circ}C$), and no acid wash was used. Table 8 lists the auto-
clave experiments performed with wood (Douglas fir softwood)
and wood-related materials. The catalytic effect of zinc
chloride in the solubilization of wood was investigated.
The reaction variables which were studied included reaction

Table 7
Coal Autoclave Experiments

(50 gm Wyodak Coal, -30 +60 mesh; 250 gm $ZnCl_2$)

Run No.	Temp. ($^\circ$C)	H_2 Pressure (psig)	Time (min)	Solvent (gm)	Additives (gm)
2	275	500	30	CH_3OH-25	Zn-4; $CaCl_2$-20
3	275	500	30	CH_3OH-25	Zn-4; ZnO-5; $CaCl_2$-20
4	275	500	30	CH_3OH-25	Sn-7; $CaCl_2$-20
5	275	500	30	CH_3OH-25	$CaCl_2$-20
6	275	500	30	CH_3OH-25	Mo-6; $CaCl_2$-20
7	275	500	30	CH_3OH-25	Al-2; $CaCl_2$-20
8	275	800	30	CH_3OH-30	Zn-1
9	275	800	30	CH_3OH-30	Zn-4; ZnO-2; $CaCl_2$-11
10	275	500	30	CH_3OH-25	Fe-1; $CaCl_2$-20
12	250/200/250	500	30/30/30	CH_3OH-25	Zn-1; O_2-20 psig
13	275	500	30	CH_3OH-25	Ni-1; $CaCl_2$-20
14	275	500	30	CH_3OH-25	Co-1; $CaCl_2$-20
15	275	500	30	CH_3OH-25	Mn-1; $CaCl_2$-20
16	275	800	30	CH_3OH-25	Fe-10
17	275	800	30	CH_3OH-25	Fe-25
19[a]	275	500	30	CH_3CN-12.5	
33	275	800	30	CH_3OH-35	Oleic acid-7.5
34	275	800	30	CH_3OH-35	Malonic acid-2.6; $NiCl_2$-5.4, $FeCl_2$-3.6
35	275	800	30	CH_3OH-35	Urea-4.6; $NiCl_2$-5.4; $FeCl_2$-3.6
36	275	800	30	CH_3OH-45	ZnS-7.1; $NiCl_2$-5.4; $FeCl_2$-3.6

Run No.	Temp. ($^\circ$C)	H_2 Pressure (psig)	Time (min)	Solvent (gm)	Additives (gm)
37[b]	225	800	60	CH_3OH-24	$SbCl_3$-228
38	275	800	30	CH_3OH-35	$NiCl_2$-5.4; $FeCl_2$-3.6
39	275	500	30	CH_3OH-25	$SbCl_3$-25
40[c]	200	800	60	none	$SbCl_3$-152.8
41	275	800	30	CH_3OH-35	Hexyl mercaptan-1.5; $NiCl_2$-5.4; $FeCl_2$-3.6
42	275	800	30	CH_3OH-35	Dodecyl p-toluene sulfonate-1.4
43	275	800	30	CH_3OH-35	
44	275	800	30	CH_3OH-35	Zn-4
45[d]	275	800	30	CH_3OH-64	$CaCl_2$-158
46	275	500	30	CH_3OH-25	Bipyridine-2
47	275	500	30	CH_3OH-25	$Zn(CN)_2$-5
48[e]	250		60	H_2O -75 C_2H_5OH-75	$FeCl_3$-50; CO-200 psig
49[f]	275	500	30	C_2H_5OH-15	90% H_3PO_4-150
50	275	800	30	CH_3OH-25	ZnO-7
51	275	800	30	CH_3OH-35	Zn-8
52	275	500	30	CH_3OH-25	AgCl-2.5
53	275	500	30	CH_3OH-25	$CuCl_2$-6.7
54	300	500	30	CH_3OH-25	
55[g]	275	800	30	CH_3OH-35	
56	275	500	30	CH_3OH-25	Sodium ferrocyanide-5
57	275	500	30	CH_3OH-25	NH_4Cl-5; ZnO-3.8
58	275	300	30	CH_3OH-25	$FeCl_3$-6.8; $FeCl_3$-5; CO-300 psig
59[h]	275	500	30	CH_3OH-35	
60	275/325/275	800/500/800	30/30/30	CH_3OH-28/0/14	Zn-6

Run No.	Temp. ($^\circ$C)	H_2 Pressure (psig)	Time (min)	Solvent (gm)	Additives (gm)
61	275	500	30	CH_3OH-25	Zn-8; Dodecyl p-toluene sulfonate-1.4
62	275	500	30	CH_3OH-25	NH_4CL-5; ZnO-3.8; Dodecyl p-toluene sulfonate-1.4
63	275/275/275	800/800/800	15/15/15	CH_3OH-35/0/	Zn-8
64[i]	275	500	30	CH_3OH-25	
65	275	500	30	CH_3OH-25	$GaCl_3$-2.5
66	275	500	30	CH_3OH-25	ZnI_2-7.5
67	275/300/325	800/800/800	15/15/15	CH_3OH-35/0/	Zn-8
68	275/300	800/800	15/15	CH_3OH-35/0	Zn-8
69	275/300/325	800/0/0	15/15/15	CH_3OH-35/0/	Zn-8
70	275	800	15	CH_3OH-35	Zn-8
71	275	800	0	CH_3OH-35	Zn-8
72	325	800	30	CH_3OH-35	Zn-8
73	275/300/325	800/800/800	15/15/30	CH_3OH-35/0/	Zn-8
74	275/300/325/340	800/800/800/800	15/15/15/15	CH_3OH-35/0/0/0	Zn-8
75	275	800	30	CH_3OH-45	$NiCl_2$-5.4; $FeCl_2$-3.6
76	275/300/325	800/800/800	15/15/0	CH_3OH-35/0/	Zn-8
77	300	800	30	CH_3OH-35	Zn-8
78	250/275//300/325	800/0//800/0	10/10//10/10	CH_3OH-35/0//0/0	Zn-8
79	250/275//300/325	800/0//800/0	10/10//10/10	CH_3OH-35/0//0/0	
81	250/275//300/325	800/0//800/0	10/10//10/10	CH_3OH-65/0//0/0	Zn-8
82	275/300	800/800	15/30	CH_3OH-35/0	Zn-8

Run No.	Temp. ($^\circ$C)	H_2 Pressure (psig)	Time (min)	Solvent (gm)	Additives (gm)
83	250/275//300/ 325	800/0//800/ 0	10/10//10/ 10	CH_3OH-35/0//Zn-8; $NiCl_2$-5; 0/0 Ammonium Molybdate-5	
84	275/325	800/800	15/30	CH_3OH-35/0 Zn-8	
85[j]	250/275//300/ 325	800/0//800/ 0	10/10//10/ 10	CH_3OH-15/0//Zn-8 0/0	
86	250/275//300/ 325	800/0//800/ 0	10/10//10 10	CH_3OH-50/0//Zn-8 0/0	

Footnotes to Coal Autoclave Experiments

a. 12.5 gm CH_3OH added

b. No $ZnCl_2$ added

c. 91.3 gm $ZnCl_2$ added

d. 79 gm $ZnCl_2$ added

e. 50 gm $ZnCl_2$ added

f. 35 gm $ZnCl_2$ added

g. Substrate was dried MTC 49 (Product of Run 49)

h. 200 gm $ZnCl_2$ added

i. -60 + 100 mesh coal used

j. Reactor plugged

Table 8. Biomass Autoclave Experiments

Run No.	Temp. ($^\circ$C)	H_2 Pressure (psig)	Time (min)	Substrate (gm)	$ZnCl_2$ (gm)	Solvent (gm)
11	250	500	60	Cellulose-17.5	250	MeOH-50
18	250	500	60	Cellulose-17.5	250	Water-25
20	250	500	60	Lignin-50	250	MeOH-50
21	250	800	60	Wood flour-20	250	MeOH-50
22	225	800	60	Wood flour-20	250	MeOH-50
23	200	800	60	Wood flour-20	250	MeOH-50
24	250	800	60	Wood chips-20	250	MeOH-50
25	250	500	60	Wood chips-20	250	MeOH-50
26	250	200	60	Wood chips-20	250	MeOH-50
27	250	800	30	Wood chips-20	250	MeOH-50
28	250	800	0	Wood chips-20	250	MeOH-50
29	225	500	60	Wood chips-20	250	MeOH-75
30	225	500	60	Wood chips-20	250	MeOH-25
31	225	500	60	Wood chips-20	250	MeOH-50
32	225	200	60	Wood flour-20	250	MeOH-50

temperature (between 200 and 250°C); reaction time (between 0 and 60 min.) and hydrogen pressure (between 200 and 800 psig).

The Soxhlet extraction technique described above is both time-consuming and tedious. A long delay between the end of the reaction and time for obtaining the extraction yield further makes this technique unsuitable. A simpler, quicker, and less tedious means for determining the reaction yield should be investigated.

A detailed gas collection and analysis, coupled with the analysis of trace constituents in the wash-water stream and materials volatilized during vacuum oven drying through vacuum distillation of the washed MTC, will be useful in calculating an accurate mass balance of the reacting system.

The use of methanol instead of water to extract $ZnCl_2$ from the reaction products should be investigated. A considerable savings in energy will be made in concentration of the $ZnCl_2$-CH_3OH solution. An additional advantage is that the concentrated solution of $ZnCl_2$ can then be recycled without further treatment.

ANALYTICAL PROCEDURES

Elemental Analysis

The elemental content of the reaction products (carbon, hydrogen, nitrogen, sulfur, chlorine, and metals) was determined by the University of California Microanalytical Laboratory. All the samples were submitted in a tightly

sealed vial placed inside a bottle containing desiccant. The carbon, hydrogen, and nitrogen analyses were performed by combustion in pure oxygen at $950^{O}C$ in a Perkin-Elmer Model 240 automated elemental analyzer.

Sulfur and chlorine were measured by combustion in pure oxygen at $850^{O}C$ to form gaseous SO_2 and Cl_2. These off-gases were absorbed in a 3% hydrogen peroxide solution to form SO_3^- (H_2SO_4) and Cl^- (HCl). In the case of sulfur, the sulfate was precipitated with $BaCl_2$, and the $BaSO_4$ formed was weighed to determine the amount of sulfur in the original sample. With respect to chlorine, the chloride was titrated with a standard $AgNO_3$ solution to determine the chlorine content of the sample. The ash content was then measured from the weight of the uncombusted material.

Oxygen was not analyzed for, and the oxygen content was obtained by difference. Metals were determined by atomic absorption in a Perkin Elmer Model 360 Atomic Absorption Spectrophotometer. Samples were initially digested in a solution of concentrated sulfuric acid and 30% hydrogen peroxide to destroy all organic matter. The resulting solution was diluted, and the metal content was obtained by comparing its absorbance with known standards.

Scanning Electron Microscopy

Photomicrographs of several samples representing a broad range of reaction conditions were obtained with 20 KeV electrons in an AMR 1000 scanning electron microscope (SEM).

The samples, comprising melt-treated coal or wood and extraction residues, were sprinkled onto conductive adhesive-coated copper plates that were later placed on SEM mounting stubs. A thin film of gold was vacuum-evaporated onto the samples to render them conductive and thereby minimize charging.

In many cases, three magnifications were utilized in examining the samples. A lower magnification of 250X, in some cases, allowed a complete view of a large portion of the particle and in certain instances, an easy scanning of the entire sample. Higher magnifications of 1000X and 3000X were used when specific areas of the sample merited a more detailed examination.

Gel-Permeation Chromatography

The molecular-weight distribution of selected extracts was determined on a Waters Associates Model 6000A-U6K-440 gel-permeation chromatograph (GPC). The samples were prepared by dissolving 2 mg of fresh extracts in 1 ml. of pyridine. The solutions obtained were filtered through Millipore Teflon-type FH filters of 0.5 mm pore size. Twenty microliters of the solution were injected into three 25 cm columns connected in series containing $1000\overset{o}{A}$, $500\overset{o}{A}$, and $100\overset{o}{A}$ microstyragel. Pyridine was used as the elution solvent at a flow rate of 1 ml/min. A chart speed of 1 cm/min was used throughout the study.

The GPC was equipped with an ultraviolet absorbance

detector fitted with both 313 and 365 nm filters, such that monitoring of absorbance as a function of elution volume could be achieved at both wavelengths on a dual pen strip chart recorder. The 313 nm wavelength was selected for this study because of its greatest relative absorbance of condensed aromatic ring compounds.

The GPC column fractionates components of a mixture according to their molecular size, the heavier components coming out first. At 313 nm, the major light-absorbing species are fused-ring aromatic compounds.

Unequal absorbance by different compounds could obscure the actual concentration information obtainable from the GPC. This could reduce the usefulness of the GPC analysis as an absolute measure of molecular weights distribution. As a result of this shortcoming, no molecular weights were as-signed to any of the GPC tracings. Hence, comparisons were only made on the effect of single reaction variables on molecular-weight distribution.

Gas Chromatography/Mass Spectrometry (GC/MS)

In order to fully characterize the reaction products, gas samples from some runs were collected and analysed using a GC/MS. The gaseous products were collected in evacuated 150 ml stainless steel sampling cylinders at the end of the reaction, prior to cooling.

The GC/MS analyses were carried out by Dr. Amos Newton and co-workers at Lawrence Berkeley Laboratory, using a

Finnigan Instruments Model 4023. This system comprises of a Finnigan Model 9610 gas chromatograph, a Finnigan 4000 quadrupole mass spectrometer, and a Model 2400 Finnigan/Incos data system with mass spectral libraries.

The 9610 gas chromatograph is a microprocessor-controlled unit, in which the column oven can operate from $-100^{\circ}C$ to $+400^{\circ}C$ in either isothermal or temperature-programmed mode, and uses either packed or capillary columns. A glass column measuring 2 mm in diameter by 2 m in length and packed with 3% OV-225 on Chromosorb W/HP was used. Helium was used as the carrier gas; a typical GC flow rate of 20 ml/min was employed.

The quadrupole mass filter has a rated resolution of 400, and in practice is capable of unit mass resolution to 1000 a.m.u. The ionizer is an electron impact source with a rhenium filament, producing an electron current up to 0.5 mA at energies from 10 to 150 eV. Usual scan conditions in this study were 0.25 mA at an ionization energy of 70 eV.

The entire mass range of the effluent gases was scanned every few (0.5-5) seconds, to obtain a complete mass spectrum of every peak eluted from the column. The mass spectrum of each chromatographic peak was then recalled and compared with mass spectra of known compounds in two mass spectral libraries each containing approximately 25,000 compounds which could be independently searched. By matching unknown mass spectrum with a known spectrum, identification was reasonably likely.

Melting Point Determination

The melting points of the extracts from various runs were determined using a 120V Mel-temp. apparatus. A small quantity of each sample was introduced into a capillary tube, which was subsequently inserted into the Mel-temp. unit. An applied voltage, usually between 30 and 70V, was selected on a variable autotransformer so that a small rise in temperature ($1^{o}C$/min) was maintained.

The effect of temperature, reactor residence time, and various additives on the melting points of the different extracts was examined. Replicate melting point determination was conducted and the results are shown in Table 9. The results are highly reproducible.

Solid-State Cross-Polarization Carbon-13 NMR

The solid state CP-^{13}C NMR analyses were carried out by Professor Alex Pines and co-workers in the Chemistry Department of University of California, Berkeley. A double resonance spectrometer operating in heterodyne mode with an intermediate frequency of 30 MHz was used. The magnet is a wide-bore superconducting solenoid. The radio-frequency sections are mostly homebuilt from commercial hybrids, and the digital section is constructed around an on-line PDP 8/e minicomputer. A detailed description of the equipment and the procedures used is given elsewhere (W12).

The various regimes in the spectrum are shown in Figure 7. These regimes were identified from spectra for a wide

Table 9.   Replicate Melting Points of MTC Fractions

Run[+] No.	Melting Points ($^{\circ}$C)	
	Oils	Asphaltenes
9	90-96	130-139
	89-95	126-137
10	72-98	124-146
	73-100	122-145
39	62-73	161-196
	59-71	162-198
41	56-70	166-222
	57-71	167-220
42	52-64	142-203
	53-66	144-201

+   Reaction conditions are given in Table 7.

Measurements by Michael Johnson.
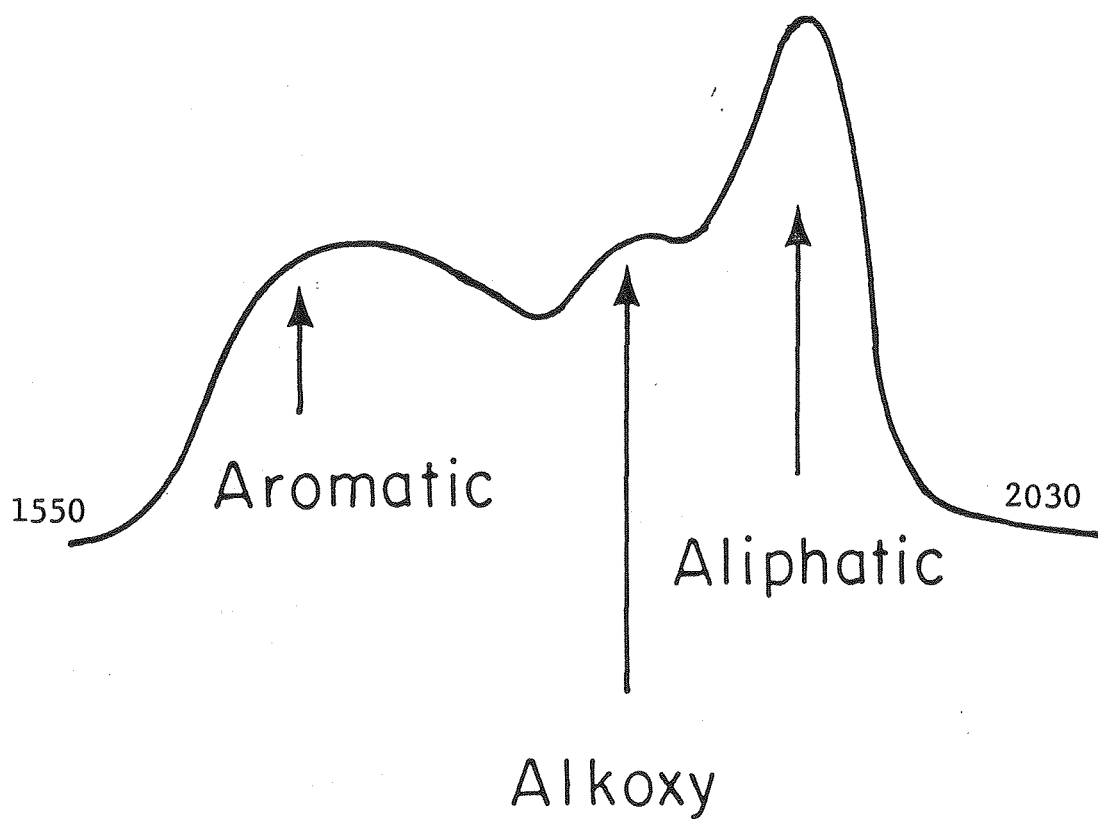
Scale: 1 point = 50Hz

XBL 804-658

Figure 7 . Identification of various regimes within a
CP– ^{13}C NMR spectrum.

range of chemical compounds identified as probably constituents of coal.

The general accuracy of this method is ±5% absolute, for the relative areas of aliphatic, aromatic, and alkoxy groups. Changes in spectrum within one set of samples have probably somewhat better relative accuracy than the ±5%.

CALCULATION PROCEDURES

The calculation procedure used in this study was developed by John Shinn, while an investigator on this project (S5), who has provided detailed explanations of the various calculation steps. A sample calculation procedure is given in Table 10.

Table 10. Sample Calculation Procedure for Run 51

MTC recovered = 34.20 gm

Microlab. analysis

	Wt. (%)	Wt. recovered (gm)	Wt. fed (gm)
C	67.29	23.01	22.97
H	6.48	2.22	1.88
N	0.75	0.26	0.36
Zn	4.33	1.48	0.00
Cl	3.27	1.12	0.00
Ash	14.00	4.79	5.24

Extraction data: MTC extracted = 2.128 gm; Cyclohexane

Extract = 0.543 gm; Toluene Extract =

0.274 gm

Pyridine Extract = 1.209 gm; Residue =

0.310 gm

Nitrogen analyses: Pyridine Extract, 3.04% or 0.035 gm;

Residue, 0.6% or 0.002 gm

$ZnCl_2$ in MTC   = gm Cl+gm Cl/1.08 (gm Cl/gm Zn in $ZnCl_2$)

= 1.12+1.12/1.08 = 2.16 gm

"Excess Zn"   = total Zn-Zn in $ZnCl_2$

= 1.48-1.04 = 0.44 gm or 0.55 gm as ZnO

True Ash = total ash−excess Zn (as ZnO)

= 4.79−0.55 = 4.24 gm

O+S = MTC−C−H−N−Zn−Cl−true ash

= 34.2−23.01−2.22−0.26−1.48−1.12−4.24

= 1.87 gm

% Recovery of Each Element = (gm recovered/gm feed)x100

Element	% Recovery
C	100.18
H	118.09
N	72.22
O+S	24.62
Ash	80.92

Incorporation ratio (R) = (% C recovery−95)/95

= (100.18−95)/95

= 0.055 gm incorporated C/gm coal C

Organic matter extracted = $\dfrac{\text{(C+H+N+O+S recovered)(MTC extracted)}}{\text{MTC recovered}}$

= (23.01+2.22+0.26+1.87)(2.128)/34.2

= 1.70 gm

Pyridine retention = Cyclohexane extract+Toluene extract+ Pyridine extract+Residue−MTC extracted

= 0.543+0.274+1.209+0.310−2.128

= 0.208 gm

Fraction of pyridine in pyridine extract

$$= \text{gm N in Pyridine Extract}/(\text{gm N in Residue+Pyridine extract})$$

$$= 0.035/(0.035+0.002)$$

$$= 0.946$$

Pyridine retained in pyridine extract

$$= \text{gm pyridine retained x fraction pyridine in pyridine extract}$$

$$= 0.208 \times 0.946$$

$$= 0.197 \text{ gm}$$

Cyclohexane solutility $= 100 \times \text{Cyclohexane extract}/\text{Organics extracted}$

$$= 100 \times 0.543/1.70$$

$$= 31.94\%$$

Toluene solubility $= 100 \times \text{Toluene extract}/\text{Organics extracted}$

$$= 100 \times 0.274/1.70$$

$$= 16.11\%$$

Pyridine solubility $= 100 \times (\text{Pyridine extract-Pyridine retained in Pyridine extract-}ZnCl_2\text{ in extracted MTC})/\text{Organic extracted}$

$$= 100 \times (1.209-0.197-(2.16)(2.128/34.2))/1.7$$

$$= 51.62\%$$

Total pyridine solubility = Cyclohexane sol.+Toluene Sol.+ Pyridine sol.

$$= 31.94+16.11+51.62$$

$$= 99.67\%$$

Corrected solubility or minimum coal-derived solubility

$$= 1-(1-\text{total solubility})(1+R)$$

$$= 1-(1-0.9967)(1+0.055)$$

$$= 99.65\%$$

CHAPTER III

RESULTS OF COAL INVESTIGATIONS

EFFECT OF CO-CATALYSTS AND ADDITIVES

Previous work (S5) in this research group led to high solubilization of coal, but gave relatively low conversion to oils which constitute the desired product. Increased conversion to oils appeared to require relatively high hydrogen pressure and increased catalyst activity and was generally accompanied by an increase of H/C ratio in the MTC.

Metal Additives

The effect of several metals on product distribution is shown in both Figure 8 and Table 11. Figure 8 shows that all metals except nickel and aluminium increased the yield of oils, and also the H/C ratio. Of these, zinc was the most effective. Table 11 shows that tin, molybdenum, aluminium, and iron were all better than zinc in increasing the combined yield of oils and asphaltenes.

The superiority of zinc metal both for increasing the yield of oils and for improving the H/C ratio of all the product fractions (see below) led to further investigations involving the addition of zinc metal.

Further Studies with Zinc Metal

Table 12 shows the effect of added zinc metal on conversion. The presence of zinc results in nearly 50% increase in the yield of oils and a large increase in the H/C ratio.

Figure 9 shows that the yield of oils increases with increasing loading of zinc. It also shows that both gas consumption during the reaction and the H/C ratio of the melt
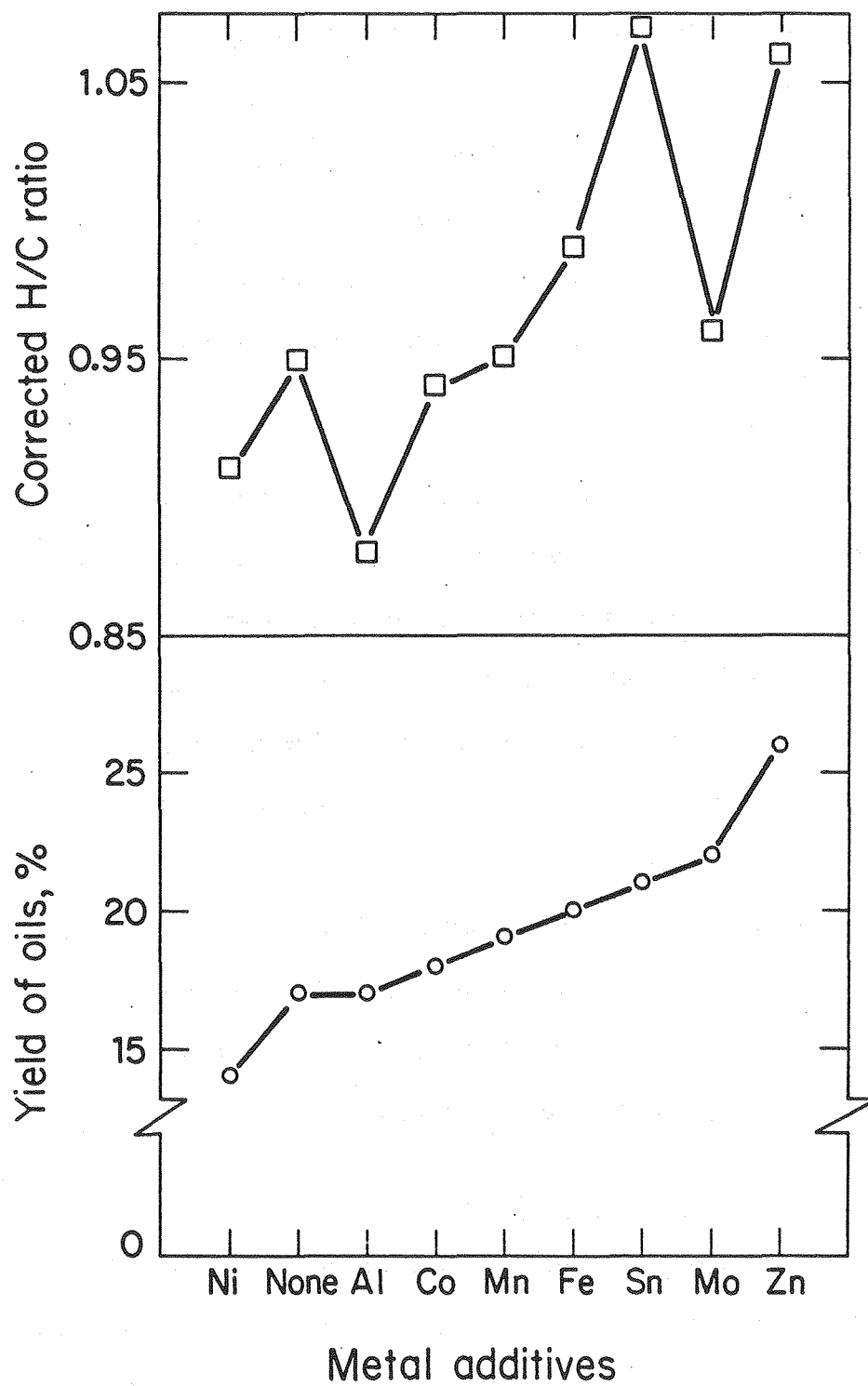
XBL 802-8328B

Figure 8 . Effect of metallic additives on conversion.

Table 11. Effect of metallic additives on conversion
(250 gm $ZnCl_2$, 50 gm Coal, 25 gm CH_3OH;
275^OC, 500 psig H_2, 30 min.)

Run No.	Additives*	Cumulative Pct. Daf.-Soluble			Corr. Sol.	Corr. Atomic H/C Ratio
		Cyclo-hexane	Toluene	Pyridine		
5	none	17	31	89	88	0.95
2	Zn	26	39	85	84	1.06
4	Sn	21	44	84	83	1.07
6	Mo	22	44	91	90	0.96
7	Al	17	44	85	82	0.88
10	Fe	20	44	89	88	0.99
13	Ni	14	28	80	77	0.91
14	Co	18	36	78	75	0.94
15	Mn	19	35	96	95	0.95

* Amounts used are shown in Table 7.

Table 12. Effect of Added Zinc Metal on Conversion

(250 gm $ZnCl_2$, 50 gm Coal; $275^{\circ}C$, 30 min.)

Run No.	Additives (gm)	CH_3OH Loading (gm)	H_2 Pressure (psig)	Cumulative Pct. daf.-Soluble			(gm ret. CH_3OH/ gm coal org.)	Corr. Atomic H/C Ratio
				Cyclo-hexane	Toluene	Pyridine		
5	none	25	500	17	31	89	0.11	0.95
2	Zn (4)	25	500	26	39	85	0.10	1.06
43	none	35	800	22	37	100	0.12	1.01
44	Zn (4)	35	800	30	46	100	0.12	1.03
51	Zn (8)	35	800	32	47	100	0.05	1.15
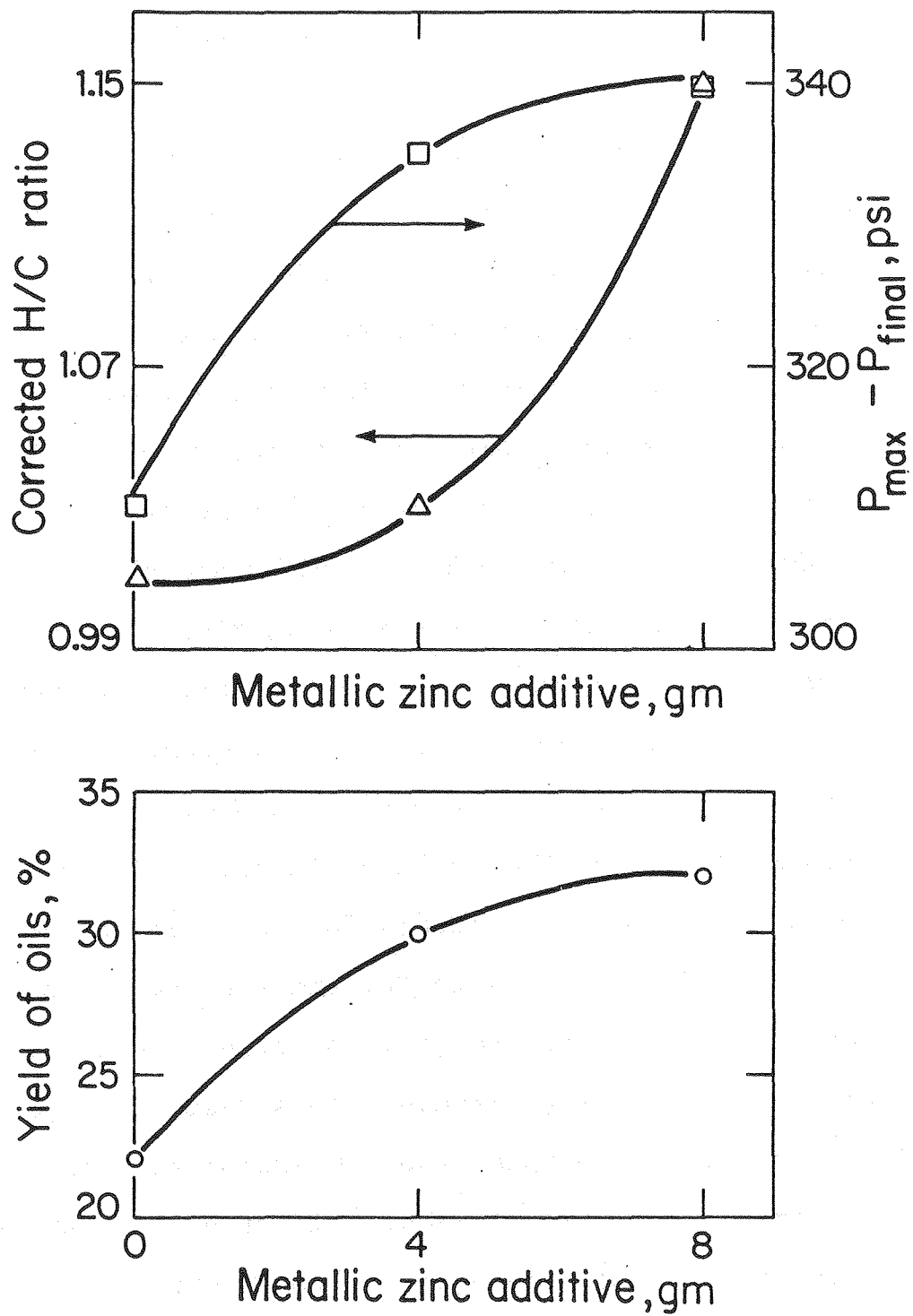
XBL 802-8329B

Figure 9 . Effect of metallic zinc on the quality
of conversion products.

treated coal increases with increasing loading of metallic zinc. This strongly suggests that the addition of zinc metal results in further activation of molecular hydrogen leading to increased hydrogenation. Zinc loading beyond 3% of the melt was not attempted, because at this loading there was evidence of incomplete solubility of zinc in the melt.

The yield of asphaltenes remains unchanged (Figure 10) as the zinc loading increases, whereas the production of pre-asphaltenes decreases. Since the decrease in the production of preasphaltenes is comparable to the increase in yield of oils, addition of zinc could be said to aid the conversion of preasphaltenes to oils. The effect of zinc metal on the H/C ratio of the melt treated coal and the various product fractions is given in Table 13. Zinc considerably increases the H/C ratio of the MTC and extraction products.

Figure 11 shows that at both 275 and 325^OC, metallic zinc addition results in roughly 50% increase in the yield of oils. At 325^OC (Run 78, with Zn; and Run 79, without Zn), zinc addition increases the yield of asphaltenes while decreasing that of preasphaltenes. This raises the possibility that the route of preasphaltene conversion to oils is through the intermediary of asphaltenes. Differences in the reaction time render comparison between the reactions at 275^OC and those at 325^OC inaccurate.

Zinc Oxide as an Additive

The catalytic effect of zinc oxide alone and with zinc
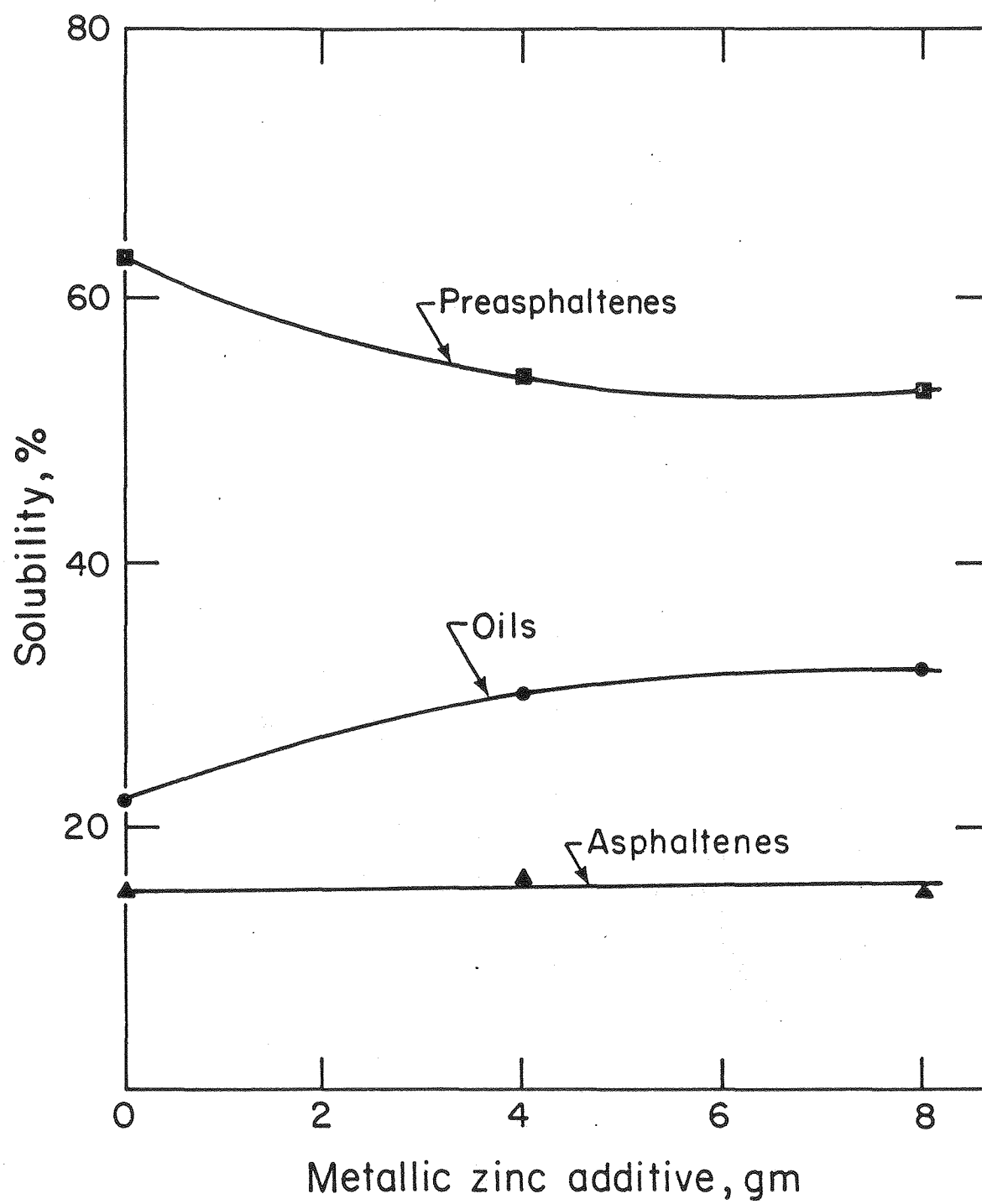
Figure 10.   Effect of metallic zinc on conversion.

XBL 804-657

Table 13. Effect of Added Zinc Metal on Quality Products

Samples	Without Zinc (Run 43)			With Zinc (Run 51)		
	Yield wt. %	Corr. H/C Ratio	M.P. $^\circ$C	Yield wt. %	Corr. H/C Ratio	M.P. $^\circ$C
Melt-treated Coal	-	1.01	-	-	1.15	-
Oils	22	1.26	62- 89	32	1.31	58- 88
Asphaltenes	15	1.07	155-183	15	1.10	201-259
Preasphaltenes	63	0.88	-	53	0.94	-
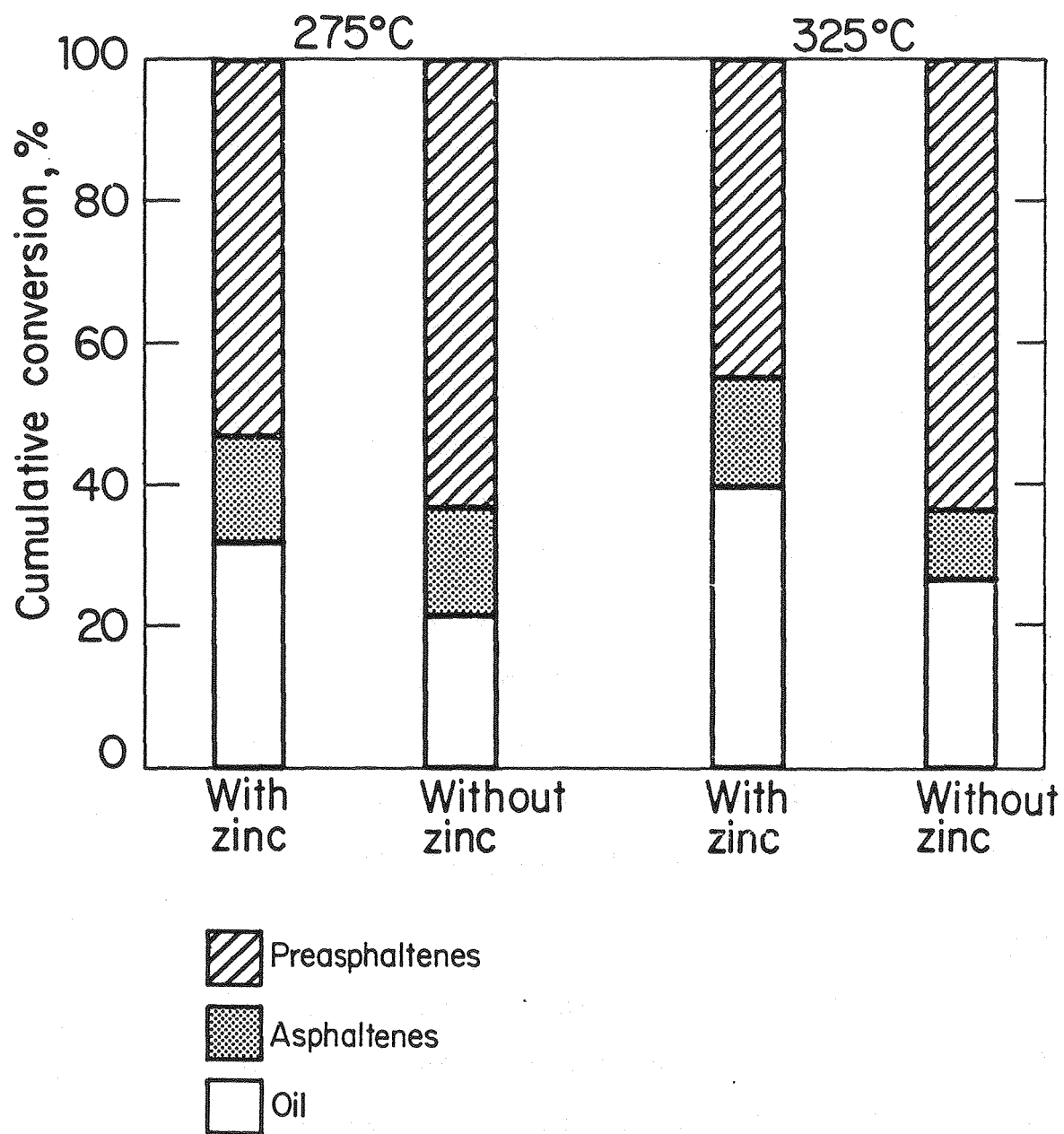
Figure 11. Effect of metallic zinc on product distribution.

metal was investigated, and the results are shown in Table 14. Zinc oxide can act as an effective scavenger for any hydrogen chloride released in the reaction. As the reagent grade $ZnCl_2$ used for this study contains small amounts of ZnO, the effect of the latter on coal conversion is important.

The addition of both zinc and zinc oxide decreases the yield of oils and in the absence of metallic zinc, zinc oxide reduces the catalytic activity of zinc chloride resulting in a lower solubilization of coal. It is obvious that the addition of zinc oxide is not beneficial.

The effectiveness of metallic additives on the hydrogenation of coal may have been reduced by their inadequate solubility in the melt, leading to mass-transfer limitations. Utilizing more soluble inorganic salts was a possible alternative, and is discussed in the next section.

Inorganic Salts

The effect of inorganic salts on the product distribution is shown in Table 15. Addition of silver chloride or cupric chloride to the zinc chloride melt, resulted in complete conversion of the coal to pyridine-soluble materials. The improvement occurred in the yield of preasphaltenes; no significant changes in the yield of oils and asphaltenes was observed.

Ammonium chloride and zinc oxide increased the preasphaltene yield and the H/C ratio. Zinc oxide was added as an

Table 14.   Effect of Zinc/Zinc Oxide Additives on Conversion
(250 gm $ZnCl_2$, 50 gm Coal; 275°C, 30 min.)

Run No.	Additives (gm)	CH_3OH Loading (gm)	H_2 Pressure (psig)	Cyclo-hexane	Toluene	Pyridine	Corr. Sol.	Corr. Atomic H/C Ratio
				Cumulative Pct. daf.-Soluble				
5	none	25	500	17	31	89	88	0.95
2	Zn (4)	25	500	26	39	85	84	1.06
9	Zn (4) ZnO (2)	30	800	20	45	82	81	1.09
3	Zn (4) (ZnO (5)	25	500	25	37	84	81	1.08
50	ZnO (7)	25	800	17	29	72	68	0.97

77

Table 15. Effect of Inorganic Additives on Conversion

(250 gm $ZnCl_2$, 50 gm Coal; 275°C, 500 psig H_2, 30 min.)

| Run No. | Additives[+] | CH_3OH Loading (gm) | Cumulative Pct. daf.-Soluble | | | R (gm ret. CH_3OH/ gm coal org.) | Corr. Atomic H/C Ratio |
			Cyclo-hexane	Toluene	Pyridine		
5	none	25	17	31	89	0.11	0.95
52	Silver chloride	25	15	28	100	0.17	0.91
53	Cupric chloride	25	16	28	100	0.20	0.83
57	Ammonium chloride Zinc oxide	25	17	30	99	0.15	0.98
47	Zinc cyanide	25	18	31	95	0.12	1.01
65	Gallium chloride	25	14	26	91	0.21	0.80
66	Zinc oidide	25	14	27	98	0.18	0.89
75*	Nickel chloride Ferrous chloride	45	30	45	100	0.18	0.99
36*	Zinc sulfide Nickel chloride Ferrous chloride	45	32	46	91	0.23	1.00

+ Amounts used are shown in Table 7.

* 800 psig H_2 pressure.

78

acceptor for HCl, a possible decomposition product of ammonium chloride, so as to study the effect of NH_4Cl alone.

Both zinc iodide and zinc cyanide increased the yield of preasphaltenes, but the former lowered the yield of oils and the latter had no effect on either the yield of oils and asphaltenes. Gallium chloride lowered the yields of both oils and asphaltenes. All the inorganic salts added to the melt increased the incorporation of methanol, and except for ammonium chloride and zinc cyanide, lowered the H/C ratio.

Since most coals contain sulfur compounds, some zinc chloride is probably converted into zinc sulfide during coal conversion. The effect of zinc sulfide was investigated. Nickel and ferrous chlorides were added as co-additives, on the basis that the divalent sulfide ion group might form bridges between two dissimilar metallic species and perhaps leading to increased overall reaction. Compared to nickel and ferrous chlorides alone, zinc sulfide resulted in a reduced yield of preasphaltenes and an increased methanol incorporation.

Complexants

Complexing agents capable of introducing two dissimilar metallic species at the same site in the coal molecule was studied in an effort to accelerate cracking and hydrogenation concurrently. The effect of complexants is shown in Table 16.

Urea drastically reduced the solubilization of coal,

Table 16. Effect of Complexants on Conversion
(250 gm ZnCl$_2$, 50 gm Coal; 275°C,
800 psig H$_2$, 30 min.)

Run No.	Complexants[+]	CH$_3$OH Loading (gm)	Cumulative Pct. Daf.-Soluble			R (gm ret. solv./ gm coal org.)	Corr. Atomic H/C Ratio
			Cyclo-hexane	Toluene	Pyridine		
38	Nickel chloride Ferrous chloride	35	24	35	100	0.12	1.02
35	Urea Nickel chloride Ferrous chloride	35	12	22	73	0.55	0.62
34	Malonic acid Nickel chloride Ferrous chloride	35	25	35	96	0.15	1.02
41	Hexyl mercaptan Nickel chloride Ferrous chloride	35	26	40	100	0.14	1.03
5*	none	25	17	31	89	0.11	0.95
46*	Bipyridyl	25	19	32	94	0.17	0.89
56*	Sodium ferrocyanide	25	16	29	83	0.15	0.93

+ Amounts used are shown in Table 7.

* 500 psig H$_2$ pressure.

80

suggesting that it formed a very strong complex with zinc chloride and contributed to its deactivation. Malonic acid slightly reduced the conversion. Under reaction conditions, it may have decarboxylated to give acetic acid (S14), which has been shown to reduce the catalytic activity of zinc chloride (S5).

The other potential complexants studied had no significcant effect on the product distribution.

Wetting Agents

The reaction between a solid and a liquid is greatly dependent on the effectiveness of contact between the liquid and the solid. Between zinc chloride and coal, contact is principally established through capillary uptake or direct inhibition which may be very responsive to changes in surface tension, as influenced by addition of wetting agents.

The wetting agents selected and their effect on product distribution are shown in Table 17. Dodecyl paratoluene sulfonate (DPTS) increased the yield of oils by nearly one fourth, while the H/C ratio remained unchanged. Oleic acid increased the yeild of oils by 18%, but was massively incorporated.

OTHER CATALYTIC SYSTEMS

Only a small part of the zinc chloride melt serves as catalyst, while the bulk provides the reaction medium. Hence the addition of cheaper inorganic compounds that might

Table 17. Effect of Wetting Agents on Conversion
(250 gm $ZnCl_2$, 50 gm Coal, 35 gm CH_3OH;
$275^O C$, 800 psig H_2, 30 min.)

Run No.	Additives	Cumulative Pct. daf.-Soluble			R (gm ret. solv./ gm coal org.)	Corr. Atomic H/C Ratio
		Cyclo-hexane	Toluene	Pyridine		
43	none	22	37	100	0.12	1.01
33	Oleic acid	26	39	100	0.69	0.65
62	Dodecyl para-toluene sulfonate	27	40	100	0.16	1.01

+ Amounts used are shown in Table 7.

substitute as a medium without reducing the catalytic activity would be of interest. This will definitely reduce the catalyst loading and ultimately decrease the processing cost.

Antimony Chloride

In general, the ability of a Lewis acid to accept an electron pair is greater, as the electronegativity of the central atom and the attached atom is increased and with the number of the attached atoms. On this basis, antimony chloride would be expected to be a stronger Lewis acid than zinc chloride particularly since Sb is more electronegative than Zn and also bonded to three chloride atoms as against only two for Zn. Moreover, antimony chloride has relatively low melting and boiling points; melting at 74°C and boiling at 220°C (P6).

Antimony chloride has shown extremely high catalytic activity, good selectivity to liquid products, and insensitivity to hydrogen sulfide (W13). In addition, $SbCl_3$ offers the prospects of not needing methanol and by its high vapor pressure, can easily penetrate the coal particles. For more direct comparison with zinc chloride/methanol system, antimony chloride/methanol was selected for study.

The catalytic activity of antimony chloride in coal conversion is shown in Table 18. At 225°C, 75% of the carbon content of coal is converted to pyridine-soluble materials, compared with only 40% conversion obtained when using the zinc chloride/methanol system. In the absence of methanol and at a quite low temperature of 200°C, antimony chloride added

Table 18. Effect of Antimony Trichloride on Conversion
(50 gm Coal)

Run No.	Catalyst*	CH_3OH Loading (gm)	Temp. (°C)	Time (min)	H_2 Pressure (psig)	Cumulative Pct daf-Soluble			Corr. Sol.	Corr. Atomic H/C Ratio
						Cyclo-hexane	Toluene	Pyridine		
49[+]	$ZnCl_2$	50	225	60	800	–	16	46	40	1.09
37	$SbCl_3$	24	225	60	800	8	14	75	75	1.32
5	$SnCl_2$	25	275	30	500	17	31	89	88	0.95
39	$SnCl_2$ $SbCl_3$	25	275	30	500	15	29	92	91	0.86
31[+]	$ZnCl_2$	50	200	60	200	–	9	16	0	0.93
40	$ZnCl_2$ $SbCl_3$	none	200	60	800	1	3	30	30	0.95

– Not determined.

* Amounts are shown in Table 7.

+ Shinn (S5).

84

to zinc chloride converts over one quarter of the carbon content of coal to pyridine-solubles.

Many chlorides dissolve in the melt to give conducting solutions (C5). A small amount was added to the zinc chloride-methanol system; the reaction when conducted at a slightly elevated temperature showed diminished catalytic activity.

Further investigation of the antimony chloride-methanol system was discontinued because of its relatively high cost, its corrosive attack on the reactor, and the difficulty in its separation from the reaction products. The difficulty in separation from reaction products is due to antimony chloride producing insoluble oxychlorides such as $SbOCl$ and $Sb_4O_5Cl_2$ when dissolved in water (C5).

Phosphoric Acid

Use of massive amounts of catalyst with an attendant high cost of recovery makes it desirable to use the cheapest catalyst available that has reasonable activity. Coal liquefaction cannot be unique to molten-halide Friedel-Crafts catalysts. It is possible that by selecting proper reaction conditions, similar results might be obtained with some liquid protic acid such as phosphoric, hydrofluoric or sulfuric acid.

Phosphoric acid is a relatively strong acid, essentially non-oxidizing. It provides a source of protons which can lead to cracking reactions by a carbonium-ion mechanism. It is compatible with decomposition products of the heteroatoms in coal and in case catalyst recycle is desired, any carbonaceous

residues can be eliminated through oxidative regeneration.

McLean (M9) studied the effect of a wide range of concentrations of phosphoric acid on coal conversion. He showed that 85 to 95% range, the remainder being water, gave the best conversion results. In the absence of additives, less than 25% of the carbon content of coal was converted to pyridine-soluble materials. This poor conversion was believed due to phosphoric acid activating the coal to give rapid bond cleavage without commensurate fragment stabilization, so that repolymerization then produces refractory insoluble materials.

In this study whose results are shown in Table 19, ethanol was added to the phosphoric acid to cap the scission fragments, whereas the zinc chloride was added to raise the hydrogenation activity. The solubilization of coal was low. This could be due to insufficient activation of coal (leaving the bulk unreacted) or excessive activation (leading through repolymerization to insoluble materials). The possibility of having produced insoluble char-like materials was investigated by reacting the sample from Run 49 with $ZnCl_2$ under the complete-conversion conditions. This led to near complete conversion, and shows that if insoluble materials were formed, they are not refractory. Nevertheless, the yields from phosphoric acid treatment remain extremely unattractive.

Calcium Chloride with Zinc Chloride

The substantial cost of zinc chloride makes it desirable to reduce the catalyst loading while maintaining good

Table 19. Effect of Phosphoric Acid on Conversion
(275°C, 800 psig H_2, 30 min.)

Run No.	Substrate (gm)	Catalyst[+]	Solvent	Cumulative Pct daf-Soluble			R (gm ret. solv./ gm coal org.)	Corr. Atomic H/C Ratio
				Cyclo-hexane	Toluene	Pyridine		
49[#]	Coal (50)	90% H_3PO_4 $ZnCl_2$	C_2H_5OH	5	8	32	0.11	0.88
55	PTC (34)*	$ZnCl_2$	CH_3OH	14	29	98	0.17	0.86
43	Coal (50)	$ZnCl_2$	CH_3OH	22	37	100	0.12	1.01

* PTC – Phosphoric acid treated coal (Product of Run 49).

\+ Amounts used are shown in Table 7.

\# 500 psig H_2 pressure.

contact between catalyst and coal. Hence a relatively inexpensive salt is sought that would dilute the zinc chloride melt without seriously reducing its catalytic activity. Calcium chloride was chosen for this study. Added in small amounts, it reduces the exchange of zinc ion into coal mineral matter, and is neutral in its effect on the catalytic activity of zinc chloride (S5).

Table 20 shows that massive amounts of calcium chloride drastically reduce the coal conversion to only 20% of pyridine-soluble materials. Thus a massive amount of calcium chloride, or the solvent needed to dissolve it, destroys the catalytic activity of zinc chloride. As one factor, calcium chloride in large amounts probably reduces the compatibility of zinc chloride melt and coal. As another, increasing polychloro-zinc anions could reduce the concentration of zinc cation which may well be the active catalyst. As a third factor, heteroatoms released from coal may reduce the effective concentration of zinc chloride as in the following reaction:

$$ZnCl_2 + NH_3 = ZnCl_2 \cdot NH_3$$
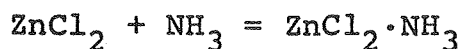
All these factors aggravate the relative scarcity of the zinc cations, and eliminate the possibility of using calcium chloride in large amounts.

EFFECT OF REACTION VARIABLES

Various reaction variables were studied to determine

Table 20. Effect of Massive Amounts of Calcium Chloride on Conversion
(50 gm Coal; 275^OC, 800 psig H_2, 30 min.)

| Run No. | Catalyst (gm) | CH_3OH Loading (gm) | Cumulative Pct. daf.-Soluble | | | R (gm ret. CH_3OH/ gm coal org.) | Corr. Atomic H/C Ratio |
			Cyclo-hexane	Toluene	Pyridine		
-*	none	-	0	1	12	-	0.98
43	$ZnCl_2$ (250)	35	22	37	100	0.12	1.01
45	$ZnCl_2$ (79) $CaCl_2$ (158)	64	3	5	21	0.44	0.60

* Untreated coal.

their effect on product distribution.

Temperature

The effect of operating up to 300°C was studied and the results are shown in Table 21. Comparing the runs at 275 and 300°C, there is no incentive to operate at the higher temperature. Increasing the temperature, increases the incorporation of methanol and reduces the corrected H/C ratio.

The minor effect of temperature up to 300°C, on both coal solubilization and product distribution, can be ascribed to a combination of reasons: firstly, it may be that all the reaction of a given type (like the cleavage of C-O bonds) is accomplished at 275°C such that operating at 300°C is not helpful. Secondly, Table 30 shows that total pressure increases with temperature, this increase being attributed to methanol and its dehydrogenation product, dimethylether, in the gas phase. This will reduce the methanol concentration in the liquid phase and therefore decrease the effectiveness of increased reaction rate at 300°C.

Conversion of preasphaltenes into oils requires the cleavage of C-C and C-N bond types in coal. This can be accomplished at temperatures beyond 300°C. Operating at this temperature regime demands an optimum temperature-staging procedure that can prevent char formation.

Staging and Time

Staged progression of two or more reaction temperatures was studied to search for the conditions that would give the

Table 21. Effect of Temperature on Conversion
(250 gm $ZnCl_2$, 50 gm Coal; 30 min.)

Run No.	Temp. (°C)	H_2 Pressure (psig)	CH_3OH Loading (gm)	Metallic Zinc (gm)	Cumulative Pct daf-Soluble			R (gm ret. CH_3OH/ gm coal org.)	Corr. Atomic H/C Ratio
					Cyclo-hexane	Toluene	Pyridine		
5	275	500	25	–	17	31	89	0.11	0.95
54	300	500	25	–	17	31	92	0.16	0.88
51	275	800	35	8	32	47	100	0.05	1.15
77	300	800	35	8	33	50	100	0.09	1.04

highest production of oils. The results obtained are given in Table 22.

Operating the reactor at 275°C (Run 51) and 300°C (Run 77) indicates no significant advantage for 300°C. However, reacting initially at 275°C and later at 300°C for only 15 minutes (Run 68) results in higher conversion to oils.

Reaction at 325°C (Run 72) shows an increase in oils over 275°C or 300°C but a drop in oil quality (as will be shown later) and in total conversion (implying production of insoluble materials).

By reacting the coal first at 275°C and 300°C in turn, operating at 325°C for 15 minutes (Run 67) and 30 minutes (Run 73) show complete conversion with a considerable increase in oils over Runs 68 and 72. An experiment with four 10-minute stages between 250°C and 325°C (Run 78), kinetically similar to 15 minutes at 275°C, and 15 minutes at 325°C, gave results between those in Runs 68 and 67. These results suggested that while first-stage reaction at 275°C is beneficial, no further advantage is obtained with first-stage reaction at 250°C.

Runs 67 and 73 are clearly the best of this series. From the result of Run 77, the separate stage at 300°C appears unnecessary. Kinetically, Run 67 is equivalent to 20 minutes at 275°C followed by 20 minutes at 325°C, and Run 73 is 20 minutes at 275°C followed by 35 minutes at 325°C. The slight gain in oils for the latter run is not believed sufficient to justify the longer residence time. Hence for this degree of

Table 22. Effect of Temperature Staging on Conversion
(250 gm $ZnCl_2$, 50 gm Coal, 35 gm CH_3OH, 8 gm Zn;
800 psig H_2)

Run No.	Temp. ($^{\circ}$C)	Time (min)	Cumulative Pct. daf.-Soluble			Corr. Atomic H/C Ratio
			Cyclo-hexane	Toluene	Pyridine	
70	275	15	31	45	99	1.00
51	275	30	32	47	100	1.15
77	300	30	33	50	100	1.04
68	275/300*	15/15	38	51	100	1.11
72	325	30	46	60	97	1.08
67	275/300/325**	15/15/15	51	65	100	1.11
73	275/300/325**	15/15/30	54	64	100	1.19
78	250/275//300/325*	10/10//10/10	40	56	100	1.06
74	275/300/325/340***	15/15/15/15	51	60	100	1.13
82	275/300*	15/30	35	53	98	1.10

* One recharge of hydrogen between stages.

** Two recharges.

*** Three recharges.

coal conversion, at this point in our consideration of reaction variables, two-stage operation with 20 minutes residence at 275°C and 20 minutes at 325°C seems the best.

The adequacy of the hydrogen charge for the batch liquefaction experiments was investigated. Hydrogen is consumed both in the removal of oxygen from the coal (with formation of water) and in increasing the H/C ratio above that of raw coal. Even at our highest pressure, the quantity of hydrogen charged is too close to the stoichiometric requirements. In order to rectify this situation, hydrogen was replenished once or for each stage in several tests so as to maintain a high concentration of hydrogen throughout the reaction.

In one case, a direct control experiment was made (Run 69) without mid-conversion replenishment of the hydrogen. Table 23 shows Run 67, for which fresh hydrogen was introduced during each stage of the reaction gave high yields of both oils and asphaltenes. In a flow reactor it would be possible to maintain a high hydrogen concentration throughout the reaction by introducing fresh hydrogen stream at various points along the reactor with simultaneous bleed-off of depleted gases at one or more points to reduce the water vapor concentration.

The effect of temperature beyond 300°C on the product distribution is shown in Table 22. Figure 12 shows that at 15 minutes reaction time, the yield of oils increases with temperature up to 325°C where it tends to level off. A rapid increase in yield is observed between 300 and 325°C. On the other hand, the yield of asphaltenes remains virtually

Table 23. Effect of Hydrogen Pressure (During Temperature Staging) on Conversion
(250 gm $ZnCl_2$, 50 gm Coal, 8 gm Zn, 35 gm CH_3OH; 275, 300, 325°C,
15 min. per stage, 800 psig H_2)

Run No.	Mode of H_2 Addition	Cumulative Pct. daf.-Soluble			Corr. Atomic H/C Ratio
		Cyclo-hexane	Toluene	Pyridine	
69	No recharge	46	56	100	1.10
67	Recharges between stages	51	65	100	1.11

constant whereas that of preasphaltenes decrease with increasing temperature up to 325°C.

For a 30-minute residence time, Figure 13 shows that the yield of oils increases with temperature, the bulk of the increase occurring between 300 and 325°C. A decrease in the production of asphaltenes is observed, being reduced by approximately one third at 325°C. The yield of preasphaltenes also decreases with increasing reaction temperature. This suggests that as the reaction temperature increases, the zinc chloride-preasphaltene complex is partly broken, and the preasphaltenes are further hydrocracked to produce oils either directly or through initial conversion to asphaltenes.

Increasing the reaction temperature to 340°C decreases the yield of asphaltenes, while that of preasphaltenes is increased and the yield of oils remains unchanged. However, a deterioration of the oils is observed (to be discussed later). These results point to the need to extract the oils prior to higher temperature (above 325°C) treatment. Aromatic compounds like naphthalene and methyl naphthalene with high solvent action are likely candidates as extraction solvents.

The effect of temperature on the H/C ratio of the melt treated coal and the various extraction products is shown in Figure 14. The H/C ratio of the melt treated coal increases with temperature, the sharpest increase occurring between 275 and 300°C after which a more moderate increase is observed. The oils and asphaltenes show a decrease in H/C ratio with increasing temperature. In the former, a substantial decrease
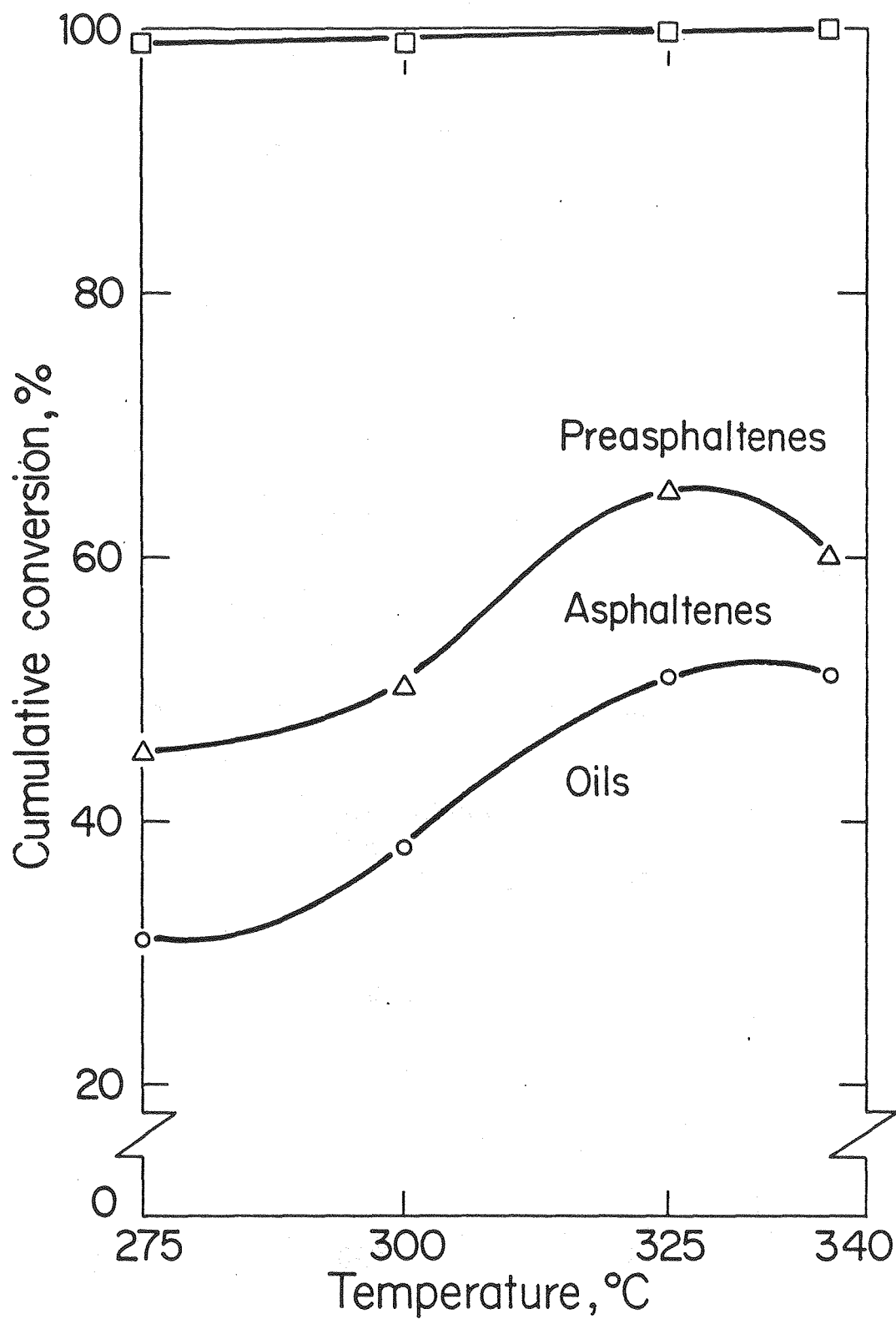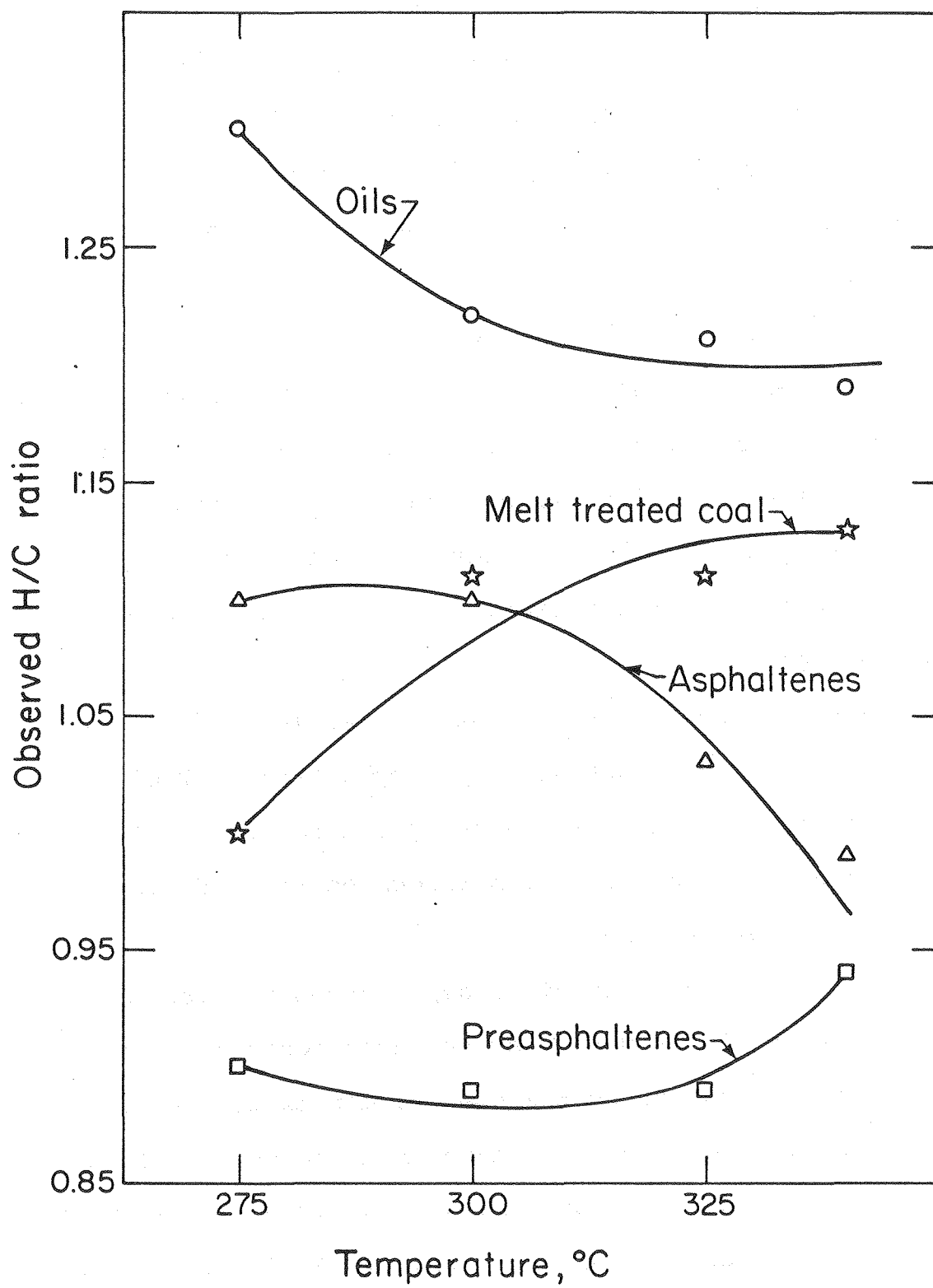
XBL 802-8332B

Figure 12. Effect of reaction temperature on conversion (staged process, 15 min.).
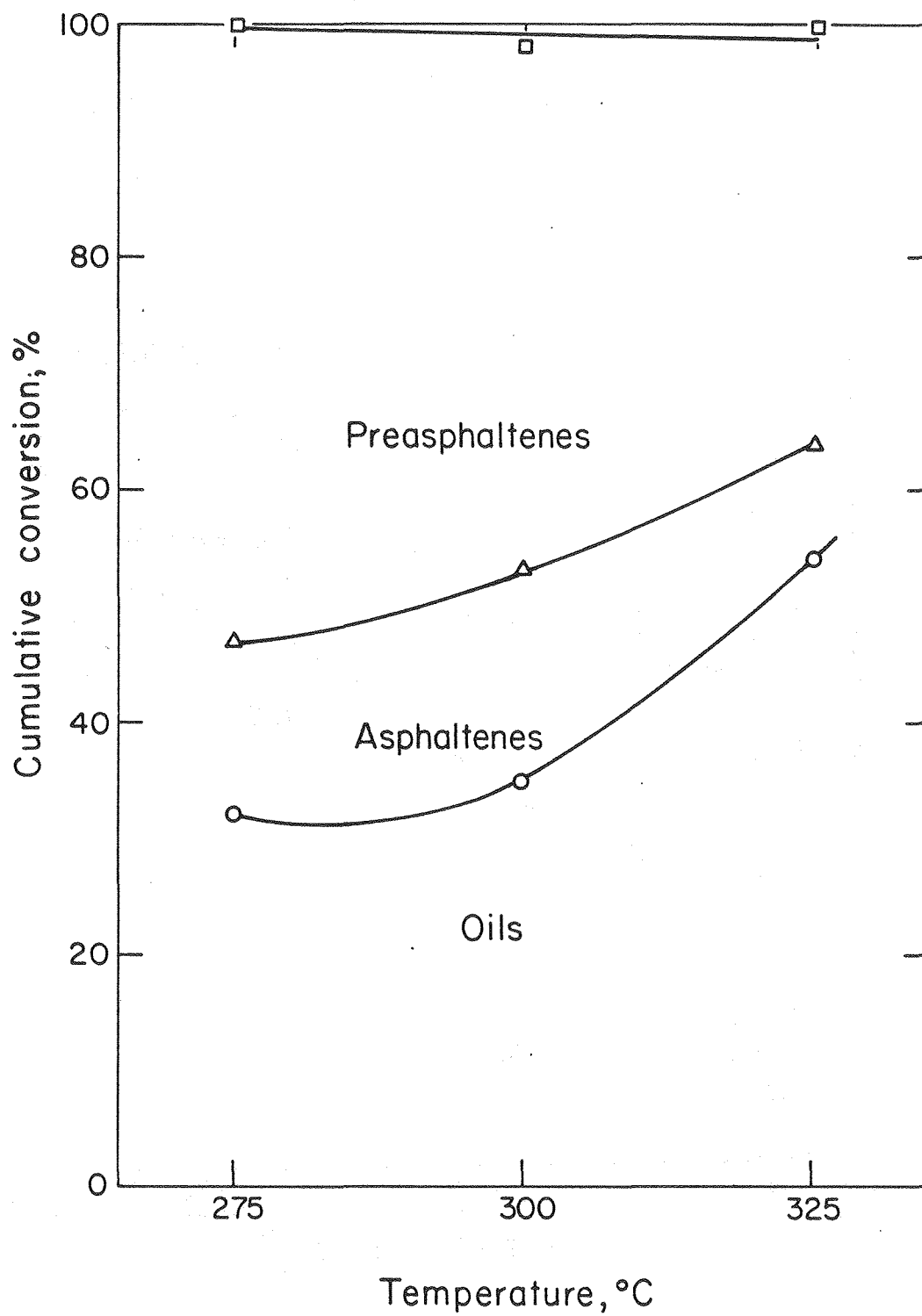
Figure 13. Effect of reaction temperature on conversion (staged process, 30 min.).

XBL 804-661

Figure 14. Effect of temperature on H/C ratio
of product fractions.

is observed between 275 and 300°C whereas no significant difference is observed between 300 and 325°C. In the latter, whereas no difference occurs between 275 and 300°C, a considerable decrease in the H/C ratio is observed above 300°C. Below 325°C, there is no significant change in the H/C ratio of the preasphaltenes, whereas a considerable increase is observed above 325°C.

The likelihood of increased hydrogenation of the preasphaltenes with higher reaction temperatures is very encouraging considering their further conversion to oils. The sharp reduction in the hydrogen content of the asphaltenes at temperatures above 300°C, further stress the importance of solvent extraction after reactions at 325°C prior to higher temperature treatment.

Figure 15 shows that increasing the yield of oils increases the nitrogen content in preasphaltenes. Table 24 shows the segregation of nitrogen in the preasphaltenes. It is interesting to observe that the nitrogen content of the oils decreases with temperature.

The nitrogen content of preasphaltenes appears to constitute a significant parameter in their conversion to oils. This clearly demonstrates the need to denitrogenate the preasphaltenes in order to facilitate their conversion to oils.

The effect of reaction time on conversion is given in Table 22 and Figures 16 and 17. Figure 16, for 275°C, shows that all the product fractions increase with reaction time. The most rapid increase is observed in the first 15 minutes.
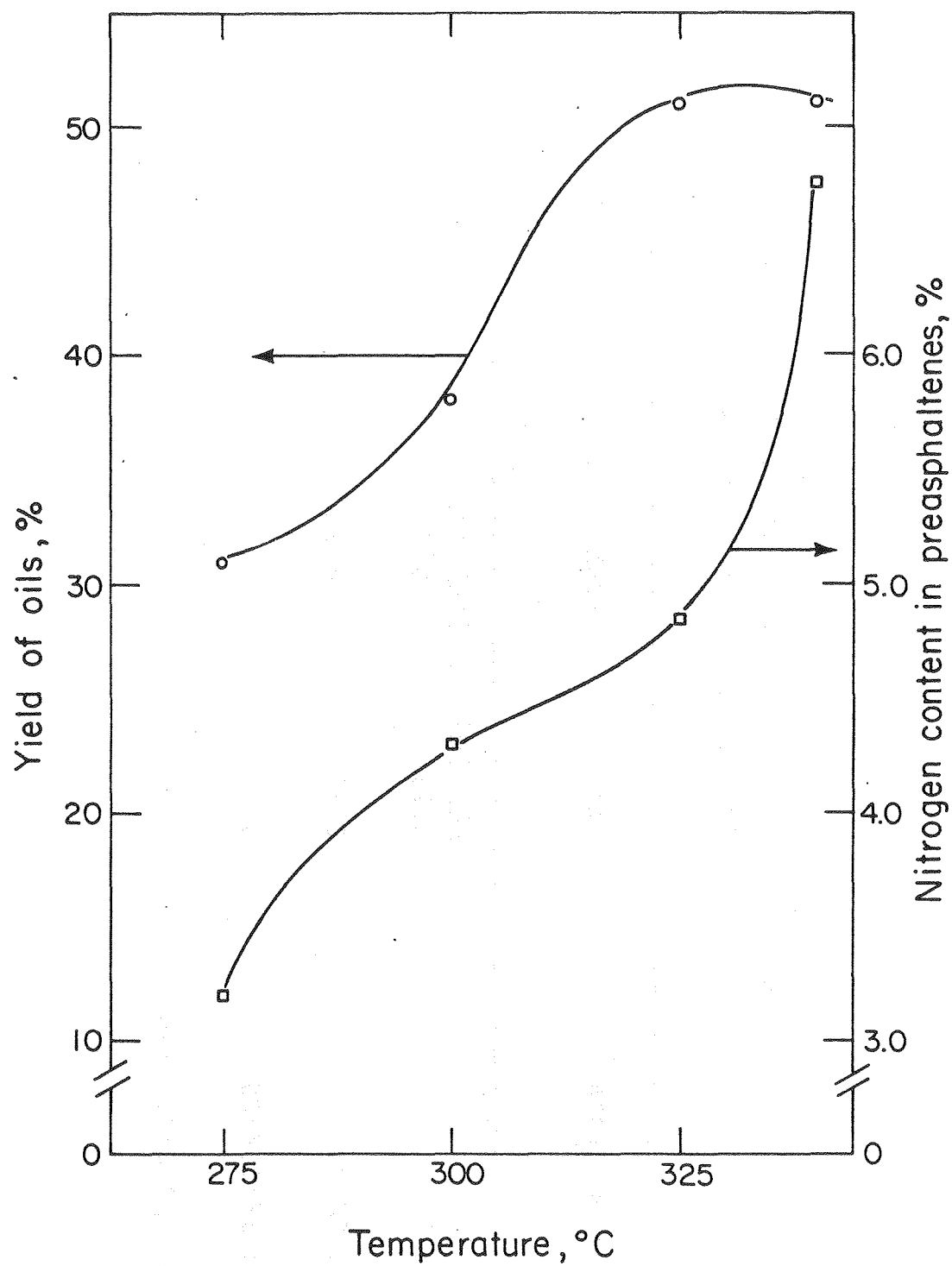
XBL 804-659

Figure 15. Variation of yield of oils with nitrogen
content in preasphaltenes.

Table 24. Nitrogen Content of Oils and Preasphaltenes
(15 min. and 800 psig H_2 per stage)

| Run No.	Temperature ($^{\circ}$C)	Oils	Preasphaltenes
		Nitrogen Content (%)	
70	275	0.29	3.20
68	275/300	0.18	4.31
67	275/300/325	0.23	4.84
74	275/300/325/340	0.13	6.76

At higher reaction time, the oils and asphaltenes level off whereas the yield of preasphaltenes slightly decrease.

At 325°C (Figure 17), following two 15-minute stages of reaction at 275° and 300°C, the yield of oils increases sharply in the first 15 minutes, and only moderately there- after. After the first 15 minutes, the conversion to sol- uble products is complete, so that subsequently the preasphal- tenes diminish by about 5%.

These effects of reaction time and temperature directly influence the H/C ratio of the melt-treated coal as shown in Figure 18. The result at 275°C and 15 minutes contact (roughly 1.0) is an important reference. Adding 15 minutes more at 275°C brings the H/C ratio to around 1.1. Substitut- ing 15 minutes at 300°C, plus heatup to 325°C, also brings the value to 1.1. The treatment at 325°C increases the oils content, and raises the H/C toward 1.2.

Methanol Loading

No significant effect of methanol loading (35 to 65 gm) on product distribution was obtained, as shown in Table 25. Possibly a very low or very high methanol loading (say 15 or 90 gm) would have shown more effect. A low loading would not give enough viscosity reduction and melting point lowering, and a high loading would lead to an excessive vapor pressure. Since an increase in methanol loading to 65 gm did not alter the yield of oils, the 35 gm used in this study remains the recommended loading.
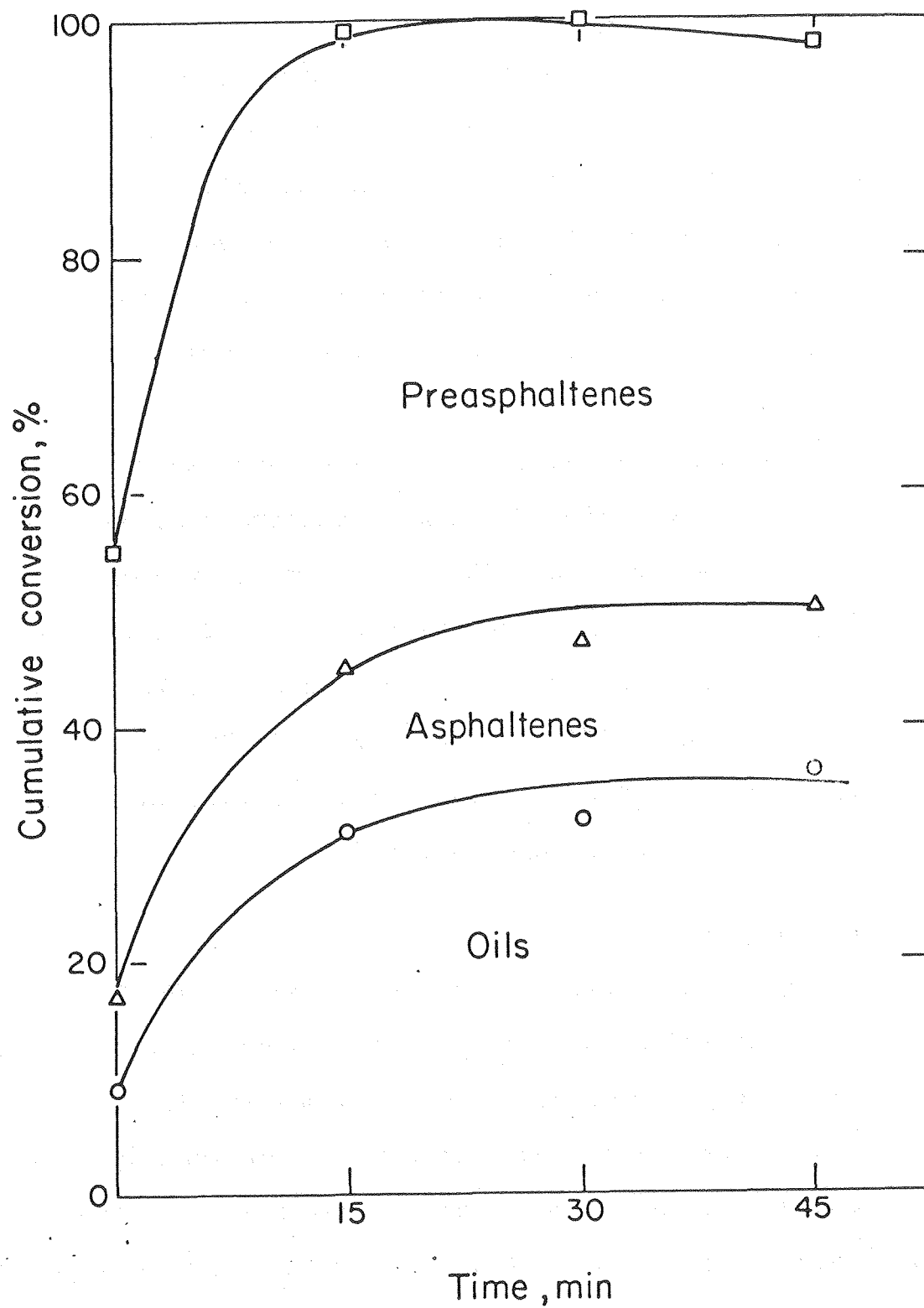
Figure 16. Effect of reaction time on conversion (275°C).

XBL 804-662
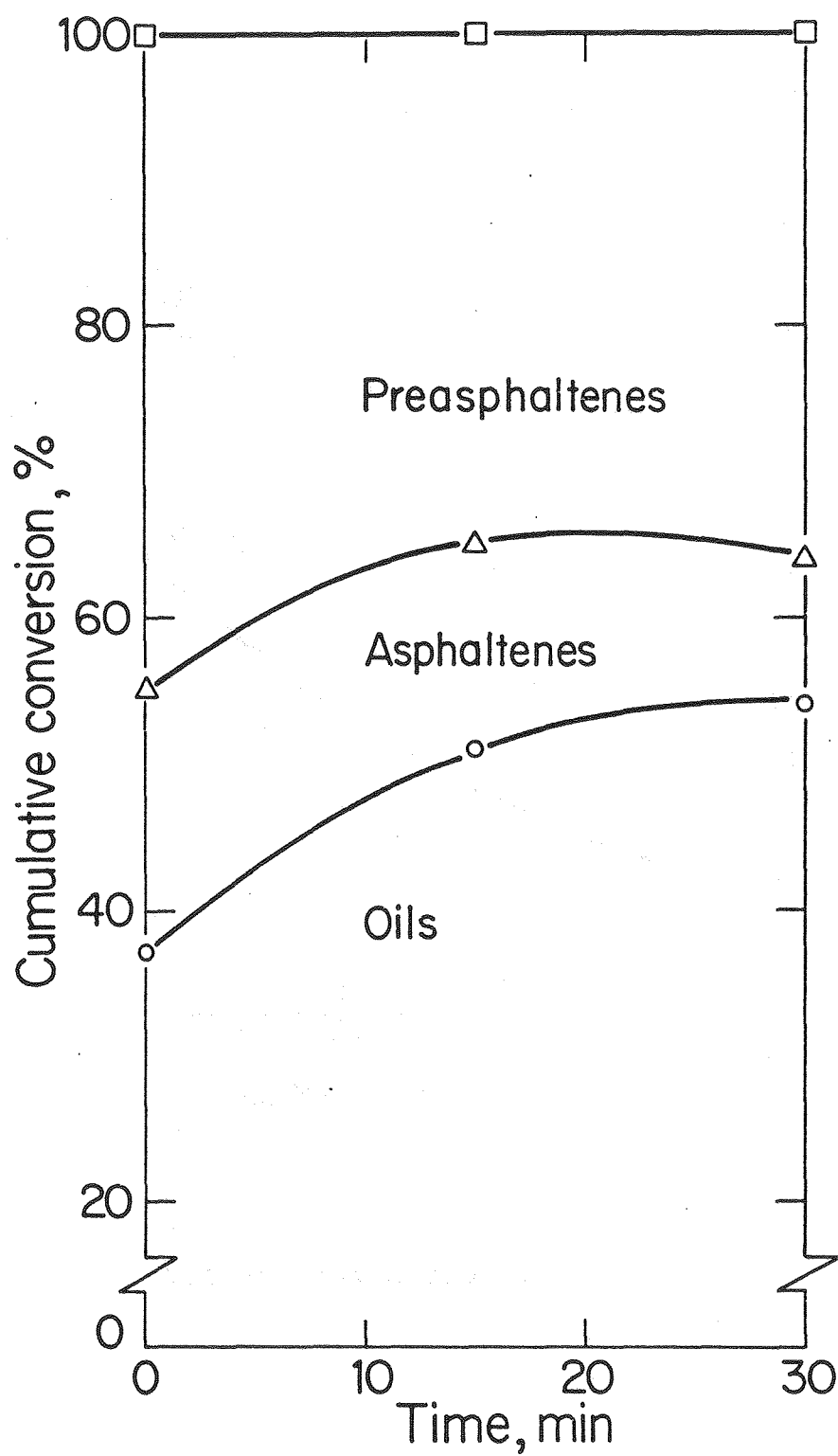
XBL 802-8331B

Figure17 . Effect of reaction time on conversion
(staged process, 325°C).
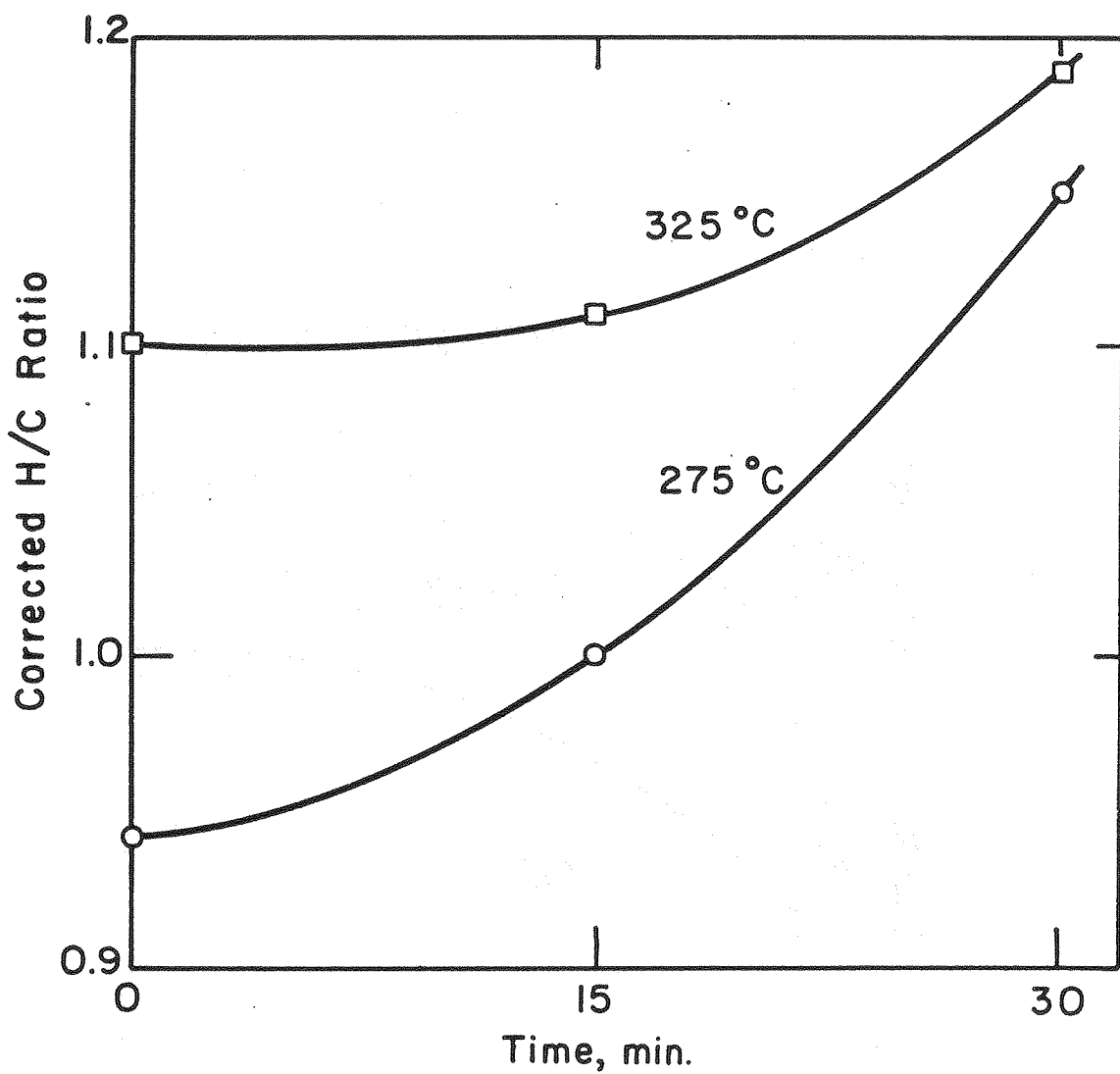
Figure 18.   Effect of reaction time on H/C ratio.

Table 25. Effect of Methanol Loading (During Temperature Staging) on Conversion (250 gm $ZnCl_2$, 50 gm Coal, 8 gm Zn; 250, 275, 300, 325°C, 10 min. per stage, 800 psig H_2 recharged after second stage)

| Run No. | CH_3OH Loading (gm) | Cumulative Pct. daf.-Soluble | | | Observed Atomic H/C Ratio |
		Cyclo-hexane	Toluene	Pyridine	
78	35	40	55	100	1.06
86	50	41	53	100	1.25
81	65	39	52	100	1.20

Coal Particle Size

The effect of particle size on coal conversion was studied, with the results shown in Table 26. It is clear that particle size, within the range studied, has no effect on either coal solubilization or product quality as measured by H/C ratio. Other investigators (C6, P7, J2) have also found that coal hydrogenation rates are largely independent of particle size. This finding indicates that mass transfer and diffusion are negligible under the present operating conditions.

The deep catalyst penetration shown in the SEM studies (to be discussed later) coupled with particle size, within the range -30 +100 mesh, being an insignificant parameter in coal liquefaction (within the conditions studied) indicate that the zinc chloride system could still be effective on very coarse particles. The resulting reduction in coal preparation cost will be beneficial.

Additional Investigations

Water-Gas Shift Reaction

Producing liquid fuels with H/C ratios in the range of 1.3 to 1.5 from a sub-bituminous coal with an initial H/C ratio of about 1.0 and an O/C ratio of about 0.2 will involve considerable consumption of hydrogen. Pure hydrogen is relatively expensive and its cost contributes a significant component in the overall cost of the coal liquefaction process. Hence any effort aimed at reducing hydrogen

Table 26. Effect of Particle Size on Conversion
(250 gm $ZnCl_2$, 50 gm Coal, 25 gm CH_3OH;
$275^O C$, 500 psig H_2, 30 min.)

Run No.	Particle Size (mesh)	Cumulative Pct. daf.-Soluble			Corr. Sol.	R (gm reg. CH_3OH/ gm coal org.)	Corr. Atomic H/C ratio
		Cyclo-hexane	Toluene	Pyridine			
5	−30+60	17	31	89	88	0.11	0.95
64	−60+100	15	28	84	82	0.09	0.96

consumption, will contribute favorably to the economic competitiveness of coal liquefaction process.

The possibility of water-gas shift reaction occuring under our reaction conditions was investigated and the result is shown in Table 27. In Run 58, a mixture of carbon monoxide and hydrogen, which is less expensive than pure hydrogen, was charged into the reactor. During the reaction, water is generated through deoxygenation reactions of coal. Production of carbon dioxide as a by-product is highly desirable since it is more economical to lose oxygen as carbon dioxide instead of water.

The higher methanol incorporation shown in Run 58 is indicative that more of the total reactive fragment-stabilization occurs through alkylation, as is generally the case at low hydrogen pressure. This, in addition to the lower H/C ratio of the melt-treated coal, demonstrate the ineffectiveness of the added carbon monoxide.

Alternate Solvent

After an extensive solvent screening test conducted by Shinn (S5), aimed toward high product solubility and low incorporation, methanol was chosen as the preferred solvent for zinc chloride. To examine the possible benefit of using a solvent containing a nitrogen atom, acetonitrile was selected for trial. Table 28 shows that acetonitrile reduces the catalytic activity of zinc chloride. It is likely that acetonitrile co-ordinates sites with the catalyst, and the results suggest that such a complex is not catalytically

Table 27. Water-Gas Shift Reaction

(250 gm $ZnCl_2$, 50 gm Coal, 25 gm

CH_3OH; 275°C, 30 min.)

Run No.	Additives	H_2 Pressure (psig)	CO Pressure (psig)	Cumulative Pct. daf.-Soluble			R (gm ret. CH_3OH/ gm coal org.)	Corr. Atomic H/C Ratio
				Cyclo-hexane	Toluene	Pyridine		
5	none	500	–	17	31	89	0.11	0.95
58	$FeCl_3$* $FeCl_2$*	300	300	15	27	77	0.22	0.85

* Amounts used are shown in Table 7.

Table 28. Effect of Alternate Solvent on Conversion
(250 gm $ZnCl_2$, 50 gm Coal; 275°C,
500 psig H_2, 30 min.)

Run No.	Solvent (gm)	Cumulative Pct. daf.-Soluble			R (gm ret. sol./ gm coal org.)	Corr. Atomic H/C ratio
		Cyclo-hexane	Toluene	Pyridine		
5	CH_3OH (25)	17	31	89	0.11	0.95
19	CH_3CN (12.5) CH_3OH (12.5)	*	13	56	0.07	0.90

* Not determined.

active. Acetonitrile is known to coordinate strongly and
thereby result in a very slow solvent exchange (J3, G4).

PRESSURE-TIME DATA

In order to monitor gas consumption and production during
reaction, the variation of total pressure with reaction time
was recorded all through each run. A typical variation of
total pressure with reaction time, as observed in a multi-
stage run, is given in Figure 19. The difference between
maximum pressure (P_{max}) and hydrogen pressure (P_{H_2}) is con-
sidered a measure of gas production; and the difference be-
tween (P_{max}) and final pressure (P_{final}) is used as a mea-
sure of gas consumption at constant methanol loading.

As Figure 19 shows, after initial pressurization with
hydrogen during heatup, the pressure increases to a maximum
which occurs at the reaction temperature. For the 275°C
stage, the pressure decreases sharply in the first two min-
utes of reaction, and more slowly later. At the end of the
reaction, the reactor is depressurized, and repressurized
at 200°C. In the 300°C stage, the pressure rises during
heatup, sharply decreases in the first five minutes, then
rises to a second maximum, followed by a slow decrease.
During the 325°C stage, the initial decrease is similar to
that at 300°C, after which the pressure buildup continues
until the end of the treatment (perhaps suggesting that some
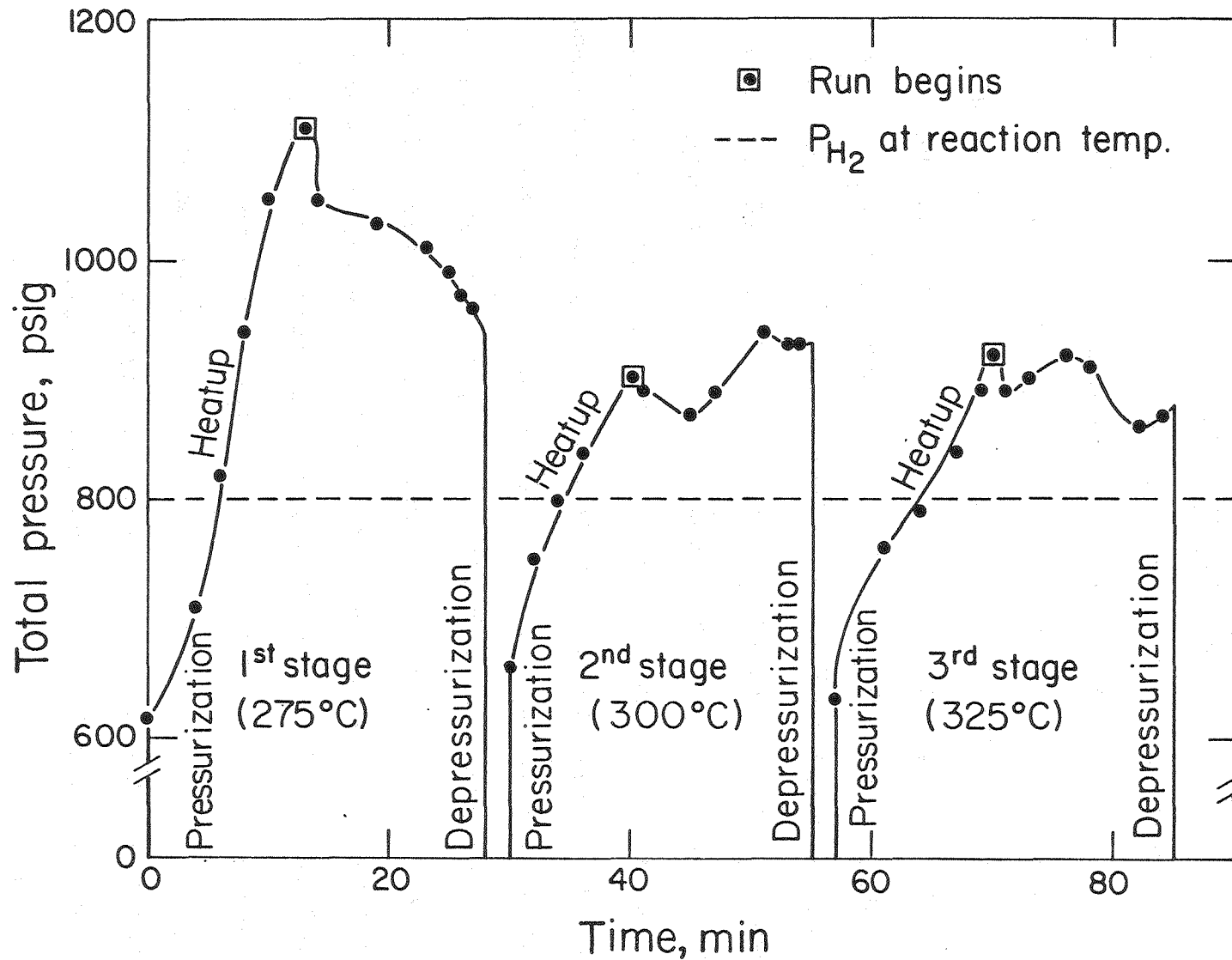decomposition or dehydration occurs).

Figure 19. Typical pressure-time relationship in a multi-stage autoclave reaction (Data from run 67).

XBL 804-664

The peak pressure observed in the 275°C stage is higher than those in the later higher-temperature stages, due probably to the loss of both water and methanol during the first depressurization.

The variation of pressure with time was studied under various reaction conditions. Addition of metallic zinc (Table 29) leads to a greater pressure drop interpreted as an increase in hydrogen consumption which correlates well with the higher H/C ratio of the melt-treated coal (Figure 9). Many inorganic salts, as additives, considerably increased the total pressure and final net gas production. Table 30 lists these additives in the order of increasing gas release; zinc oxide (with ammonium chloride) had the least effect, and zinc oidide and zinc cyanide the greatest. The gas consumed, measured by $(P_{max} - P_{final})$, is closely related to the calculated H/C ratio of the reaction product (Table 30).

Increasing the reaction temperature from 275°C to 300°C at two different methanol loadings and hydrogen pressures (Table 31) considerably increases the maximum pressure. Higher vapor pressure and increased conversion at higher temperature jointly explain the results. Measurements of the separate effects of hydrogen pressure and methanol loading were also made. Table 32 shows that higher hydrogen pressure gave a smaller buildup and a larger gas consumption, in good agreement with a higher H/C ratio. Higher methanol loading (Table 33) increases the pressure rise, and diminishes the gas consumption. The effect of other reaction

Table 29. Effect of Metallic Zinc on Pressure Variation with Time
(250 gm $ZnCl_2$, 50 gm Coal, 35 gm CH_3OH; $275^{\circ}C$, 800 psig H_2,
30 min.)

Run No.	Zinc Loading (gm)	P_{max} (psig)	P_{final} (psig)	$P_{max}-P_{H_2}$ (psi)	$P_{max}-P_{final}$ (psi)
43	none	1050	740	250	310
44	4	1030	695	230	335
51	8	1080	740	280	340

Table 30. Effect of Inorganic Additives on Pressure Variation with Time
(250 gm $ZnCl_2$, 50 gm Coal, 25 gm CH_3OH; 275°C, 500 psig H_2,
30 min.)

Run No.	Additives*	P_{max} (psig)	P_{final} (psig)	$P_{max}-P_{H_2}$ (psi)	$P_{max}-P_{final}$ (psi)
5	none	610	510	110	100
57	NH_4Cl ZnO	700	500	200	200
52	AgCl	700	540	200	160
53	$CuCl_2$	710	570	210	140
65	$GaCl_3$	710	610	210	100
66	ZnI_2	720	630	220	90
47	$Zn(CN)_2$	760	630	260	130

* Amounts are given in Table 7.

Table 31. Effect of Temperature (275 vs 300°C) on Pressure Variation with Time
(250 gm $ZnCl_2$, 50 gm Coal; 30 min.)

Run No.	Temp. (°C)	CH_3OH Loading (gm)	P_{H_2} (psig)	P_{max} (psig)	P_{final} (psig)	$P_{max}-P_{H_2}$ (psi)	$P_{max}-P_{final}$ (psi)
5	275	25	500	610	510	110	100
54	300	25	500	780	620	280	160
51*	275	35	800	1080	740	280	340
77*	300	35	800	1170	890	370	280

* 8 gm Zn added

118

Table 32. Effect of Hydrogen Pressure on Pressure Variation with Time
(250 gm $ZnCl_2$, 50 gm Coal, 35 gm CH_3OH; 275°C, 30 min.)

Run No.	P_{H_2} (psig)	P_{max} (psig)	P_{final} (psig)	$P_{max}-P_{H_2}$ (psi)	$P_{max}-P_{final}$ (psi)	Corr. Atomic H/C Ratio
59	500	810	570	310	240	0.96
43	800	1050	740	250	310	1.01

Table 33. Effect of Methanol Loading on Pressure Variation with Time
(250 gm $ZnCl_2$, 50 gm Coal; $275^{O}C$, 500 psig H_2, 30 min.)

Run No.	CH_3OH Loading (gm)	P_{max} (psig)	P_{final} (psig)	$P_{max}-P_{H_2}$ (psi)	$P_{max}-P_{final}$ (psi)	Corr. Atomic H/C Ratio
5	25	610	510	110	100	0.95
59	35	810	570	310	240	0.96

variables on the pressure variation with time is summarized in Tables 34 to 37 and presented in Appendix A.

In general, the direct relationship between gas consumption and the H/C ratio of the melt-treated coal clearly demonstrates the participation of molecular hydrogen in stabilizing reactive fragments produced during the reaction.

ANALYTICAL RESULTS

Scanning Electron Microscopy

The treatment conditions and extraction yields of samples examined by scanning electron microscope are given in Table 38. Untreated coal (Figure 20a) exhibits a compact structure with a coherent textured surface. Its structure is that of a series of layers cemented together. When treated with phosphoric acid (Figure 20b), the coal shows no severe structural change, even though cracks develop and surface roughness is reduced. However, when the sample from phosphoric acid treatment is subjected to zinc chloride-methanol treatment, extensive structural change takes place (Figure 20c), consonant with the high conversion obtained. There is an absence of solubilized materials deposited on the surface which could be due to a reduction in the yield of oils by nearly a half when phosphoric acid treatment precedes treatment with $ZnCl_2$. On the other hand, coal reacted with $ZnCl_2$ under the same conditions without previous phosphoric acid treatment (Figure 20d) shows a relatively smooth, less pitted surface, seemingly coarser grained than Figure 20c.

Table 38. Treatment Conditions and Extraction Yields for Coal Samples Examined by Scanning Electron Microscope

(250 gm $ZnCl_2$, 50 gm Coal, 35 gm CH_3OH; 800 psig H_2 per stage)

Run No.	Substrate	Temp. (^{O}C)	Time (min)	Additives (gm)	Total Solubility (pct. daf.)
0[a]	Coal	25	0	none	12
49[+]	Coal	275	30	90% H_3PO_4 (150)	24
55	PTC 49[b]	275	30	none	98
43	Coal	275	30	none	100
51	Coal	275	30	Zn (8)	100
73	Coal	275/300/325*	15/15/30	Zn (8)	100
76	Coal	275/300/325*	15/15/0[c]	Zn (8)	100

[a] Untreated Coal.

[b] 34 gm phosphoric-acid-treated coal (Dried product from Run 49).

[c] Heatup only to 325°C (less than 3 min. above 300°C).

* Three stages.

[+] Reaction conditions given in Table 7.

122
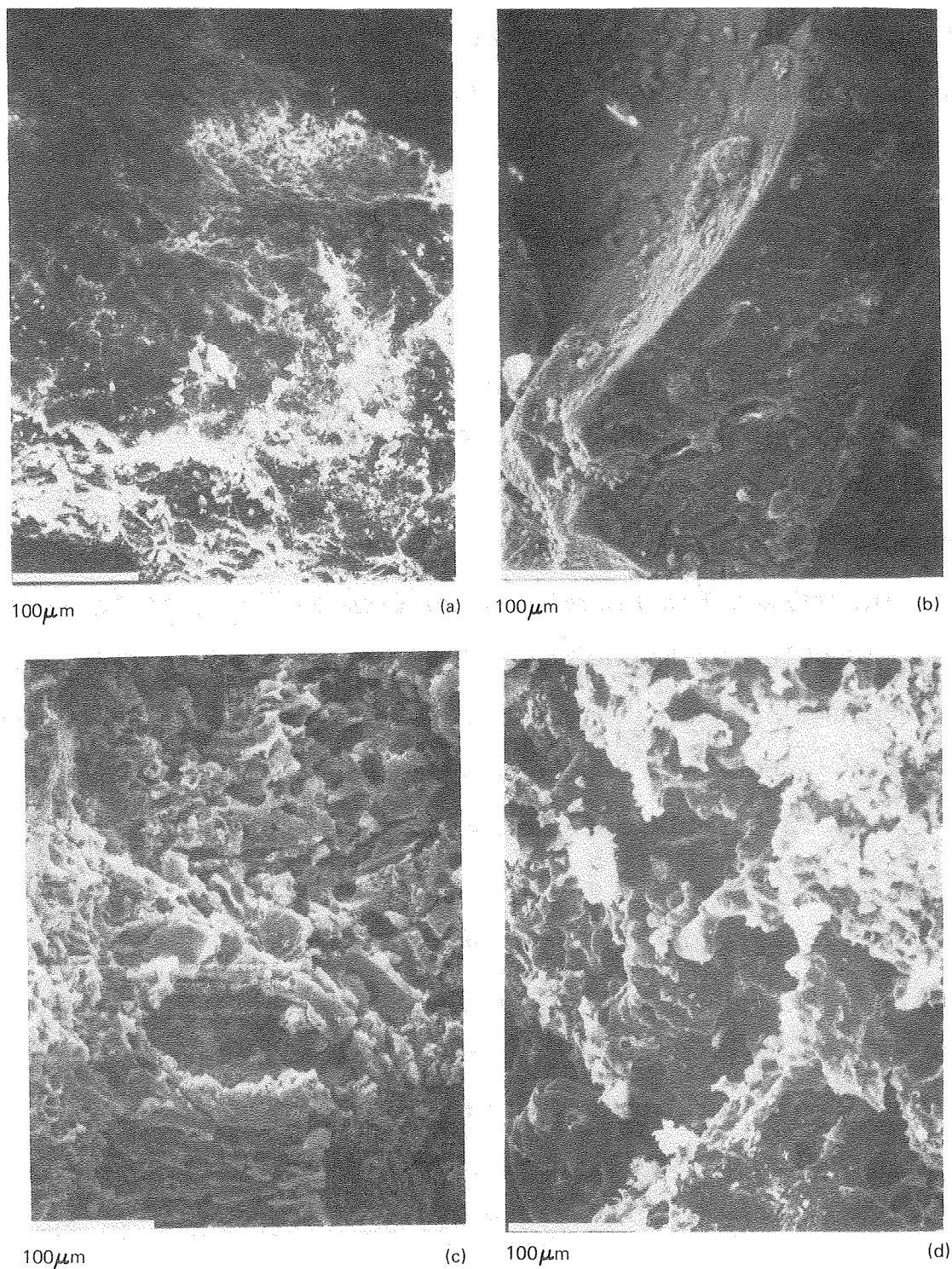
Figure 20. (a) Untreated coal

(b) Phosphoric acid treated coal (275°C, 30 min)

(c) Coal (b) after $ZnCl_2$-CH_3OH treatment (275°C, 30 min)

(d) Coal (a) after $ZnCl_2$-CH_3OH treatment (275°C, 30 min)

XBB 804-5025

The residue from the untreated coal after pyridine extraction is shown in Figure 21a, with distinct shallow cracks but no massive change. The residue from phosphoric acid treatment after pyridine extraction (Figure 21b), shows a considerable structural change, consistent with the difference in solubilization between phosphoric acid treatment (24%) and untreated coal (12%). After zinc chloride-methanol treatment of phosphoric-acid-treated coal (Figure 21c), the residue shows large aggregates of materials whereas without prior treatment with phosphoric acid, the residue (Figure 21d) is a conglomerate of fine grains.

Increasing the reaction time from $275^{O}C$ to $325^{O}C$ leads to destruction of the surface features of the treated coal due presumably to melting and resolidification of the reaction products. There was a significant increase from 32% to 54% in the yield of oils accompanied by a corresponding decrease from 53% to 36% in the yield of preasphaltenes. Figure 22a, the same as Figure 20d, shows some deposition of wax-like materials on the surface with the dramatically eroded structure of native coal beneath. After treatment at $325^{O}C$, Figure 22b shows a structureless, nearly homogeneous material.

The micrographs of the residues after pyridine extraction for coal treated at $275^{O}C$ and $325^{O}C$ are shown in Figure 23a and Figure 23b respectively. Figure 23a shows a fine grain structure of agglomerated materials that are highly condensed and compact. At the higher temperature, a uniform, relatively smooth structure consisting of extremely fine
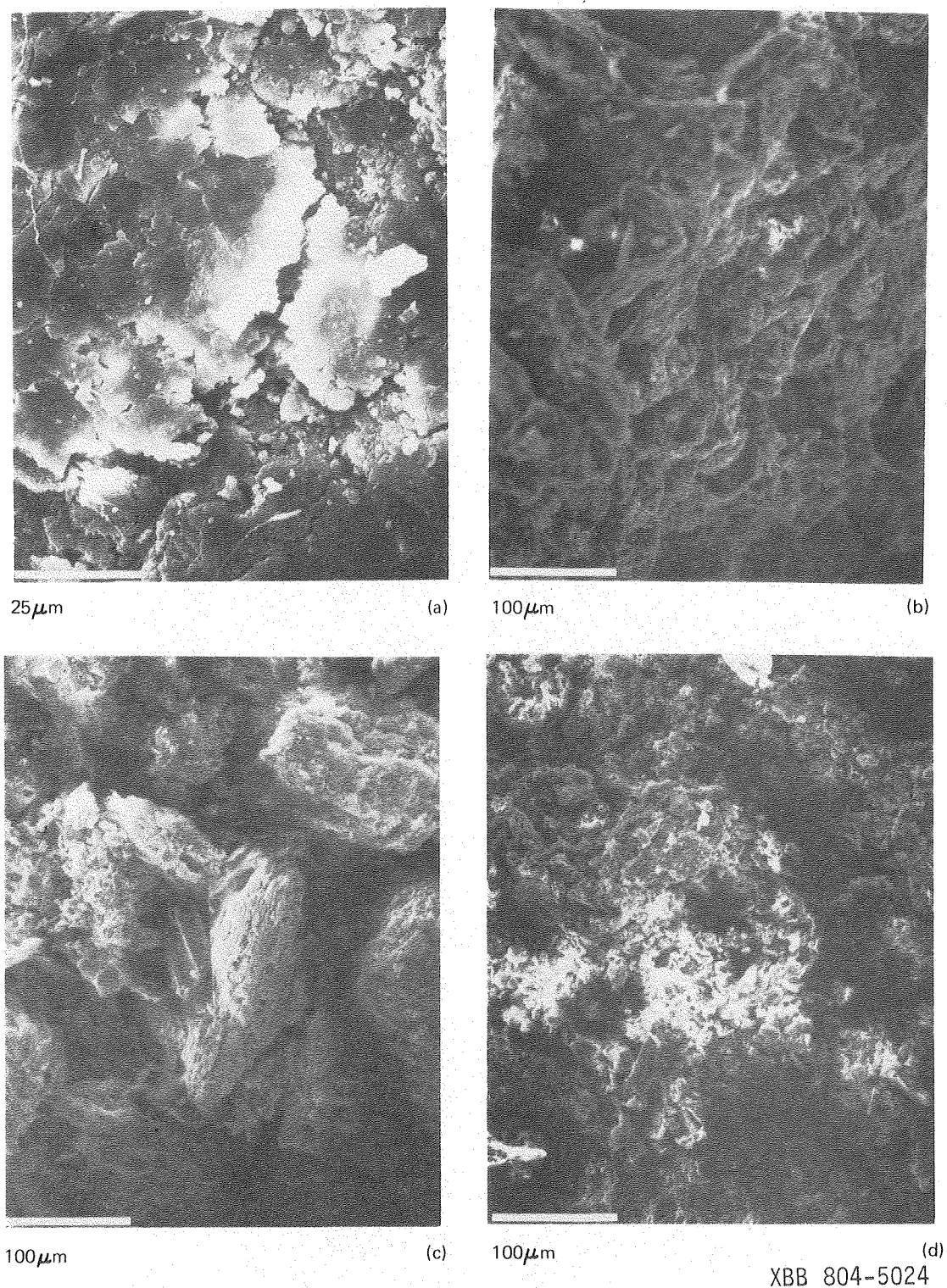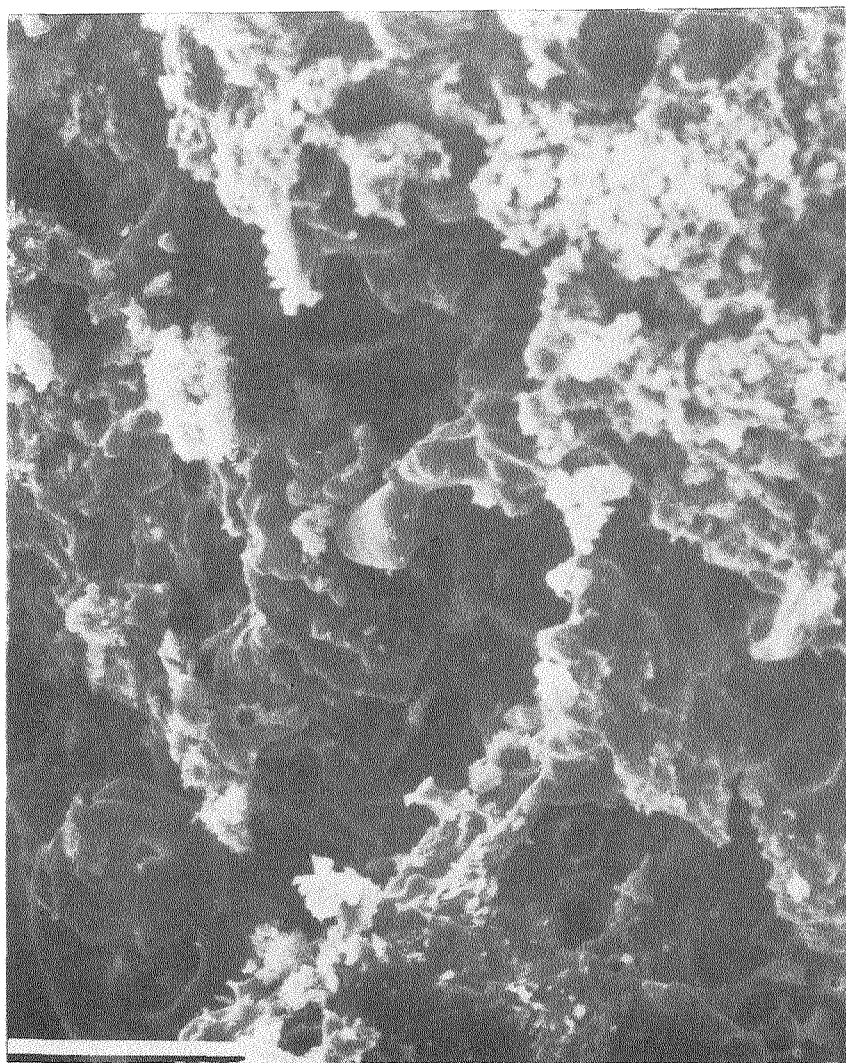
25 μm   (a)   100 μm   (b)

100 μm   (c)   100 μm   (d)

XBB 804-5024

Figure 21.   (a) Untreated coal after pyridine extraction

      (b) H_3PO_4-treated coal after pyridine extraction

      (c) Residue of (b) after $ZnCl_2$-CH_3OH treatment

      (d) Residue of (a) after $ZnCl_2$-CH_3OH treatment

100μm.   (a)   100μm   (b)

XBB 804-5015

Figure 22. $ZnCl_2$-CH_3OH treated coal (30 min)   (a) 275°C   (b) 325°C

100μm   (a)   100μm   (b)
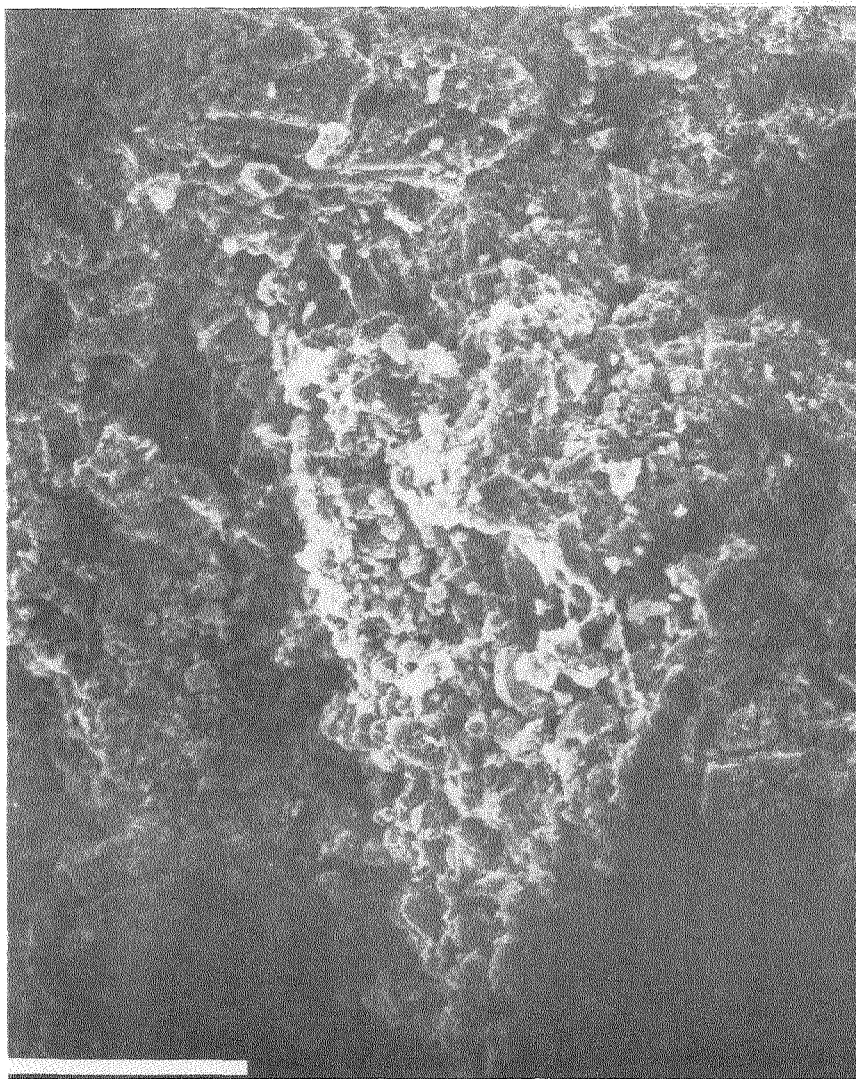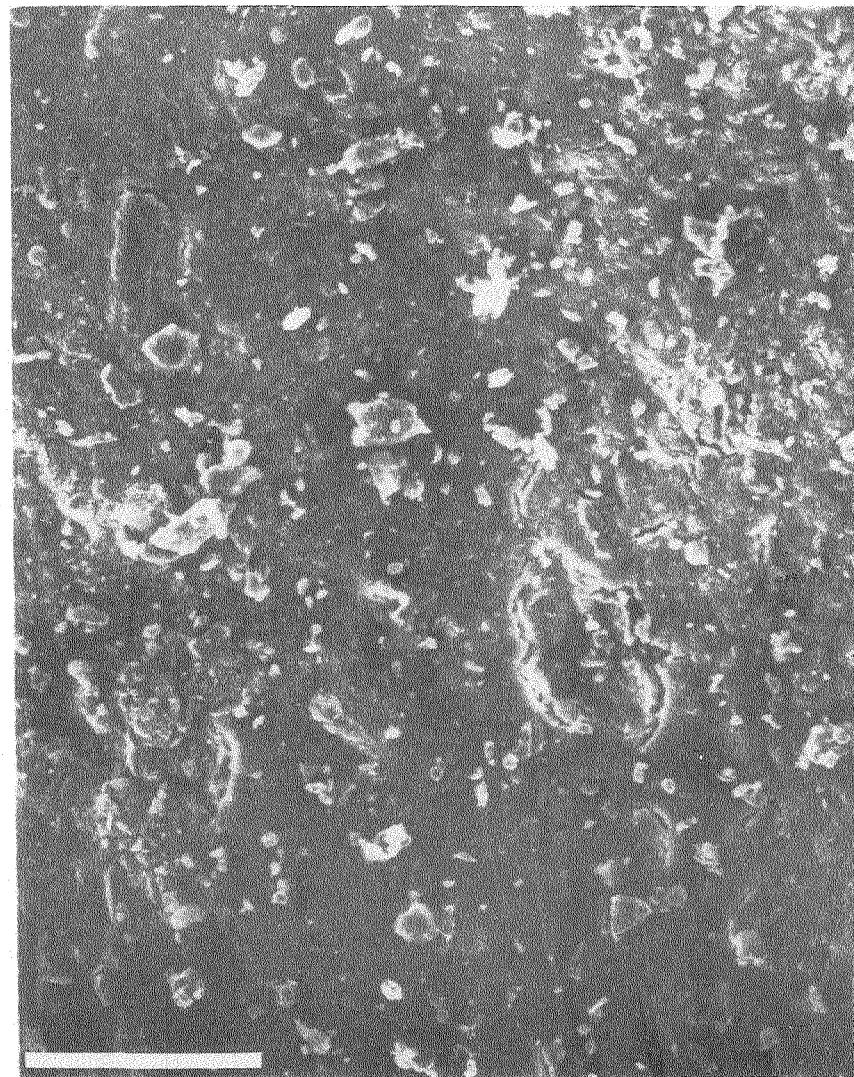
XBB 804-5016

Figure 23. ZnCl$_2$-CH$_3$OH treated coal (30 min) after pyridine extraction

(a) 275°C   (b)325°C

grain structure of agglomerated materials that are highly condensed and compact. At the higher temperature, a uniform, relatively smooth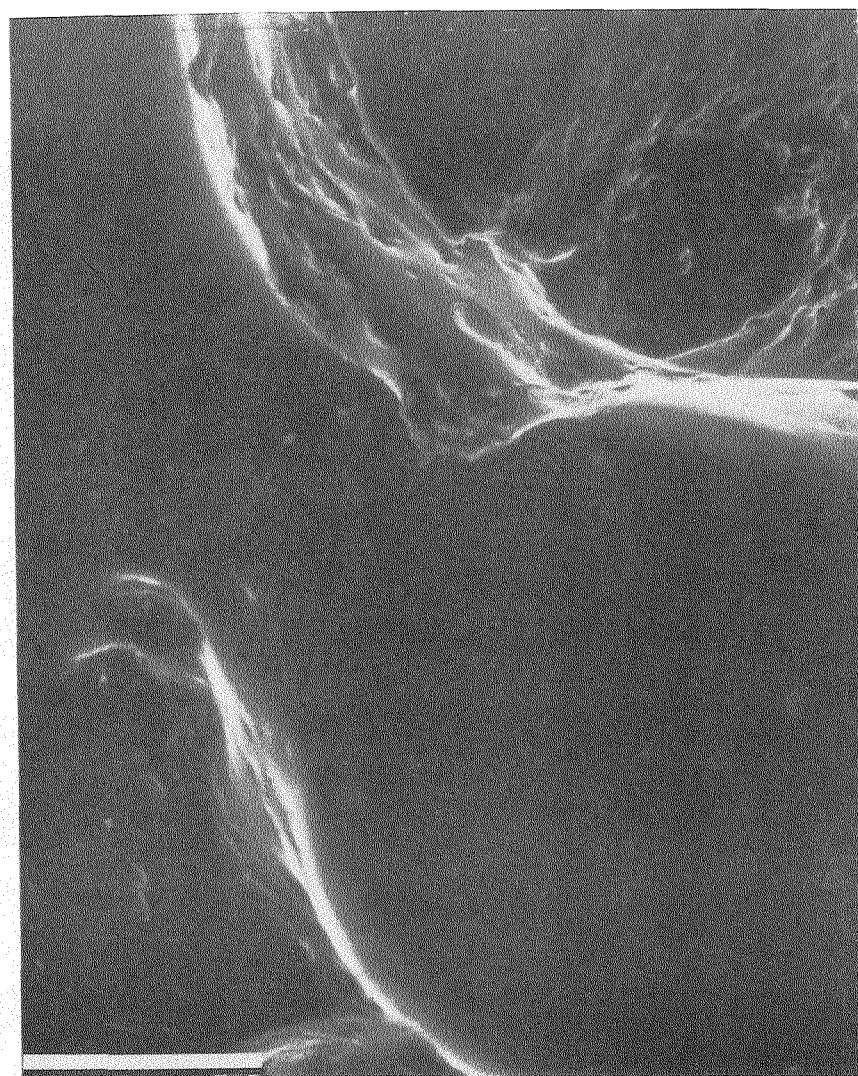 structure consisting of extremely fine grains is observed. It is most likely that at 325°C, the removal of coal is so complete that the original structure of the mineral matter collapses. The reduction in grain size of the mineral matter will increase its dispersion in the coal matrix and may enhance its subsequent catalytic activity. Ash disposal will also be aided.

Heatup of coal to 325°C, which takes less than 3 minutes above 300°C, shows a different product distribution and a structure less changed (Figure 24a). Figure 24a, for this coal reacted at 275 and 300°C, shows deposition of solubilized and later solidified materials on the surface. Figure 24b, the same as Figure 22b, has already been discussed.

Figure 25a shows the pyridine-extracted residue from Figure 24a, consisting of individual fine grains very similar to those obtained after reaction at 275°C. Figure 25b is the extraction residue after 30 minutes' reaction at 325°C (same as Figure 23b), with a homogeneous smooth structure.

Summarizing, reaction temperature, time, and conditions have very dramatic effects on the structure of the evolving solid material. It is significant that the changes obtained at 325°C appear exhaustive and complete, and that changes as extensive cannot be obtained with zinc chloride at any lower temperature.

100μm   (a)

100μm   (b)
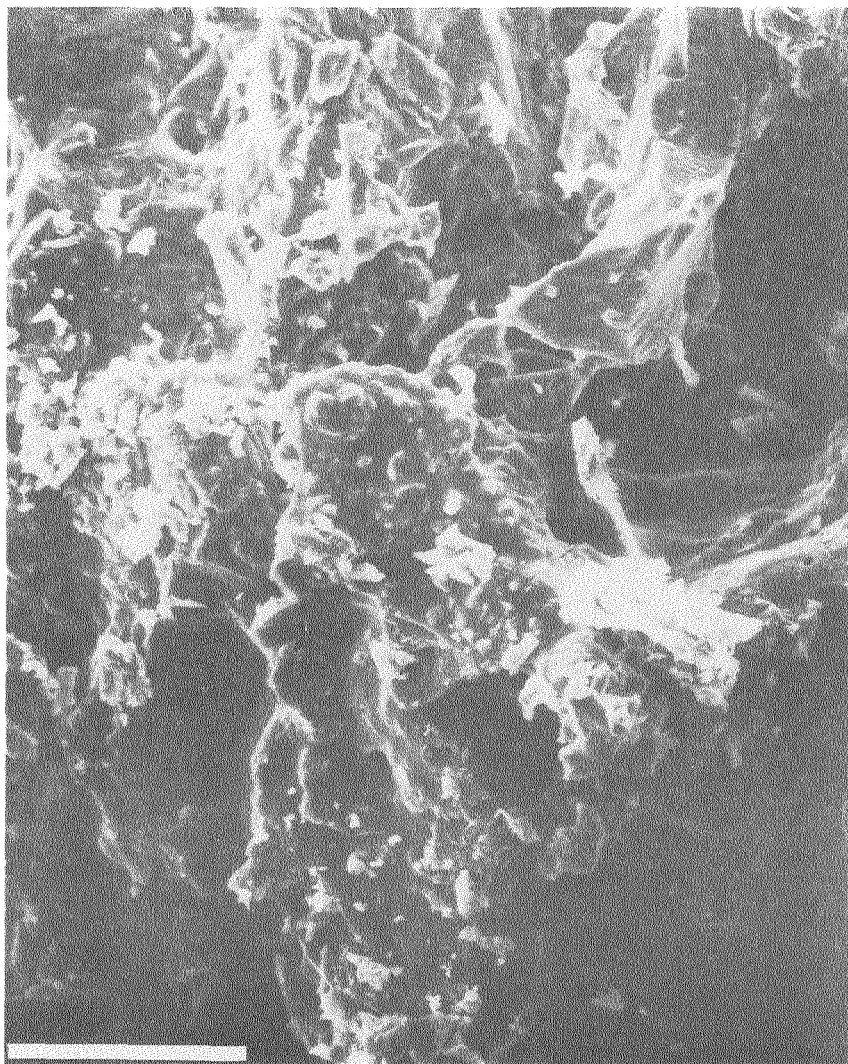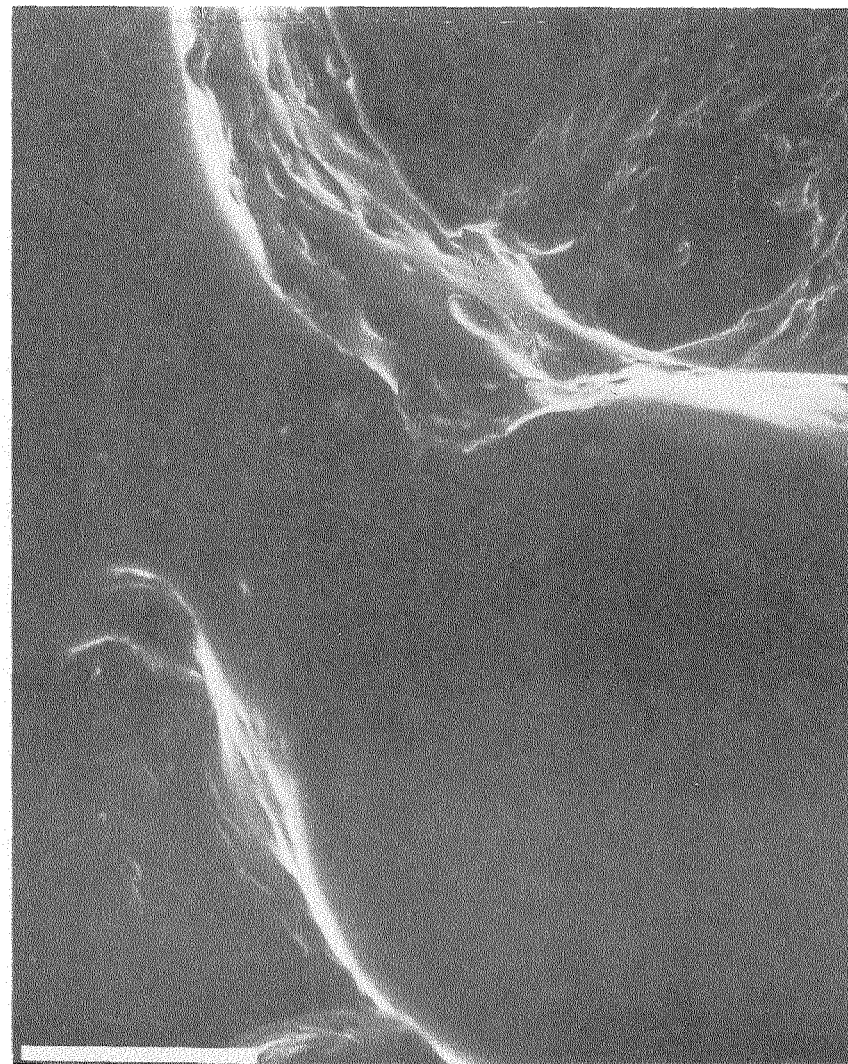
XBB 804-5017

Figure 24. $ZnCl_2$-CH_3OH treated coal (325°C)   (a) Heatup only   (b) 30 min reaction time

129

100μm (a)   100μm (b)
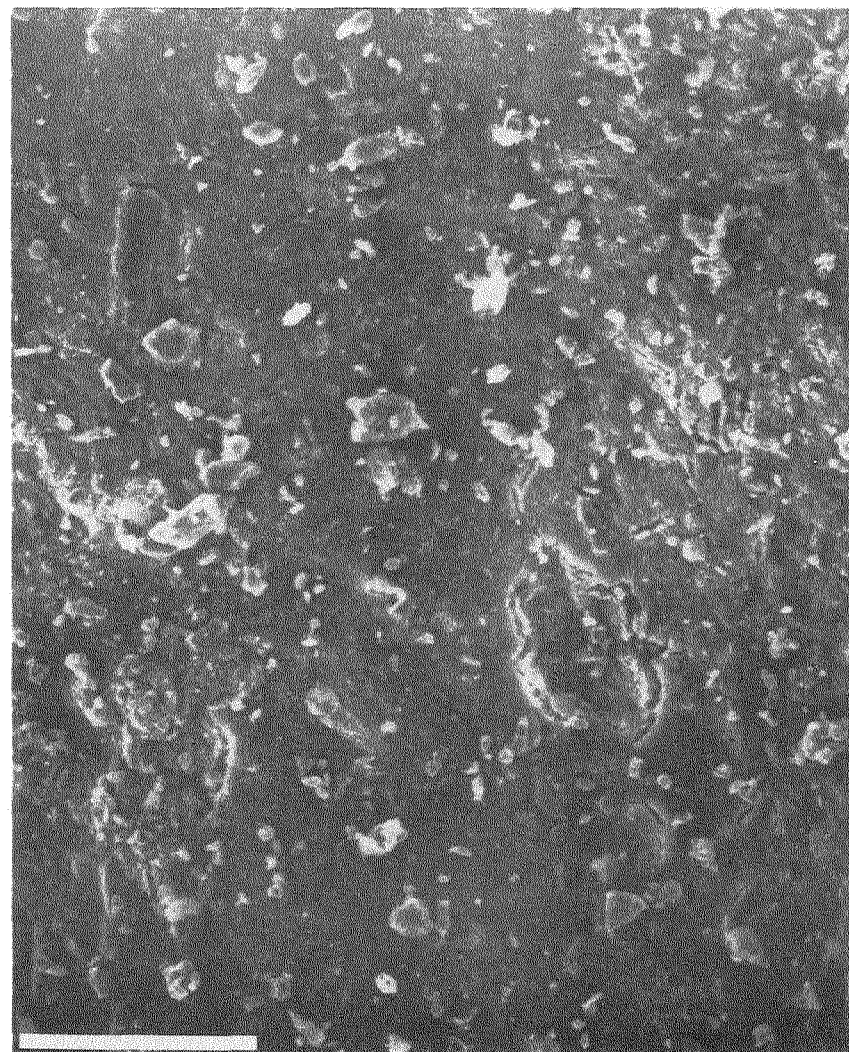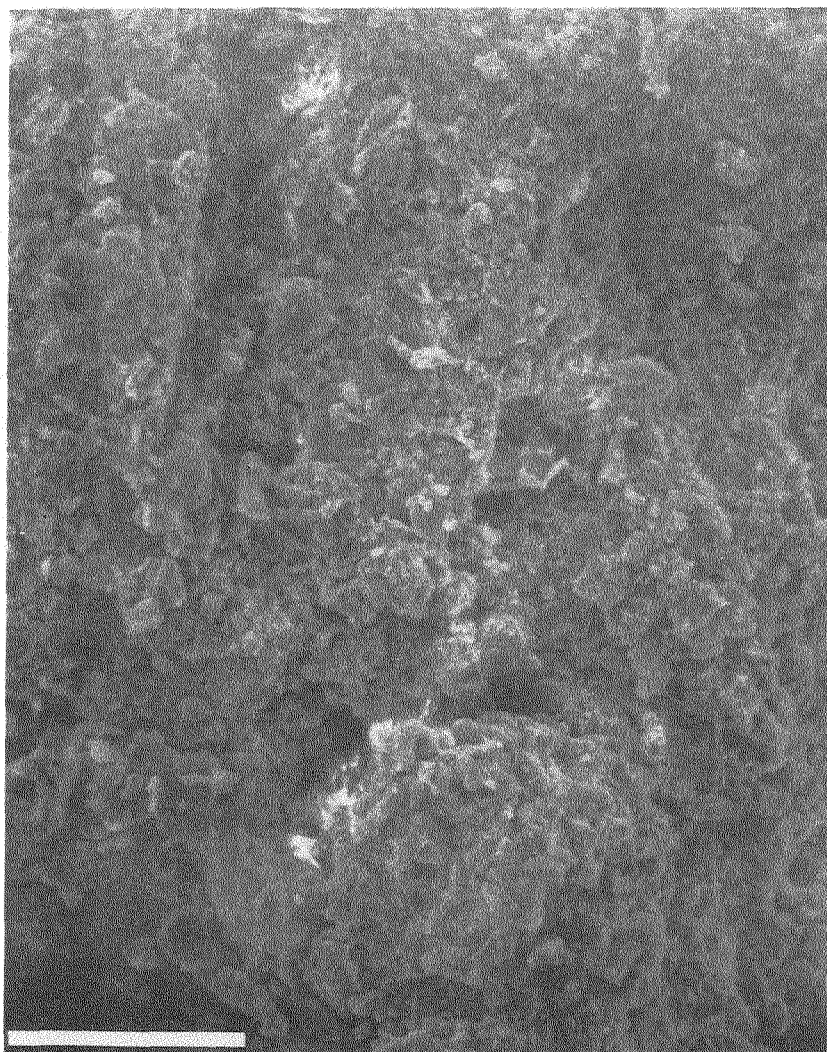
Figure 25. $ZnCl_2$-CH_3OH treated coal (325°C) after pyridine extraction
(a) Heatup only (b) 30 min reaction time

Gel-Permeation Chromatography

The effects of reaction conditions on the molecular-weight distribution of product fractions from coal were examined by gel-permeation chromatography. The runs in which these products were prepared are shown in Table 39. Previous work in this Laboratory (S5) indicated that preasphaltenes are most stable, and that molecular-weight reduction within that fraction is a prelude to asphaltene and oil formation. The effect of temperature on the molecular-weight distribution of preasphaltenes was therefore investigated.

Figure 26 shows that treatment at 325°C resulted in a molecular-weight reduction culminating in dominance by low-molecular-weight components. With the same attenuation, the area under the 325°C GPC tracing is slightly over 50% of that at 275°C. This indicates a reduction in the fused-ring aromatic structures, since at 313 nm, these are the major absorbing species. This reduction in molecular size of pre-asphaltenes after treatment at 325°C (taken together with a reduction in the amount of preasphaltenes) suggests strongly that at a higher temperature, further molecular-weight reduction of preasphaltenes may be achieved (this observation is strongly supported by a low melting point of the 325°C pre-asphaltenes as shown in Table 41).

Asphaltenes and oils (Figure 27) derived from the 325°C run show a similar shift towards lower-molecular-weight components. Despite the prospects of further reaction at higher temperature, no significant difference in the

Table 39. Treatment Conditions and Extraction Yields for Samples Examined by Gel-Permeation Chromatography

(250 gm $ZnCl_2$, 50 gm Coal, 35 gm CH_3OH; 800 psig H_2 per stage)

Run No.	Temp. (°C)	Time (min)	Additive (gm)	Cumulative Pct. daf.-Soluble		
				Cyclo-hexane	Toluene	Pyridine
43	275	30	none	22	37	100
51	275	30	Zn (8)	32	47	100
76	275/300/325*	15/15/0[+]	Zn (8)	37	55	100
73	275/300/325*	15/15/30	Zn (8)	54	64	100

* Three stages.

[+] Heatup to 325°C (less than 3 minutes residence time above 300°C).
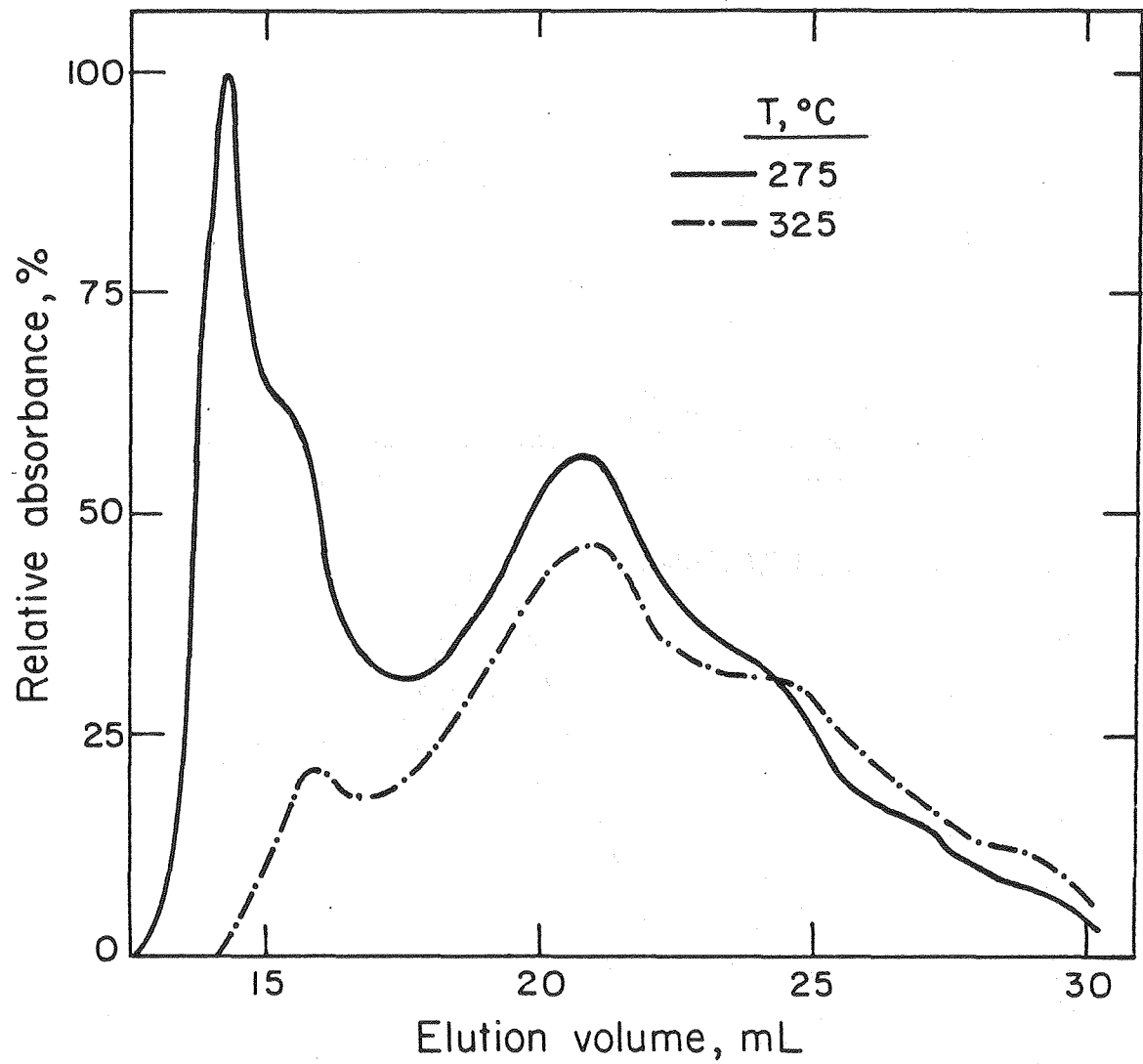
Figure 26 . Effect of temperature on elution of
preasphaltenes from a gel-permeation column.
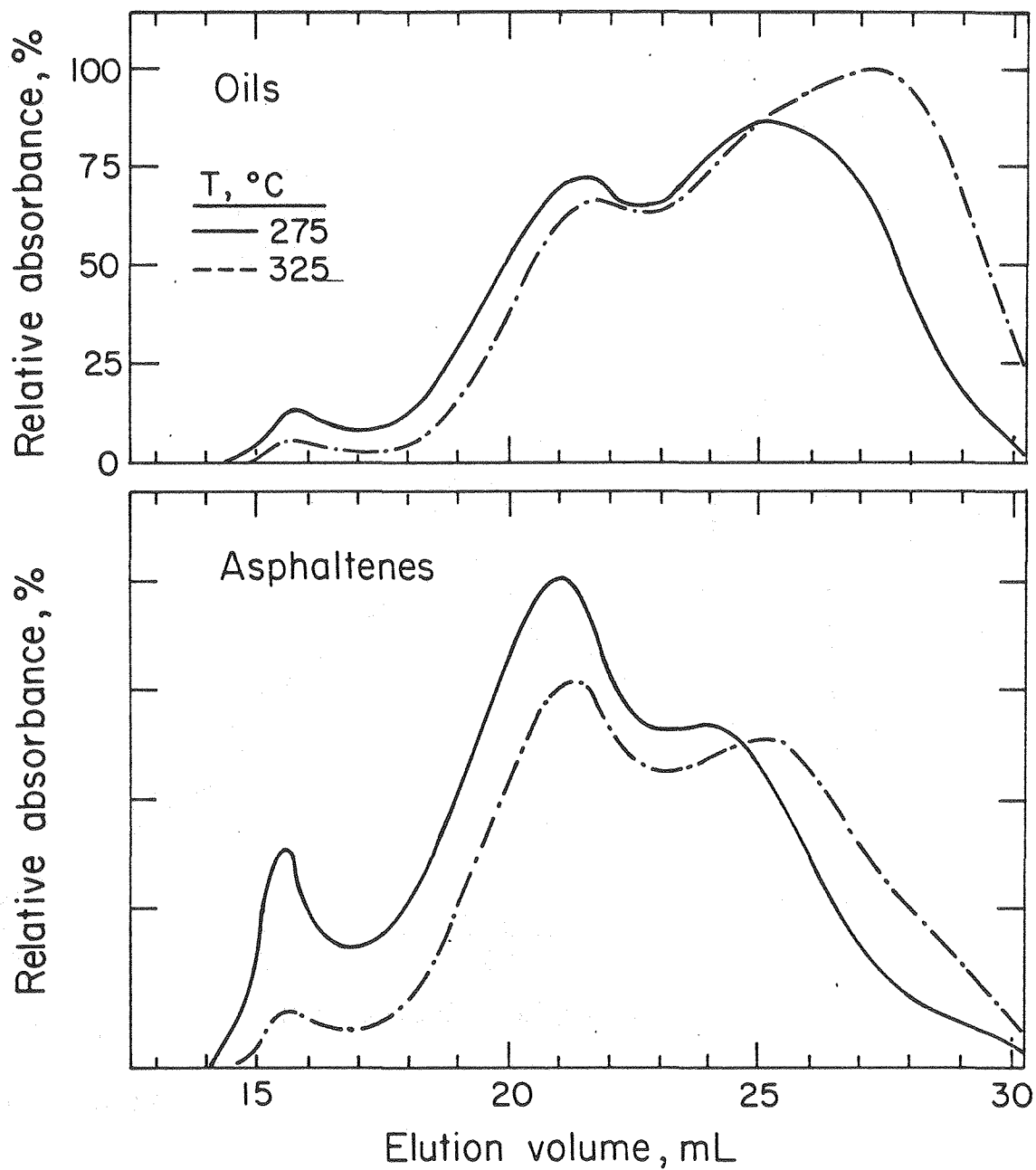
Figure 27.   Effect of temperature on elution of oils
              and asphaltenes from a gel-permeation column.

chromatograms was observed when the various product fractions from 325°C and 340°C were compared.

Figure 28 shows that reaction time has considerable effect on the molecular size distribution of preasphaltenes. Heatup to 325°C after prior treatment at both 275 and 300°C does not significantly alter the molecular size distribution when compared with the GPC tracing at 275°C, whereas after 30 minutes reaction, considerable molecular-weight reduction is observed.

The addition of metallic zinc (Figures 29 and 30) results in inclusion of higher-molecular-weight components in the oils, probably somewhat in proportion to the greater yield of oils observed with addition of metallic zinc.

Summarizing, operation at 325°C narrows the molecular-weight distribution in the preasphaltenes and may widen the distribution for the asphaltenes and oils.

Melting-Points of MTC Fractions

The extraction products from various treatments were further characterized by determination of their melting points with the assistance of Michael Johnson. The effect of reaction variables including temperature, hydrogen pressure, reaction time, and metallic additives on melting point was studied.

Because many of the comparative runs were made with added zinc metal, the effect of metallic additives on melting points will be reviewed first (Table 40). The addition of metals widens the melting-point range of both oils and

Figure 28. Effect of reaction time on the elution of oils and preasphaltenes from a gel-permeation column.
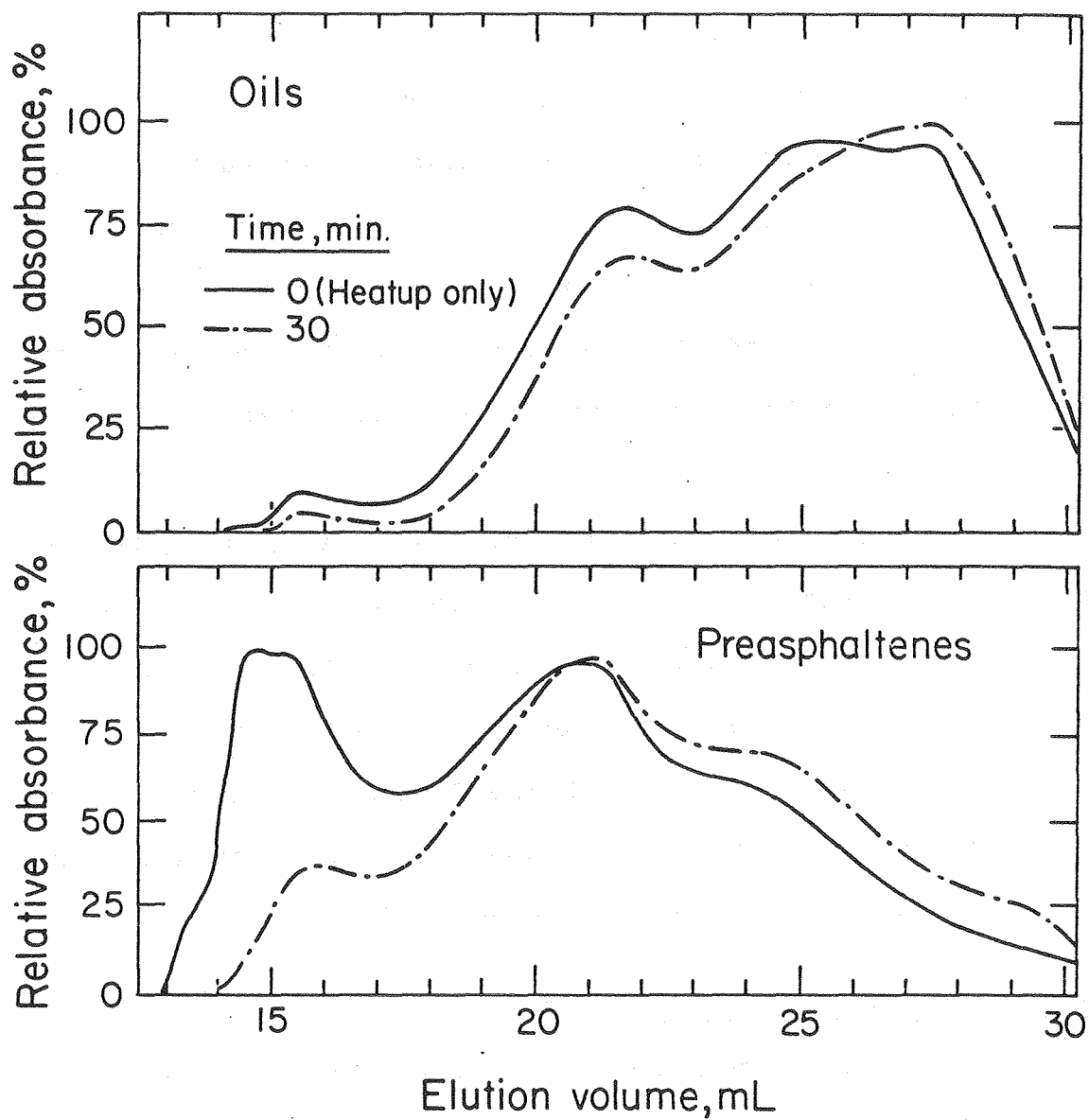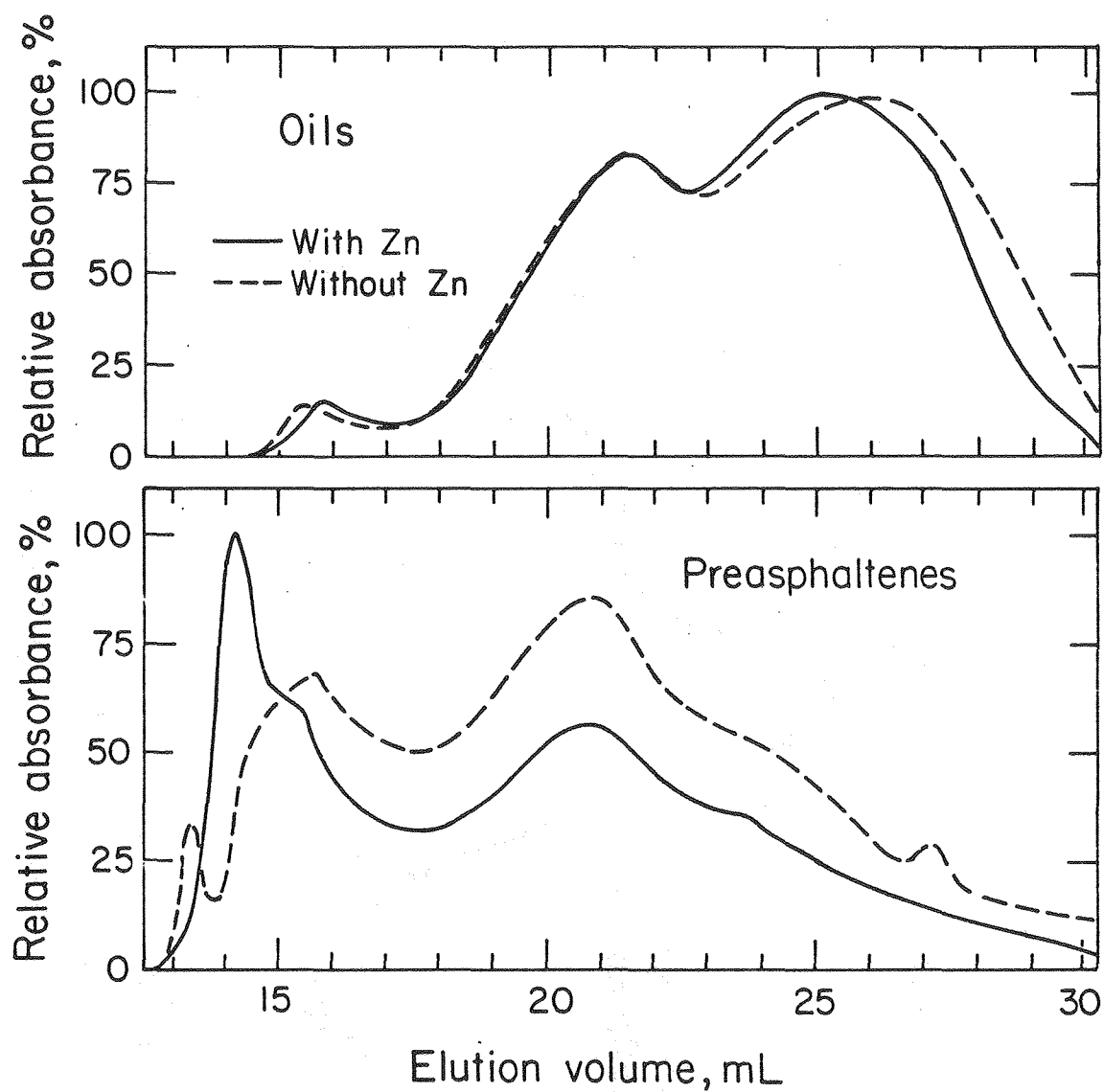
XBL 804-650

Figure 29. Effect of metallic zinc on elution of oils and preasphaltenes from a gel-permeation column.
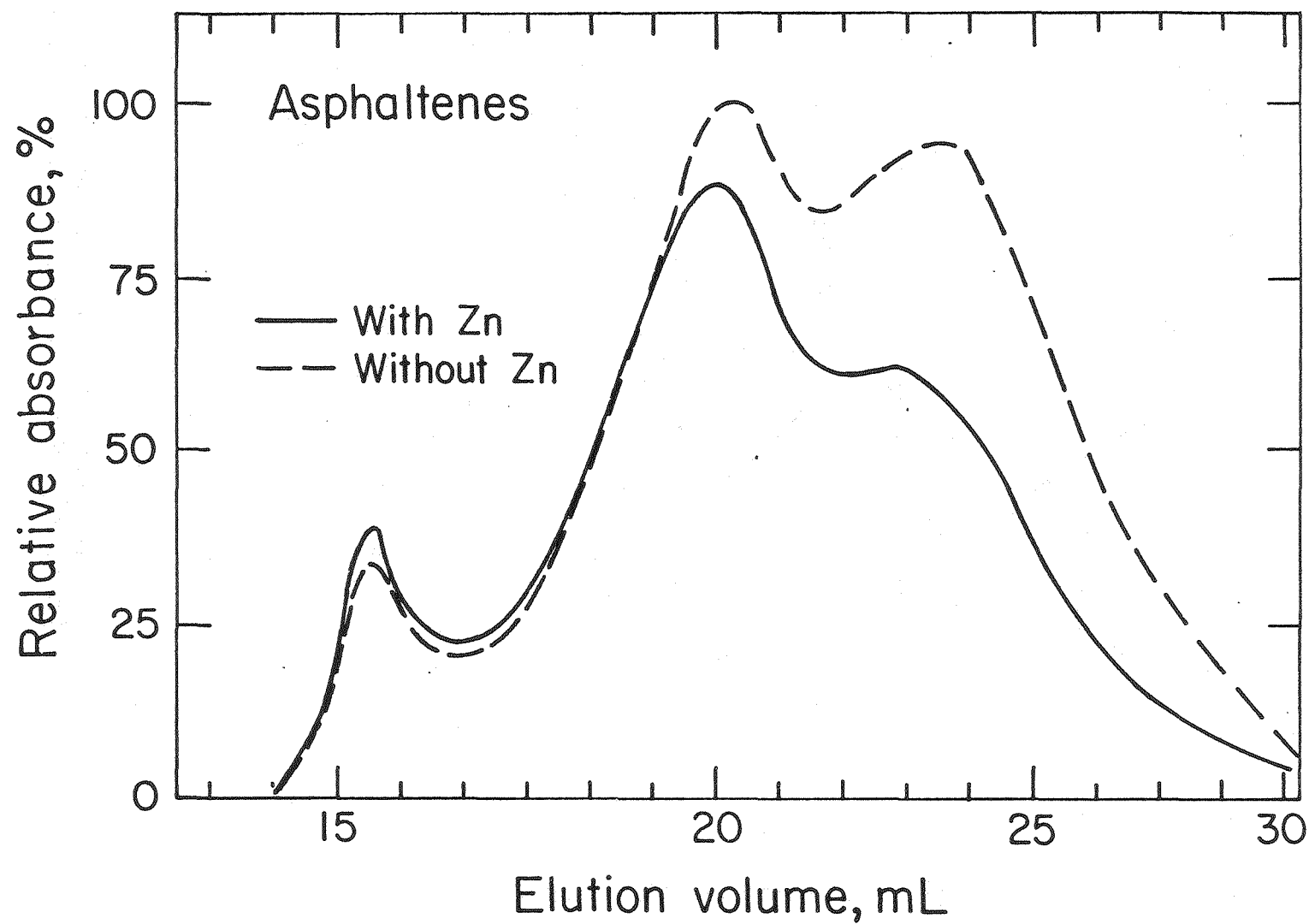
XBL 804-648

Figure 30 . Effect of metallic zinc on the elution of
asphaltenes from a gel-permeation column.

XBL 804-651

Table 40. Effect of Metallic Additives on Melting Points of Extraction Products
(250 gm $ZnCl_2$, 50 gm Coal; 275°C, 30 min.)

Run No.	Additives (gm)	CH_3OH Loading (gm)	H_2 Pressure (psig)	Melting Point (°C)		
				Oils	Asphaltenes	Preasphaltenes
4	Sn (7)	25	500	59-118	83-116	[+]271 to over 400
6	Mo (6)	25	500	60-91	108-133	over 400
10	Fe (1)	25	500	60-86	124-146	over 400
5	none	25	500	65-69	139-145	over 400
2	Zn (4)	25	500	61-96	128-168	over 400
7	Al (2)	25	500	88-106	130-179	over 400
43	none	35	800	62-89	155-183	over 400
44	Zn (4)	35	800	54-71	178-258	over 400
51	Zn (8)	35	800	58-88	201-259	over 400

[+] A small amount (less than 5%) melts below 400°C.

asphaltenes. Tin produces the lowest median melting points, and aluminium the highest.

The favorable product distribution obtained by addition of metallic zinc made further characterization of its product fractions necessary. The use of increasing amounts of zinc (Table 40) produced higher-melting asphaltenes. The oils varied irregularly, without any large change in the average melting point. No lowering of the melting points of preasphaltenes was observed.

The marked effect of increased temperature is shown in Table 41. Although 300°C (compared with 275°C) has no great effect, a further increase to 325°C produces generally lower melting-point ranges for all the products. With 30 minutes at 325°C or 15 minutes at 340°C, the oils did show deterioration.

Most remarkable is the low melting point of the preasphaltenes treated at 325°C. The preasphaltenes begin melting as low as 190°C; up to 400°C in the best case, about 30% has melted. This behavior is corroborated by indications from GPC data that the preasphaltenes obtained at 325°C contain more lower-molecular-weight components.

Increasing the temperature to 340°C results in a sharp increase in the melting point of the oils. In order to avoid such retrogressive reactions, it would be essential to extract the oils after treatment at 325°C before starting any higher-temperature treatment.

The reduction in the melting point of preasphaltenes after 340°C treatment further supports the reactivity of

Table 41. Effect of Reaction Variables on Melting Points of Extraction Products
(250 gm $ZnCl_2$, 50 gm Coal, 35 gm CH_3OH; 8 gm Zn)

Run No.	Temp. (^{O}C)	Time (min)	H_2 Pressure (psig)	Melting Points (^{O}C)		
				Oils	Asphaltenes	Preasphaltenes
51	275	30	800	58-88	201-259	over 400
77	300	30	800	64-82	167-192	over 400
68	275/300	15/15	800/800	52-73	127-169	over 400
76	275/300/325	15/15/0+++	800/800/800	52-70	160-200	*189-400+
69	275/300/325	15/15/15	800++	53-71	172-224	*189-400+
67	275/300/325	15/15/15	800/800/800	56-67	171-250	*191-400+
73	275/300/325	15/15/30	800/800/800	57-78	141-193	**197-400+
74	275/300/325/340	15/15/15/15	800/800/800/800	85-130	155-190	***140-400+

141

Up to 400°C, approximately * 15%, ** 30%, *** 35% melted; ++ Without repressurizing
+++ Heatup to 325°C (less than 3 minutes residence time above 300°C).

preasphaltenes. This strongly suggests that treatment at temperatures above 340°C could serve to convert most of the remaining preasphaltenes into oils. A multi-stage process can be envisaged, consisting of two stages at 275°C and 325°C, followed by solvent extraction of oils and asphaltenes, with further treatment of the preasphaltenes at a higher temperature.

The effect of reaction time was also observed. At 325°C, 30 minutes resulted in about 30% of the preasphaltenes melting below 400°C, whereas 15 minutes or less led to less than 15% melting.

At 300°C, increased availability of hydrogen (Run 68) when compared with Run 77 resulted in lower melting components in both oils and asphaltenes. However, at 325°C, comparison of Runs 67 and 69 shows essentially no change in melting point when the system was repressurized with additional hydrogen.

Summarizing, it can be observed that temperature has a substantial effect on melting points of the product fractions. In future studies with $ZnCl_2$ catalysis, higher temperatures may serve to convert most of the remaining preasphaltenes (35% at 325°C) into oils.

Solid-State Cross Polarization Carbon-13 NMR

The CP-^{13}C NMR technique shows great promise in the characterization of coal components, enabling one to distinguish aromatic, aliphatic, aliphatic ethers, and condensed aromatic carbon in model compounts (L6). In the present study, this technique has been applied to correlate the effects of

temperature, reaction time and addition of metallic zinc in coal conversion.

The results are shown in Figures 31 to 35 and summarized in Table 42. Comparing untreated coal and the MTC from Run 71, mere heatup to 275°C (which takes 7 minutes of reaction exposure above 200°C) increases the aromatic content from 53% to 61%. The alkoxy and aliphatic components are decreased from 11 to 8%, and 36 to 31% respectively.

Providing 30 minutes of reaction time at 275°C, with zinc (Runs 51 vs 71) renders the coal more aliphatic, consistent with the H/C ratios, 1.15 for Run 51 and 0.94 for Run 71. In both runs, the MTC is more aromatic than the untreated coal. Without the added zinc, 30 minutes at 275°C, Run 43, gives 3% more alkoxy than in Run 51 (the same alkoxy as in raw coal), and 3% less aliphatic content.

Increasing the reaction temperature to 325°C (Run 73) increases the aromatic carbon content from 57% (Run 51) to 61%. There is equally a decrease in the aliphatic carbon content from 35 to 31%. However, the increased H/C ratio of 1.19 for Run 73 when compared with 1.15 for Run 51 is consistent with a lower average molecular weight.

Gas Analysis

The effect of temperature on the distribution of gaseous components was studied using combined gas chromatography and mass spectrometry. Temperature-staged run ranging from 275°C to 340°C was selected for analysis, and the results obtained
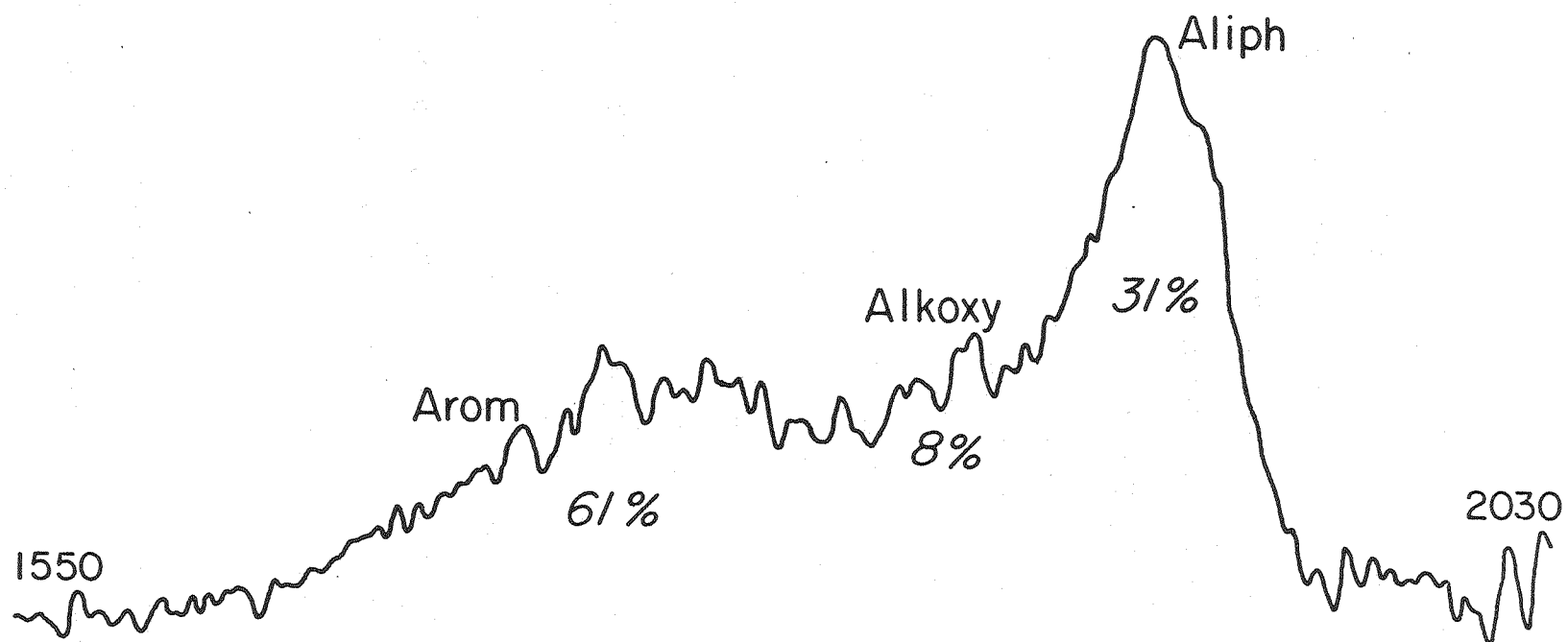
Figure 31 . CP-^{13}C NMR spectrum of melt-treated coal
(275°C, heatup only, with zinc)

XBL 804- 653
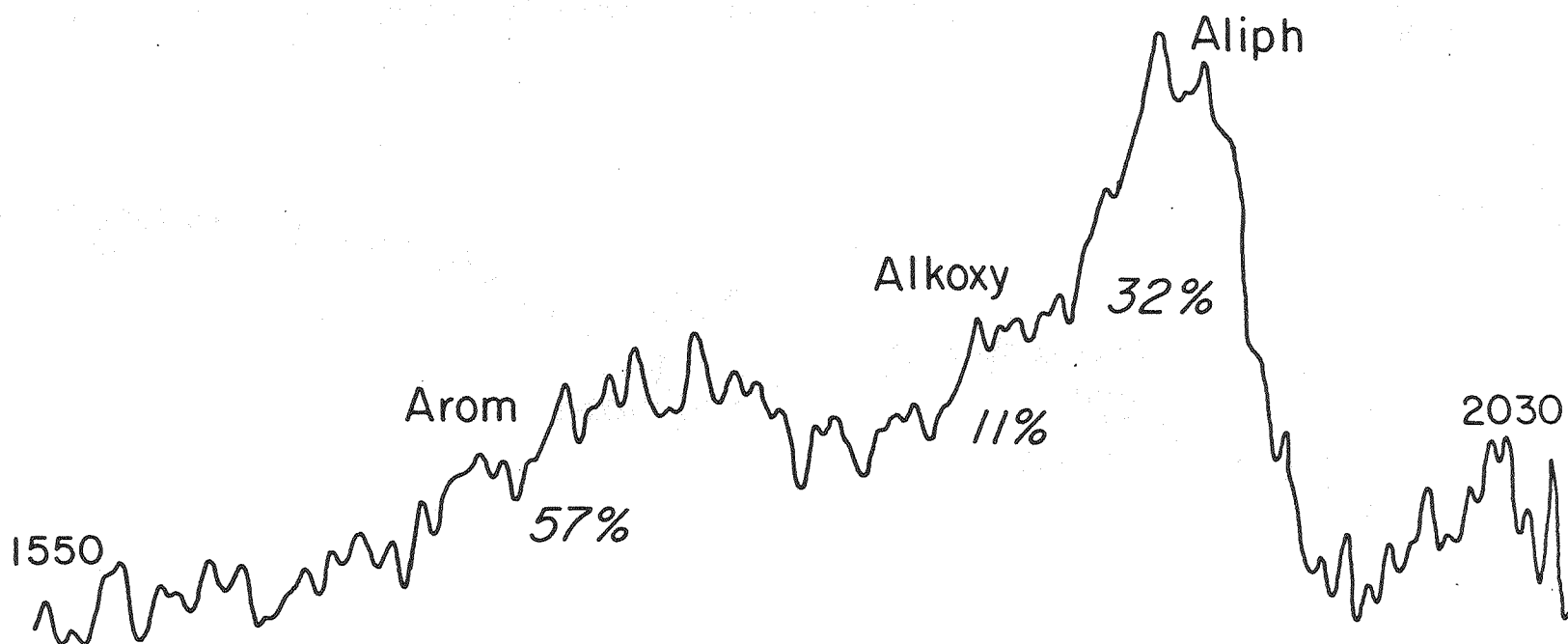
Figure 32 . CP-^{13}C NMR spectrum of melt-treated coal (275°C, 30 min, without Zn)

XBL 804-655

145
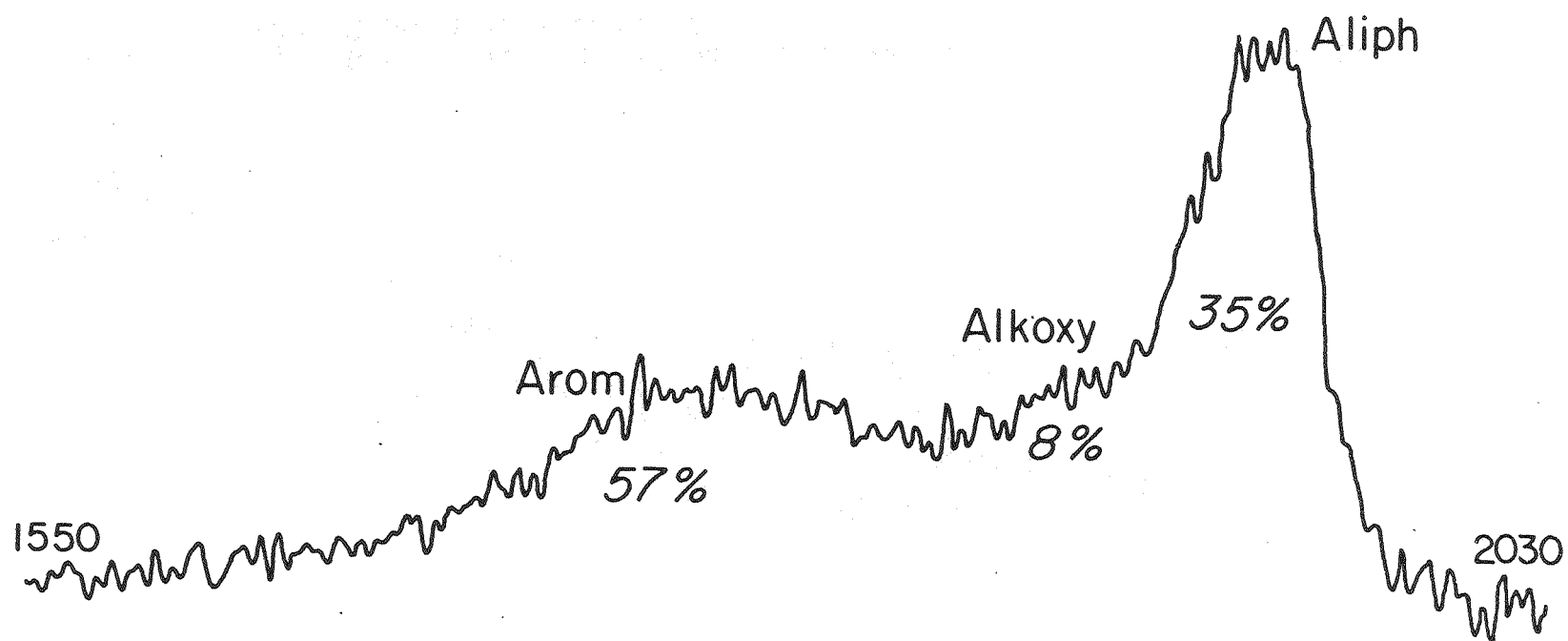
Figure 33 . CP-^{13}C NMR spectrum of melt-treated coal
(275°C, 30 min, with Zn)

XBL 804- 656
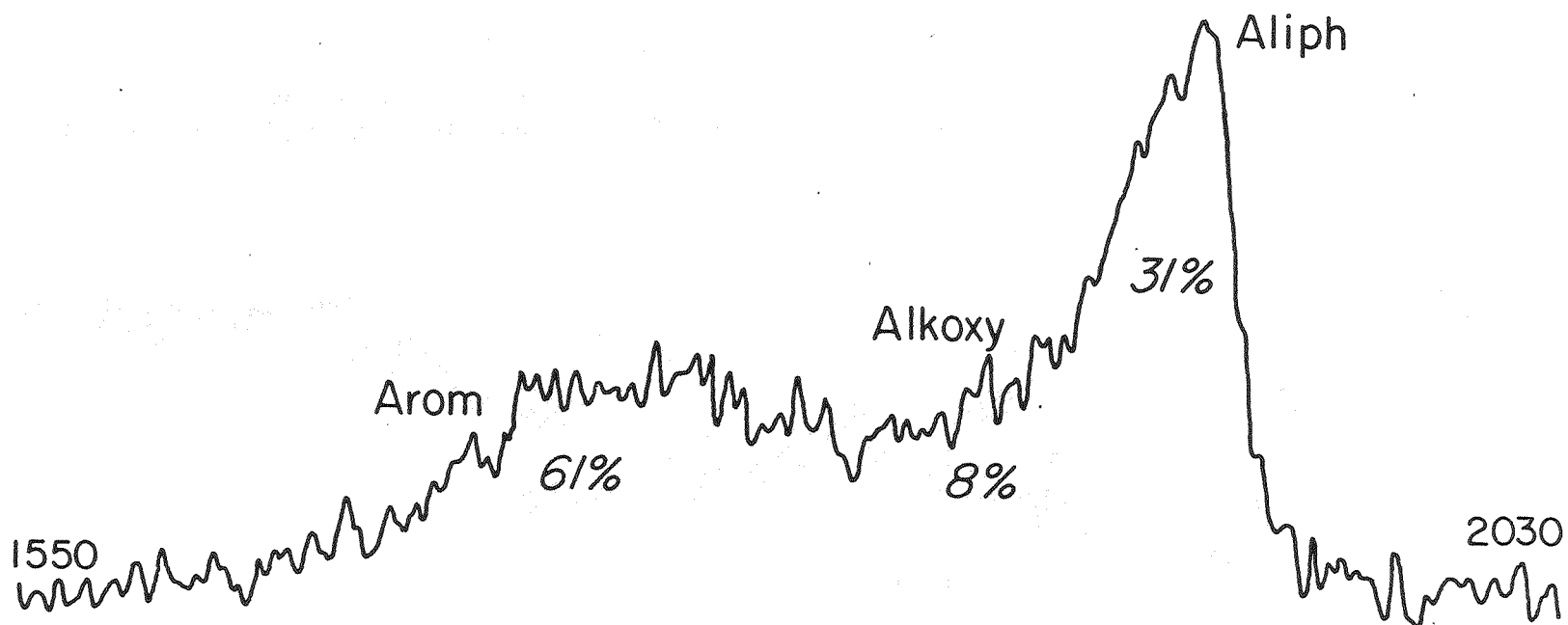
Figure 34 . CP-^{13}C NMR spectrum of melt-treated coal (325°C, 30 min, with Zn)

XBL 804-652
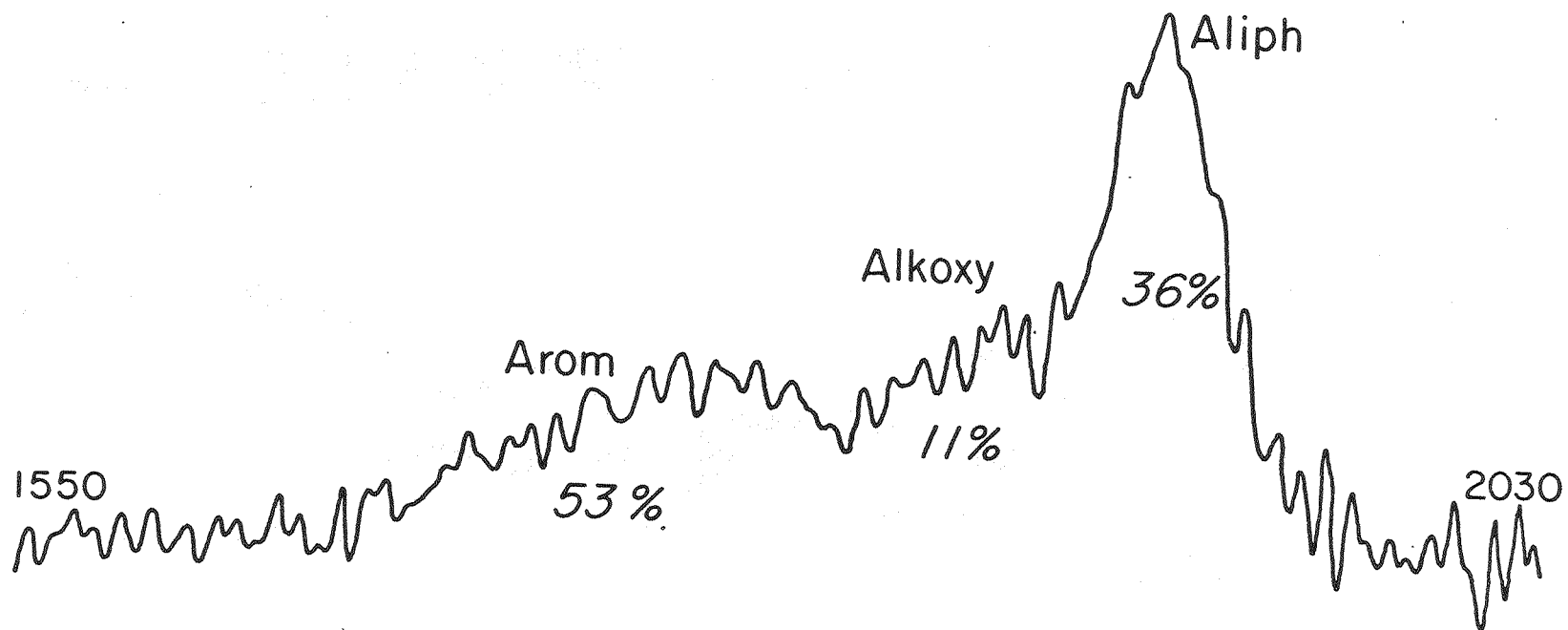
Figure 35. CP-^{13}C NMR spectrum of untreated wyodak
sub-bituminous coal.

XBL804-654

Table 42. Solid State CP-^{13}C NMR Analysis of Melt-Treated Coals

Samples	Composition (%)			Reaction Conditions
	Aliphatic	Alkoxy	Aromatic	
Untreated Coal	36	11	53	Wyodak Sub-bituminous Coal
Run 71	31	8	61	275°C, heatup only, 8 gm Zn
Run 51	35	8	57	275°C, 30 min, 8 gm Zn
Run 43	32	11	57	275°C, 30 min.
Run 73	31	8	61	325°C, 30 min, staged process, 8 gm Zn

are shown in Table 43.

Hydrogen, carbon dioxide, and butane are the major components. At $275^{O}C$, hydrogen consumption is maximum. This is supported by solubility data which show that a good percentage of the reaction occurs at $275^{O}C$. Maintaining a high concentration of hydrogen all through the reaction has been shown to be highly beneficial. However, maximum hydrogen consumption is 0.027 gm H_2/gm C or 0.016 gm H_2/gm Coal.

Dimethyl ether and methyl chloride decrease as conversion progresses. The mechanism and kinetics of their formation from methanol in this reaction system are not known. The total lost, including methanol, in the vapor is less than 10% of the methanol imput, which occurs mainly at the beginning of the reaction.

Both carbon dioxide and carbon monoxide decrease as conversion progresses. Some carbon oxides may come from mineral carbonates, some from carboxylic acids in the coal, and some perhaps from certain liquefaction reactions.

Total gaseous products amount to 4 gm at $275^{O}C$. This decreases to 2.1 gm at the $300^{O}C$ stage, with a slight increase 2.2 gm at $325^{O}C$ and a decrease to 1.8 gm at the $340^{O}C$ stage. Methanol in the gaseous products decreases sharply from 0.94 gm at $275^{O}C$ to 0.07 gm at $340^{O}C$. Total carbon loss during the four-stage depressurization is 6 gm.

There is no significant increase in the production of hydrocarbon gases as the conversion proceeds. This suggests

Table 43. Gas Analysis for Staged Pressurization and
Depressurization
(250 gm $ZnCl_2$, 50 gm Coal, 8 gm zn, 35 gm CH_3OH;
275°, 300°, 325°, 340^OC; 15 min. per stage,
800 psig H_2 in each stage.)

| | Concentration, mole − % | | | |
	275^OC	300^OC	325^OC	340^OC
H_2	78.41	90.28	90.05	90.12
CH_3OH	0.52	−	−	0.49
CH_3OCH_3	1.78	0.12	0.02	0.04
CH_3Cl	3.28	0.41	0.10	0.03
CO	1.76	0.54	0.54	0.38
CO_2	7.68	2.36	1.86	1.44
CH_4	1.44	0.52	0.73	1.44
C_3H_8	0.79	0.37	0.94	1.00
C_4H_{10}	2.44	2.99	2.63	3.20
C_5-C_8	1.89	2.00	2.75	1.51
NH_3^+	−	0.01	0.003	0.005
H_2O^+	−	0.39	0.37	0.33

+ Values inaccurate due to adsorption on column surfaces.

that even at high temperatures, gas production may be low.

There is need to determine the kinetics of the conversion of methanol to dimethyl ether and other products. This will be useful in determining the contribution of methanol to these materials in the coal liquefaction reactions. Moreover, the effects of these materials on conversion can then be determined.

DISCUSSION

The goal of this study has been to increase the conversion of coal to oils. This goal has been considerably advanced with 54% conversion at 325°C. Operating at 325°C was desirable because higher temperature treatment enhances the availability of hydrogen in the liquid phase, increases the rate of depolymerization and solubility of reaction products, and cleaves the zinc chloride-preasphaltene complex.

The increase in oil yield has been accompanied by a decrease in preasphaltenes, while the yield of asphaltenes remain relatively constant. Preasphaltenes as such are not directly usable as components of a synthetic crude oil, as they are essentially undistillable. Preasphaltenes when compared with oils have relatively high molecular weight, and are richer in nitrogen and leaner in hydrogen than the other fractions. Their conversion to oils will require removal of ring nitrogen and perhaps phenolic oxygen both demanding substantial hydrogenation.

A good understanding of the chemical factors responsi-

ble for the stability of preasphaltenes is highly necessary. This will throw more light on how their reactivity can be improved. Catalytic systems capable of liquefying preasphaltenes deserve attention. Probably candidates include soluble organometallic complexes, such as metal carbonyl stabilized by partial ligand substitution capable of withstanding the severe liquefaction conditons. Derencsenyi (D6) has already demonstrated the stability of some of these materials up to 300°C. The use of disposable catalysts like a colloidally dispersed precipitated ferrous sulfide can prove useful.

Preasphaltenes obtained from different coals and reaction conditions will prove useful as substrates in this investigation. This will determine how these factors affect their chemical nature.

The reaction involving hydrogenation through molecular hydrogen uptake of many unsaturated organic compounds is thermodynamically feasible, but kinetically less so, due in part to the stability of the hydrogen molecule. Soluble transition metal complexes, particularly several of rhodium, have demonstrated that aromatic molecules can be hydrogenated under mild conditions (A5-6, E3-4, B11, M7). Avilov and associates (A5-6, E3-4), and Holy and co-workers (H12) have reported the striking activity of N-phenylanthranilic acid complex of rhodium on aromatic compounds including benzene, anthracene and cyclohexene. As a result of the complexity and composition of the coal molecule, these commonly available hydrogenation catalysts cannot effectively withstand

the reaction conditions utilized and reaction environment generated during coal liquefaction.

However, transition metals are reported (J4) to catalyze the activation of hydrogen and thereby facilitate the hydrogenation of unsaturated organic compounds. The addition of finely powdered metallic zinc to the zinc chloride melt has considerably increased the yield of oils through conversion of preasphaltenes. Whether zinc metal influences the primary solubilization of coal directly, or only indirectly, is not now known. The favorable behavior of zinc metal may be exerted in a finely divided metallic form, or may be due to its forming liquid-phase monovalent zinc ion.

In a chronopotentiometric investigation of metal with salts, Emmons (E5) showed that monovalent zinc ions, possibly Zn_2^{++} as such or complexed, form when metallic zinc is added to zinc chloride. The formation of diatomic zinc ions, asymmetrically complexed, could provide an imbalance of polarity that would aid hydride formation from molecular hydrogen.

The ability of a catalytic complex to activate molecular hydrogen and form a metal hydride as shown in Figure 36 is a necessary, but in itself not sufficient, condition for catalytic hydrogenation. For hydrogen transfer to the preasphaltene molecules, they must themselves be co-ordinated to the metal. Here again, methanol as a solvent and as a complexant, may be playing a very important role.

Since preasphaltenes contain the bulk of the multi-ringed

$$Zn^{0} + Zn^{++} \rightleftharpoons Zn_2^{++}$$

$$Zn_2^{++} + H_2 \longrightarrow Zn_2H_2^{++}$$

$$Zn_2H_2^{++} + PA \longrightarrow PA\text{-}H_2 + Zn_2^{++}$$

$$PA\text{-}H_2 \longrightarrow \text{Distillable Products}$$
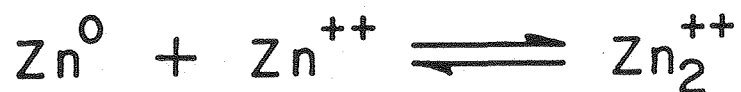
PA — Preasphaltenes

PA-H$_2$ — Hydrogenated Preasphaltene Molecules

XBL 805-5121

Figure 36. Conversion of preasphaltenes to distillable products.

aromatic compounds in coal, partial hydrogenation will render them more susceptible to loss of nitrogen or oxygen atoms, and lead to a reduction in molecular weight. Model compound studies tend to uphold this assertion. Whereas Salim (S12) observed that at $325^\circ C$, zinc chloride was incapable of cracking naphthalene, Maienschein (M10) has recently reported that at $300^\circ C$, the hydrogenated products of naphthalene, tetralin and decalin, are cracked by zinc chloride. The degree of ring opening increases with hydrogenation, resulting in nearly 50% of decalin cracking in one hour producing predominantly cyclohexane.

The eventual development of a commercial liquefaction process utilizing zinc chloride will depend to a great extent on the ability to solve zinc chloride corrosion and recovery. A zinc lined reactor is increasingly becoming attractive since metallic zinc considerably improves the yield of oils. However, the solubility behavior of zinc in the zinc chloride-methanol melt deserves attention. A steep solubility behavior is undesirable since any temperature gradient within the reactor will result in resolidification that may finally clog the reactor. A small amount of ZnO that can serve as an HCl acceptor will minimize the corrosive effect of HCl if produced during the reaction.

CHAPTER IV

RESULTS OF BIOMASS INVESTIGATIONS

Reactivity of Wood and Wood-Related Materials

The catalytic effect of the zinc chloride-methanol system on solubilizing wood and wood components is shown in Table 44. At $250^{\circ}C$ with 1 hour reaction time, water and methanol were separately used as liquefying agents in solubilizing cellulose. The methanol treatment, resulted in near complete conversion to pyridine-soluble materials with as much as one third of the solubles converted to oils. On the other hand, the zinc chloride-water system converted only 14% of the cellulose to pyridine-solubles, with no oils. The superiority of methanol over water as a liquefying agent could result from improved stabilization of reactive fragments through methylation; possible higher reactivity of zinc chloride in the methanol medium; or more rapid extraction of reaction products, leaving the unreacted cellulose more accessible to catalyst.

Lignin showed nearly 90% conversion to pyridine-solubles, about one-fifth of which represented oils. The corrected H/C ratio of 0.99 was slightly below that of unreacted lignin. The high reactivity of both lignin and cellulose, led us to expect favorable results from wood also.

Wood was studied with zinc chloride as both wood flour and chips. Both were completely solubilized under the reaction conditions, with one third of the recovered organics converted to oils.

On a dry ash-free basis, a carbon recovery of 79% is

Table 44. Zinc Chloride Solubilization of Wood and Wood Constituents

(250 gm $ZnCl_2$, 50 gm CH_3OH; $250^{\circ}C$, 500 psig H_2, 1 hour)

Run No.	Substrate (gm)	Recovered Solids, daf. basis, %			(gm ret. CH_3OH/ gm substrate org.)	Corr. Atomic H/C Ratio
		Oils	Asphaltenes	Preasphaltenes		
11	Cellulose (17.5)	35	21	38	0.62	0.42
18[+]	Cellulose (17.5)	–	1	13	0.00	0.73
20	Lignin (50)	19	19	49	0.16	0.99
21*	Wood flour (20)	31	17	52	0.30	0.86
24*	Wood chips (20)	34	13	52	0.22	0.91

[+] 25 gm H_2O.

* 800 psig H_2.

obtained with a charge of cellulose, and 90% for both wood flour and chips. Table 45 shows the amount of recovered solids for wood, as chips or flour, and wood derived lignin and cellulose. For wood (as both chips and flour) 12 to 18 gm of solids are recovered for a charge of 20 gm whereas 10 to 16 gm are recovered from a charge of 17.5 gm of cellulose. Incorporations range from 0.02 to 0.46 of retained methanol per gram of recovered organic material.

The effect of various reaction variables on wood solubilization was studied. These variables include temperature, time, hydrogen pressure, and methanol loading.

Effect of Temperature

Experiments with wood flour were conducted at temperatures of 200°, 225°, and $250^{\circ}C$, at a constant hydrogen pressure of 800 psig. The effect on conversion is shown in Table 46 and Figure 37.

Wood solubilization is highly temperature-dependent, leading (as already shown) to complete conversion at $250^{\circ}C$ but less than 10% conversion at $200^{\circ}C$. The yield of oil is also temperature sensitive; whereas no oil was produced at $200^{\circ}C$, about one third of the recovered organics at $250^{\circ}C$ was in the form of oils. At $250^{\circ}C$ also, the incorporation reaches 0.30 gram retained methanol per gram of recovered organic materials.

Reaction Time

Reaction time was varied between 0 (heatup only) and 60

Table 45. Amount of Recovered Solids in Biomass
Autoclave Experiments

Run* No.	Recovered Solids (gm)	Substrates Charged (gm)
11	16	Cellulose (17.5)
18	10	Cellulose (17.5)
20	54	Lignin (50)
21	16	Wood flour (20)
22	13	Wood flour (20)
23	12	Wood flour (20)
24	13	Wood chips (20)
25	13	Wood chips (20)
26	15	Wood chips (20)
27	13	Wood chips (20)
28	12	Wood chips (20)
29	12	Wood chips (20)
30	13	Wood chips (20)
31	18	Wood chips (20)
32	16	Wood flour (20)

* Reaction conditions are given in Table 8.

Table 46. Effect of Reaction Temperature on Conversion
(250 gm $ZnCl_2$, 20 gm wood flour, 50 gm CH_3OH; 800 psig H_2, 1 hour)

Run No.	Temp. ($^\circ$C)	Recovered Solids, daf. basis, %			(gm ret. CH_3OH/ gm wood org.)	Corr. Atomic H/C Ratio
		Oils	Asphaltenes	Preasphaltenes		
23	200	0	0	6	0.02	0.84
22	225	12	9	33	0.25	0.74
21	250	31	17	52	0.30	0.86

162
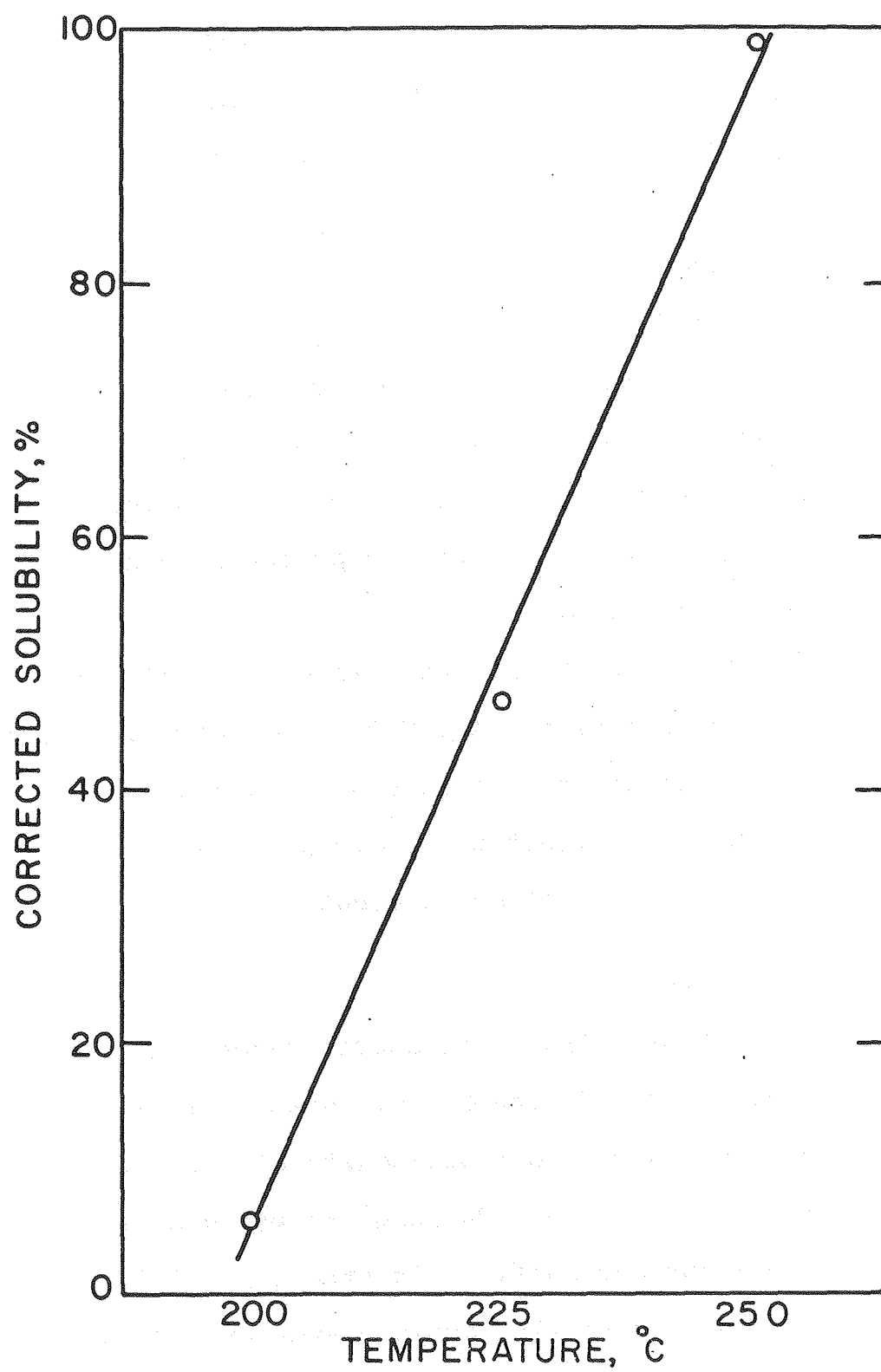
XBL795-6283A

Figure 37. Effect of temperature on solubility of wood.

minutes at 250°C. As shown in Table 47 and Figure 38, conversion is nominal with heatup only. When the reaction time is increased, 80% conversion is reached within 25 minutes, and total conversion within 60 minutes.

At the start of the reaction, wood is converted rapidly to preasphaltenes, with little or no oils or asphaltenes. Thus the initial reactions involve rupture of a relatively small number of bonds. As the reaction proceeds, the production of oils and asphaltenes increases, but beyond 40 minutes, the asphaltenes begin to revert to preasphaltenes, and the yield of oils levels off.

Figure 39 shows the increase in product H/C ratio with increasing reaction time. The H/C ratio shown in Figure 39, increases sharply at lower reaction times but approaches a constant value at 30 minutes. Correspondingly, gas consumption falls off greatly after 30 minutes.

Hydrogen Pressure

The effect of hydrogen pressure, between 200 and 800 psig at temperatures of 225° and 250°C, is shown in Table 48 and Figure 40. At 225°C, about one-fourth of the recovered wood solids after treatment at 200 psig are pyridine-soluble, and at 800 psig about one-half. In contrast, at 250°C, wood solubilization is essentially complete even at 200 psig, and the product distribution remains almost unchanged at higher pressures. The incorporation ratio, illustrated in Figure 41, decreases with increasing hydrogen pressure at both

Table 47. Effect of Reaction Time on Conversion
(250 gm $ZnCl_2$, 20 gm wood chips, 50 gm CH_3OH;
$250^{\circ}C$, 800 psig H_2)

Run No.	Time (min)	Recovered Solids, daf. basis, %			Corr. Atomic H/C Ratio
		Oils	Asphaltenes	Preasphaltenes	
28	0	0	0	11	0.87
27	30	30	15	40	0.91
24	60	34	13	52	0.91
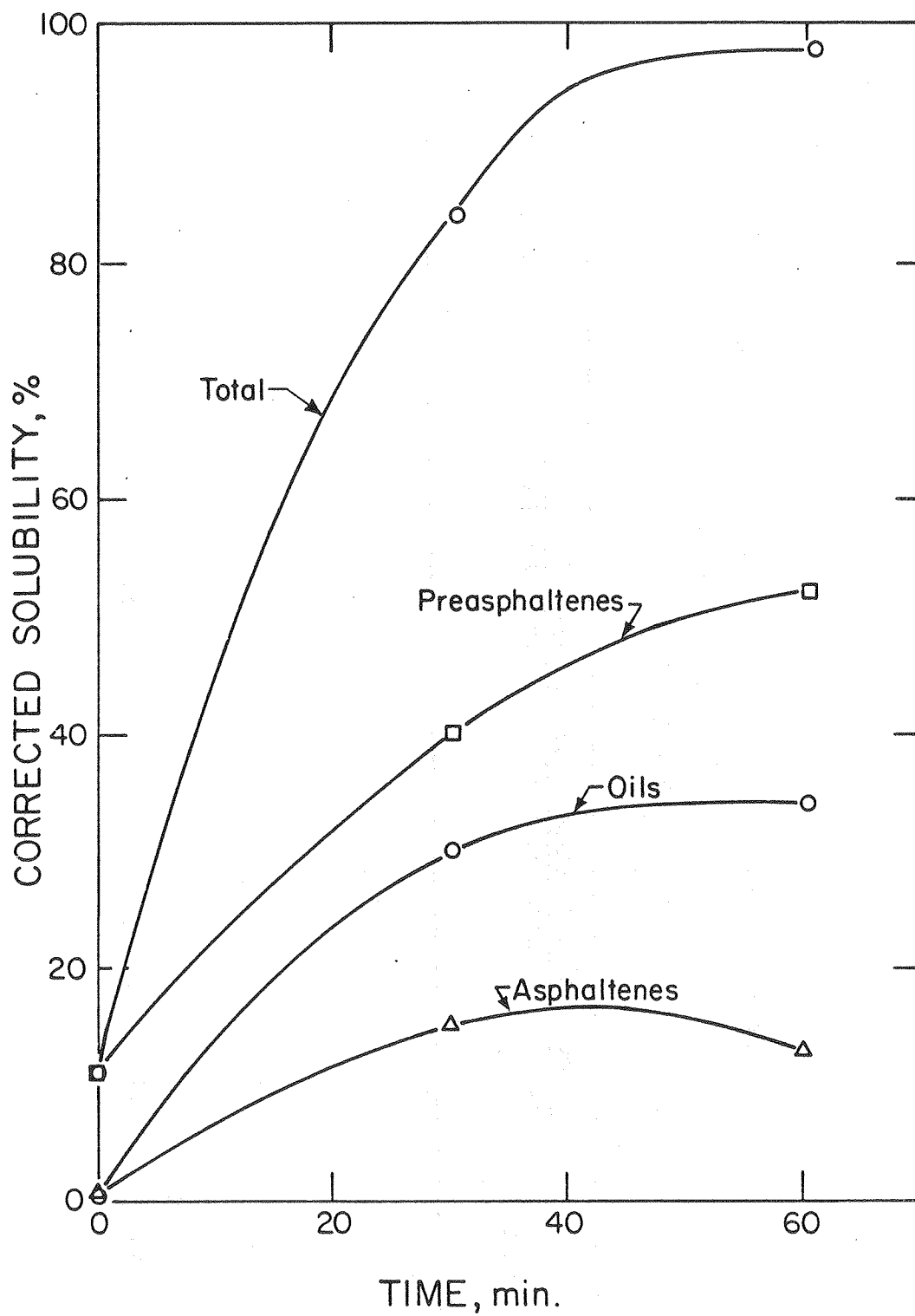
Figure 38. Effect of reaction time on
solubilization of wood.

XBL 804-628

Figure 40 . Effect of hydrogen pressure on solubility of wood.
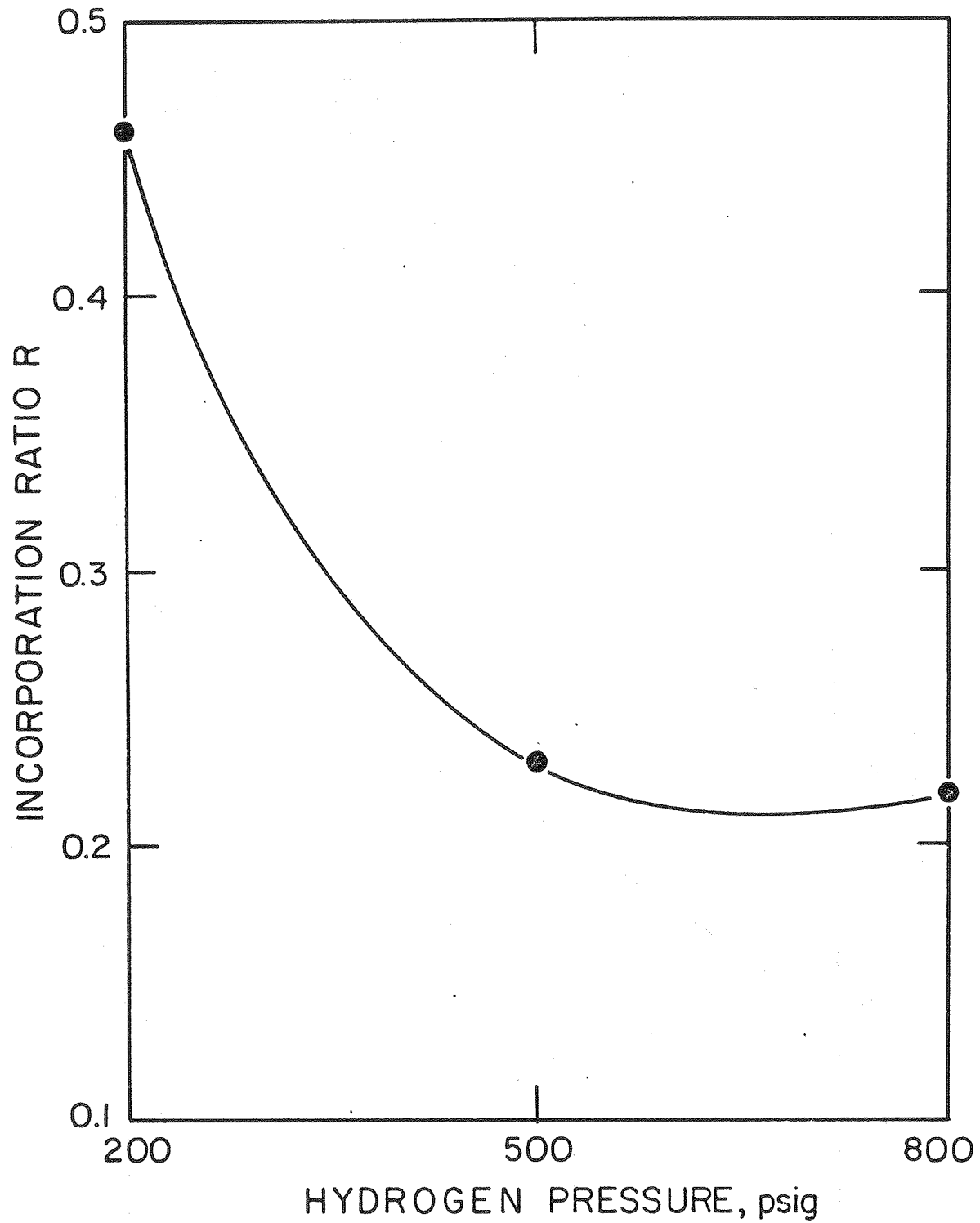
Figure 41. Effect of hydrogen on incorporation ratio.

temperatures.

The variation of corrected product H/C ratio with hydrogen pressure is shown in Figure 42. The H/C ratio increases sharply with hydrogen pressure between 200 and 500 psig, as does the gas consumption, then increases more moderately.
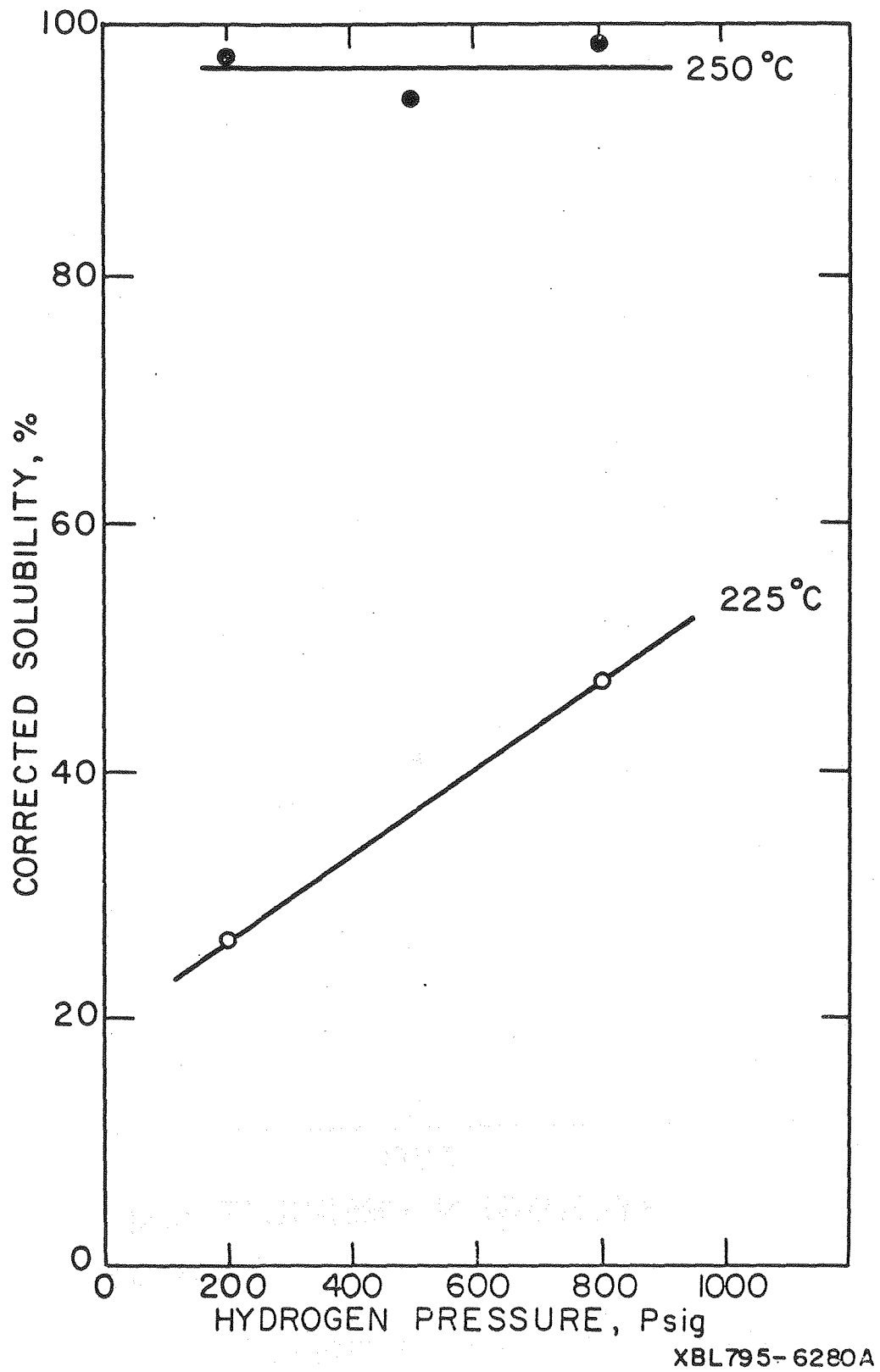
Methanol Loading

The methanol charged was varied from 25 to 75 gm, with the effects shown in Table 49 and Figure 43. Maximum conversion to soluble products at $225^{\circ}C$ occurs with about 50 gm of methanol for a zinc chloride loading of 250 gm; this approximates 0.85 mole CH_3OH per mole of $ZnCl_2$.

Scanning electron micrographs of samples of zinc chloride-methanol melt treated wood, as will be discussed later, shows that there is very good melt penetration into the wood and that reaction products are extracted thereby exposing the unreacted wood to further contact with the catalyst system. This improved contacting between wood and the melt could be due to lowering of the melt viscosity with methanol addition.

Oxygen Recovery

Oxygen functionalities, particularly alcohol-OH and ether -O-, are abundant in the various constituents of wood. The wood used for this study consists of 44 wt-% of oxygen on a dry basis. Other heteroatoms, nitrogen and sulfur, occur in insignificant amounts.

Hershkowitz (H10) and Shinn (S5), in their study of coal conversion using zinc chloride, have shown a relationship
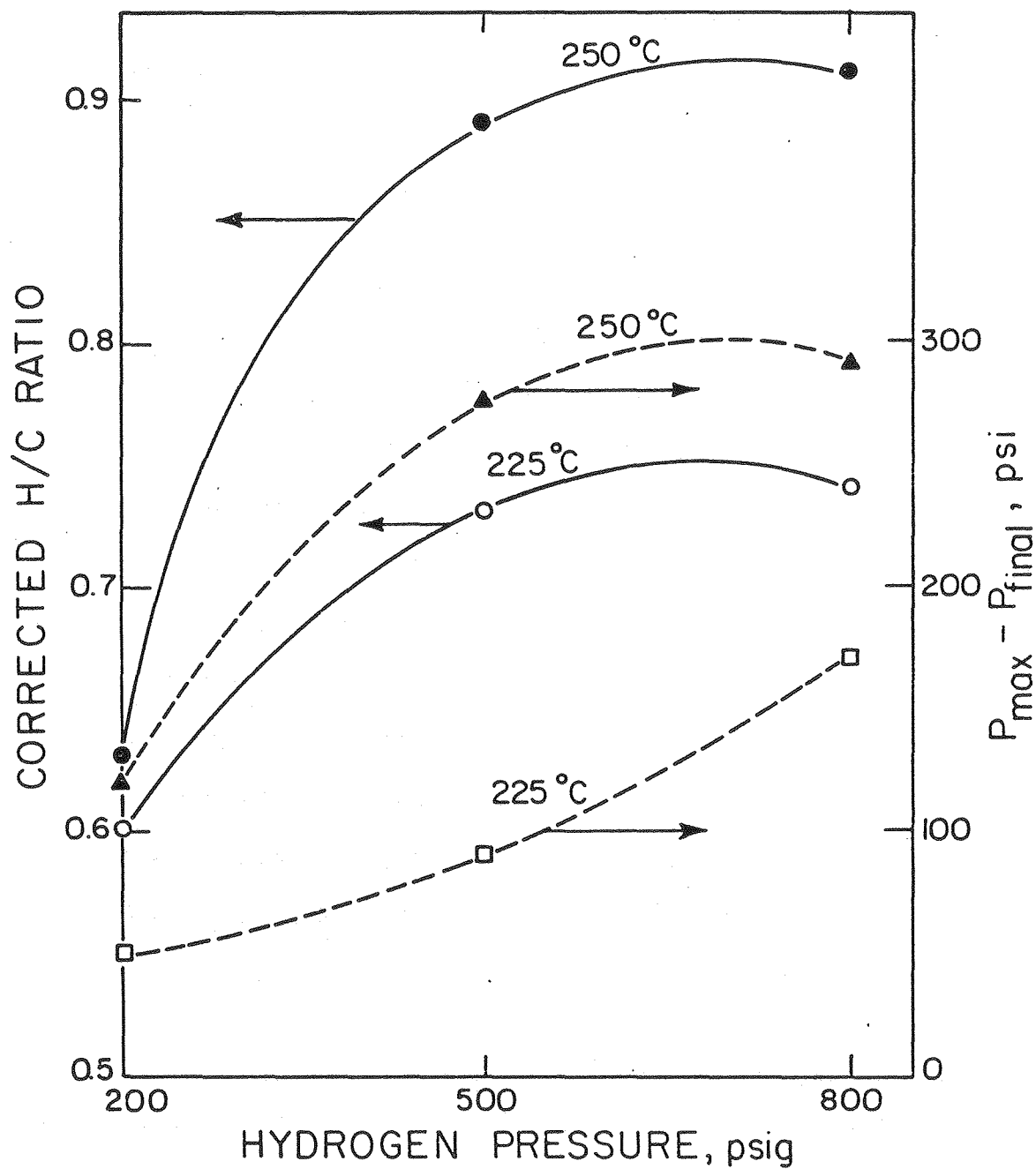
XBL 804-631

Figure 42.   Effect of hydrogen pressure on H/C ratio
             and gas consumption of $ZnCl_2$-CH_3OH treatment
             of wood.

Table 49. Effect of Methanol Loading on Conversion
(250 gm $ZnCl_2$, 20 gm wood chips; 225^OC, 500 psig H_2, 1 hour)

Run No.	CH_3OH Loading (gm)	Recovered Solids, daf. basis, %			(gm ret. CH_3OH/ gm wood org.)	Corr. Atomic H/C Ratio
		Oils	Asphaltenes	Preasphaltenes		
30	25	15	7	29	0.23	0.82
31	50	11	11	43	0.37	0.73
29	75	3	5	8	0.02	0.92
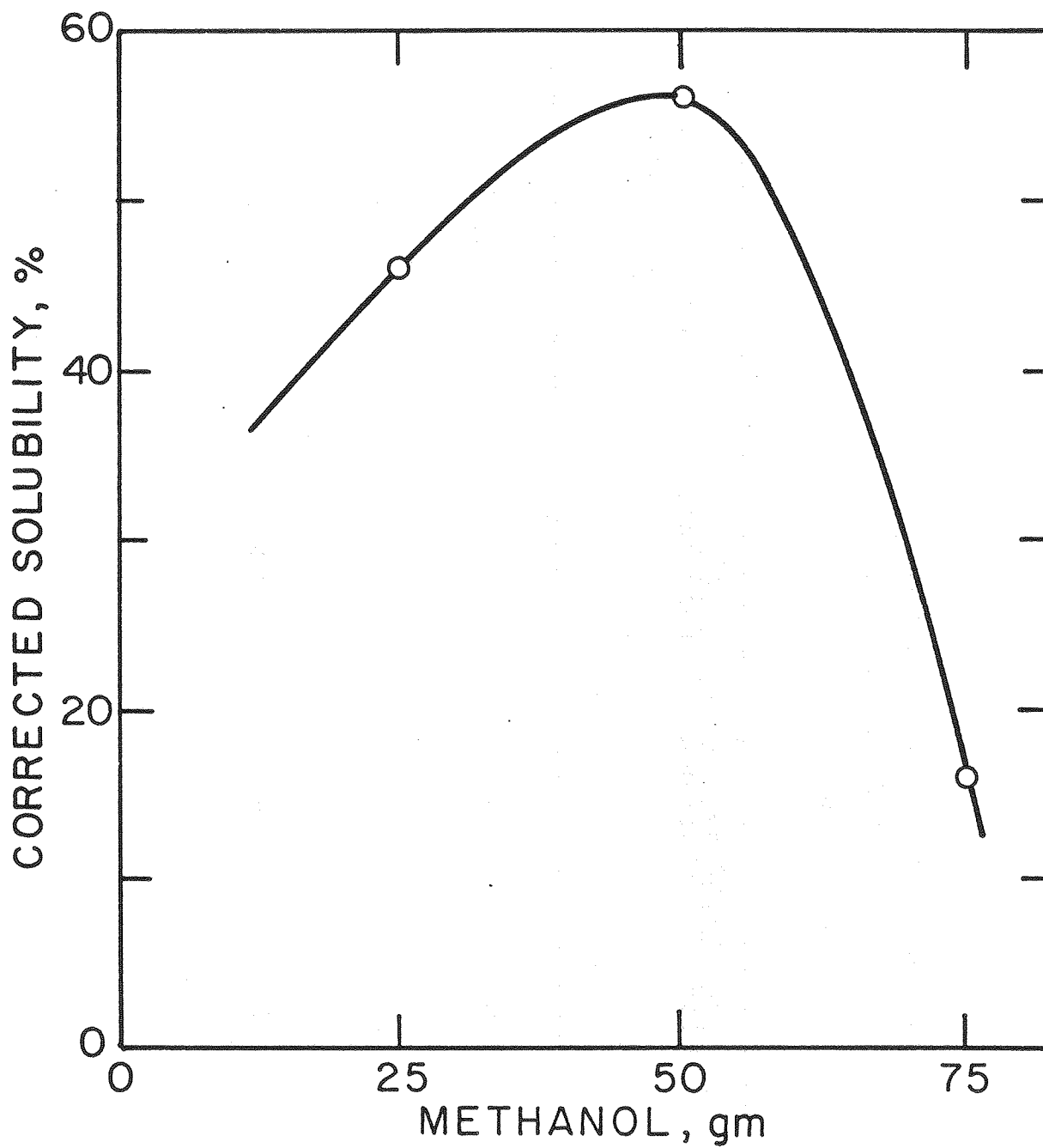
XBL 795-6284A

Figure 43. Effect of methanol loading on solubility of
wood.

between oxygen removal and coal solubilization. In the present study of wood solubilization, the effect of oxygen removal (determined by difference) is shown in Figure 44. Although data points are scattered, oxygen removal runs parallel to wood conversion. The wood constituents (cellulose and lignin), when treated separately, each conform to the general pattern. As Figure 45 shows, heatup to $250^{\circ}C$, removes about three quarters of the oxygen; the remainder is more resistant to attack, about 20% being removed in 30 minutes and about 5% highly resistant to attack even after 60 minutes. These results suggest that wood contains two kinetically distinct forms of oxygen functionality.

The effect of conversion (Runs 11, 18-32 using cellulose, lignin, and wood as substrates) on product distribution is shown in Figures 46 and 47. At low solubilization, the bulk of wood converted forms preasphaltenes, with oils and asphaltenes increasing with total conversion. As with coal, preasphaltenes are thus the first-formed product. As the reaction proceeds, preasphaltenes increase most rapidly and asphaltenes more slowly. This indicates that preasphaltenes are converted to oils either directly or through initial intermediate formation of asphaltenes.

PRESSURE-TIME DATA

A typical pressure-time relationship observed during the reactions is shown in Figure 48. The effect of different reaction variables on the pressure variation with time is shown in
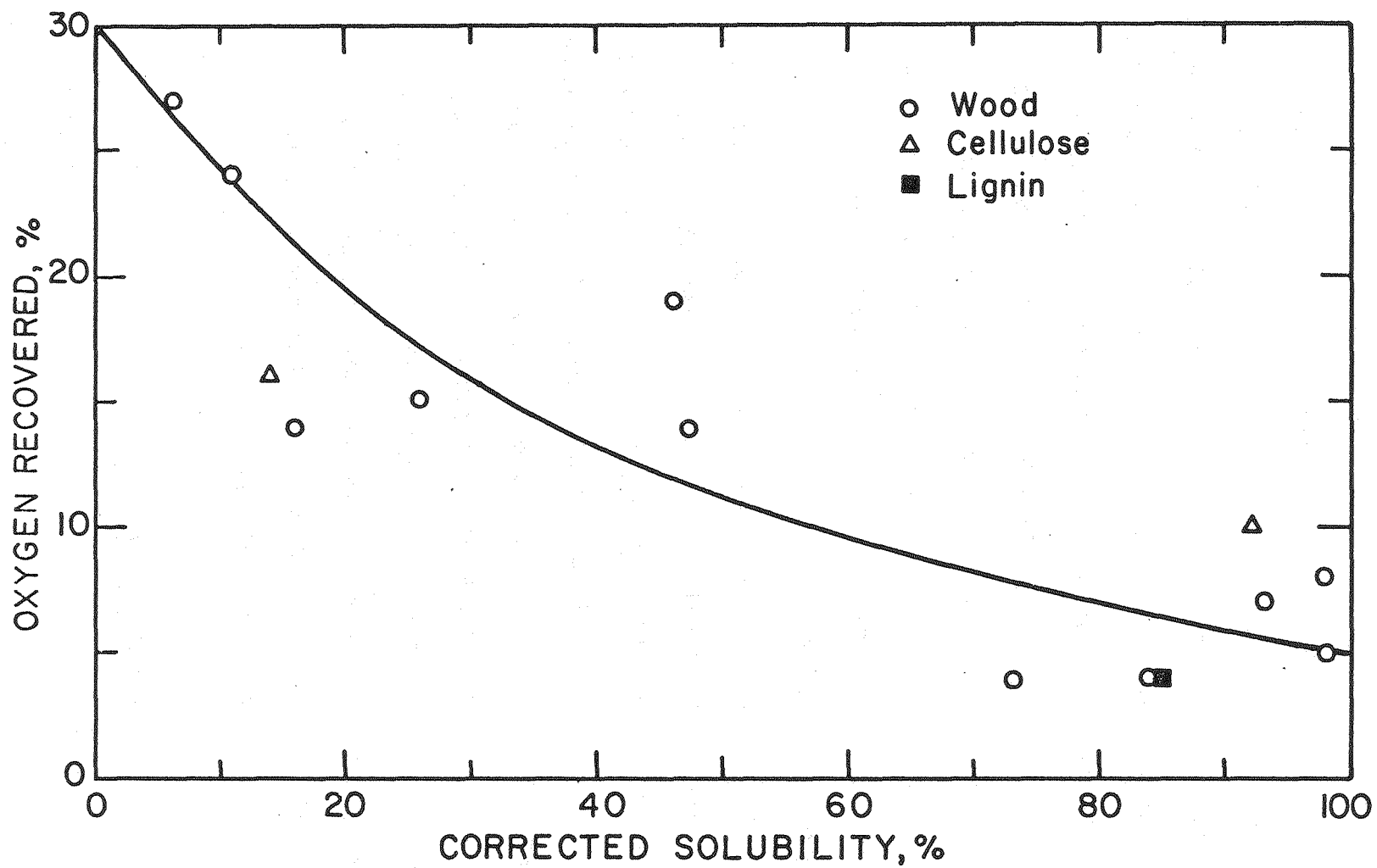
Figure 44. Effect of solubility on oxygen removal.

XBL 795-6281A

176
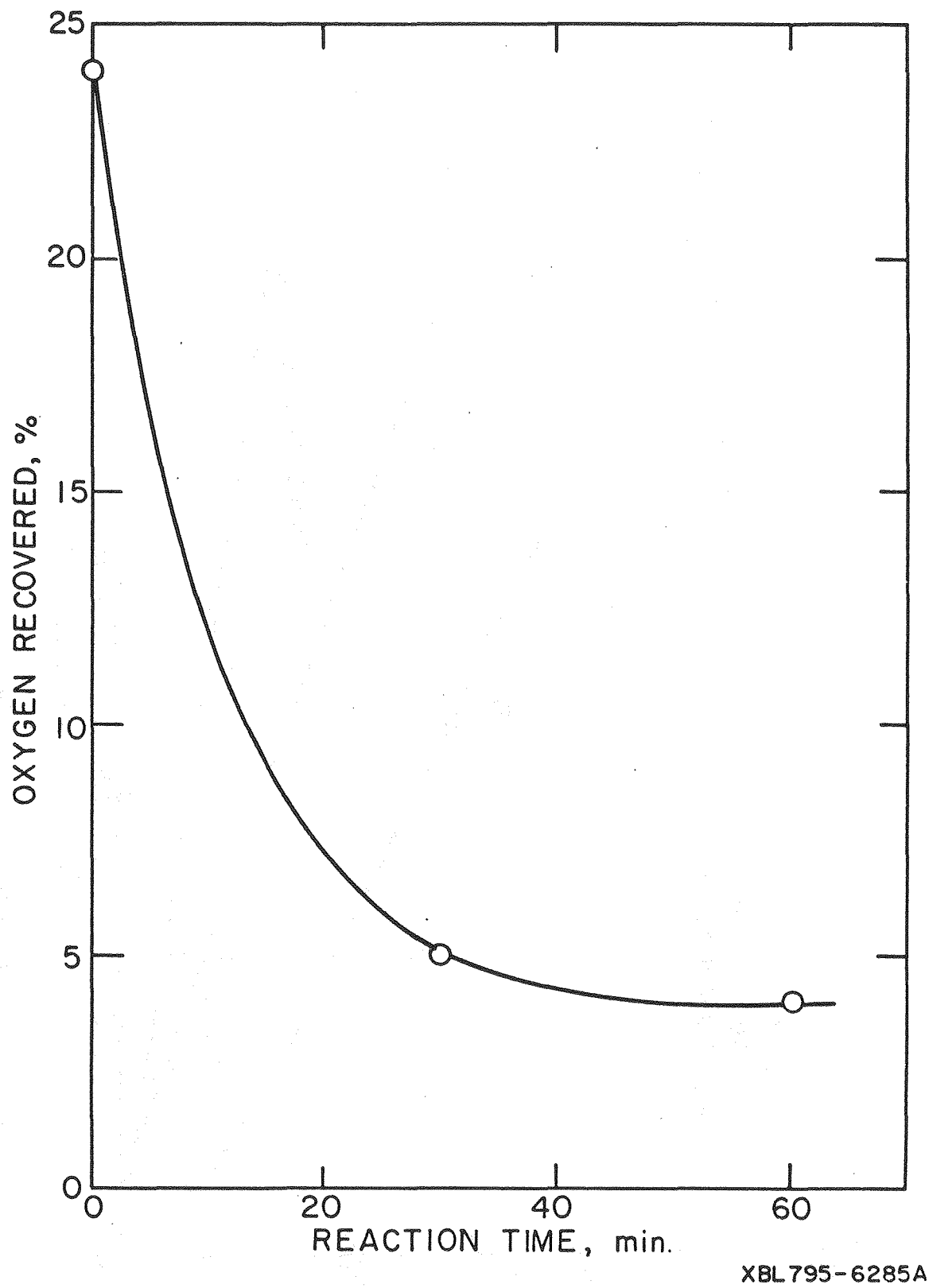
Figure 45. Effect of reaction time on oxygen removal.
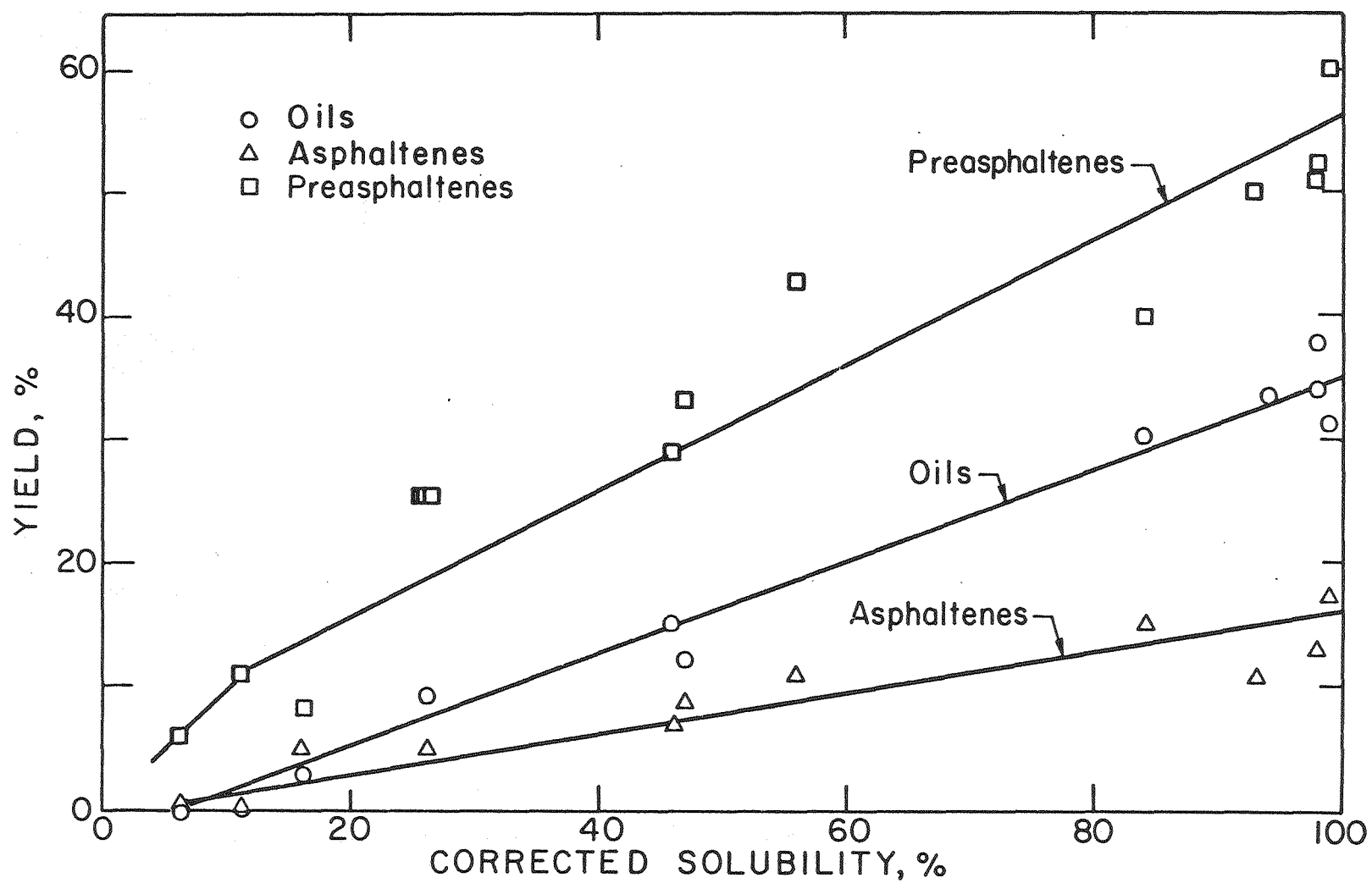
Figure 46.   Effect of conversion on product distribution.
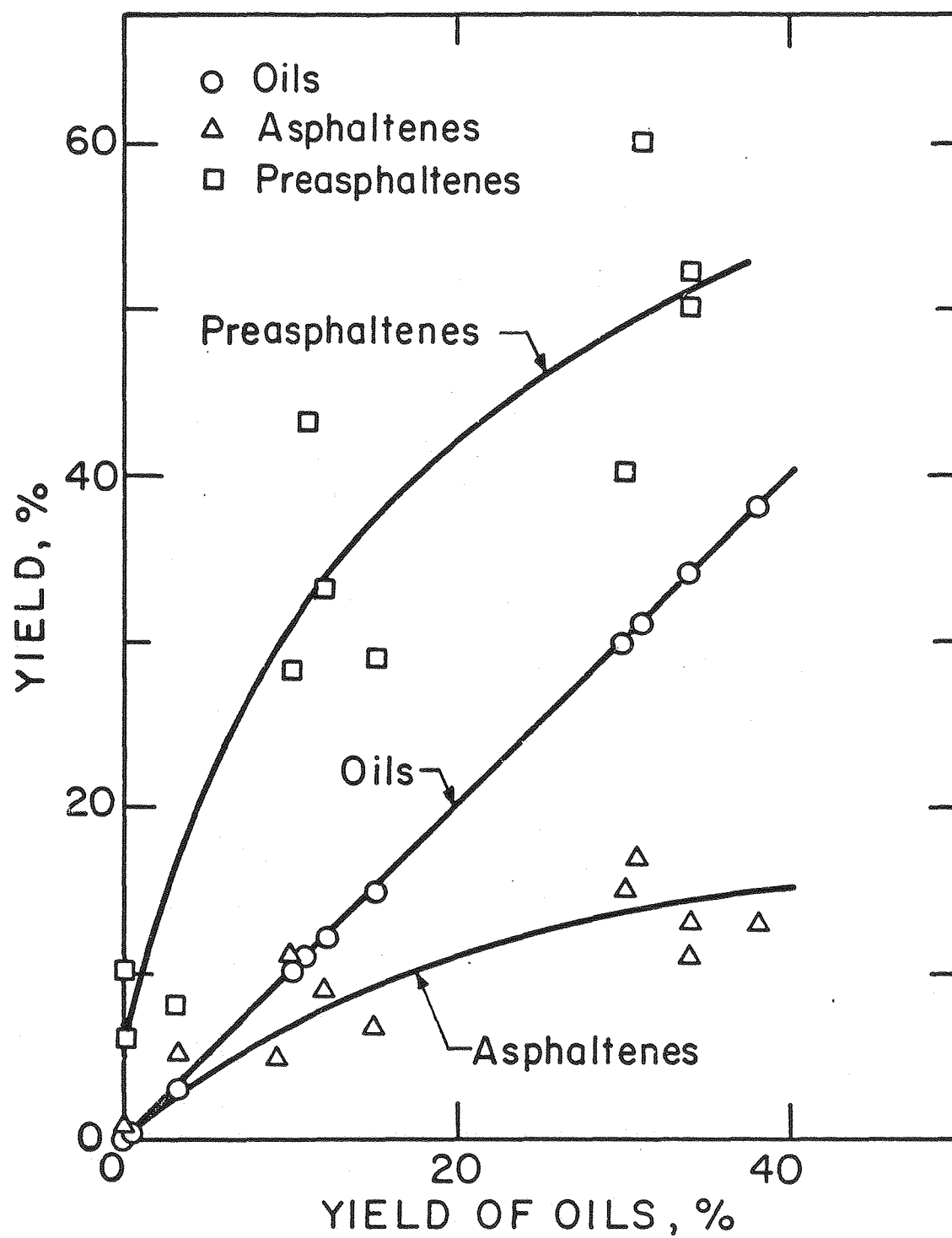
XBL 795-6286A

Figure 47. Effect of yield of oils on product distribution.

XBL795-6287A
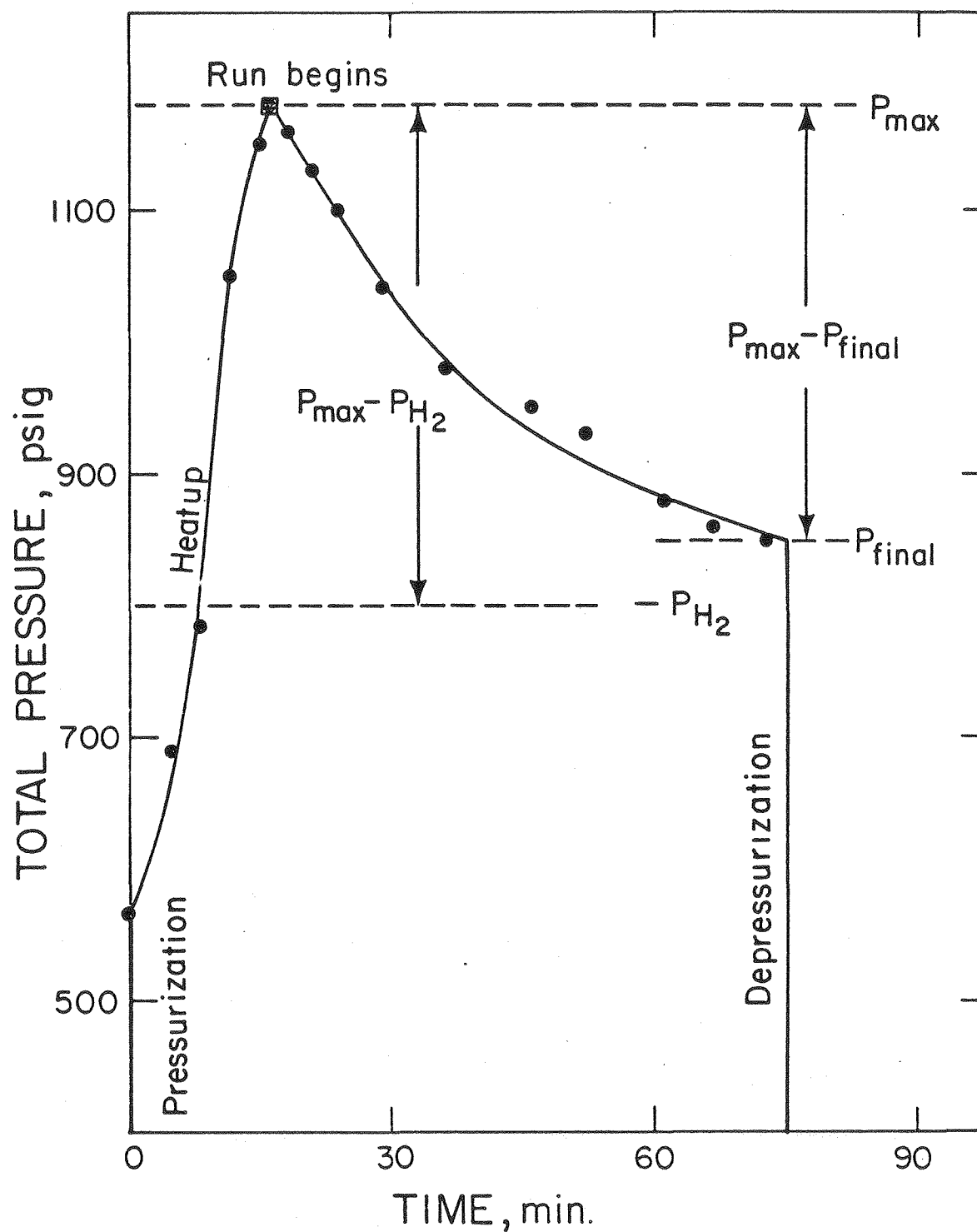
XBL 804-633

Figure 48. Typical pressure-time relationship in an
autoclave reaction (Data from run 21).

Tables 50 to 54 presented in Appendix B.

ANALYTICAL RESULTS

Scanning Electron Microscopy

The rate of wood liquefaction greatly depends on the ability of the catalyst system to penetrate the wood particles and on the ease with which reaction products can be extracted.

Residue samples from varying reaction conditions were examined with a scanning electron microscope in order to examine their structure. The reaction conditions and the pyridine solubilities of the various products examined are shown in Table 55.

Scanning electron micrographs of cellulose, Figures 49 a and b, show long bundles of materials interconnected by an irregularly woven network of thread-like and rod-like fibers. The structure shows open space between fibers suggestive of high permeability. After treatment with zinc chloride-methanol catalyst, Figure 49c, the surface topography becomes structureless, and relatively homogeneous; its surface smoothness is most likely due to solubilized material which deposited and resolidified at the end of the reaction.

The comparative effect of using $ZnCl_2$-H_2O melt instead of $ZnCl_2$-CH_3OH is examined in Figures 50a and b. For the aqueous melt, a thin layer of solubilized and redeposited product appears to overlie a relatively unreacted base structure, unlike the methanol case. When the respective products are

Table 55. Treatment Conditions and Extraction Yields for Wood and Cellulose Samples
Examined by Scanning Electron Microscope
(250 gm $ZnCl_2$)

Run No.	Substrate (gm)	Temp. (^{o}C)	Time (min)	H_2 Pressure (psig)	H_2O (gm)	CH_3OH (gm)	Total Solubility (Pct. daf.)
21	Wood flour (20)	250	60	800	0	50	99
23	Wood chips (20)	200	60	800	0	50	6
11	Cellulose (17.5)	250	60	500	0	50	92
18	Cellulose (17.5)	250	60	500	25	0	14
24	Wood chips (20)	250	60	800	0	50	98
28	Wood chips (20)	250	0	800	0	50	11

100 μm   (a)   25 μm   (b)

25 μm   (c)
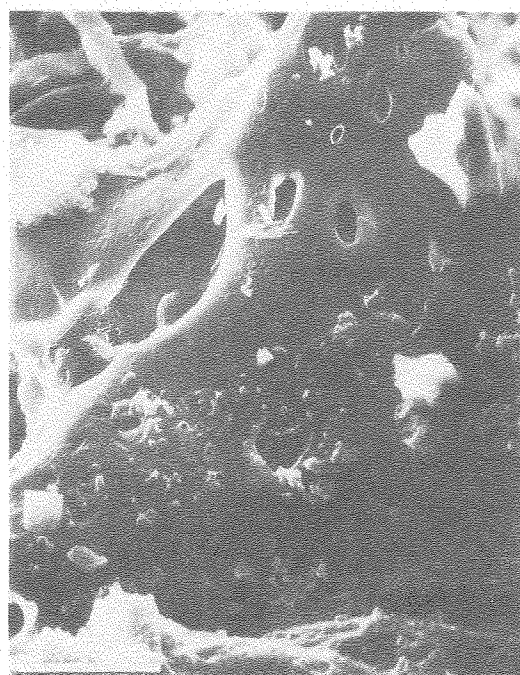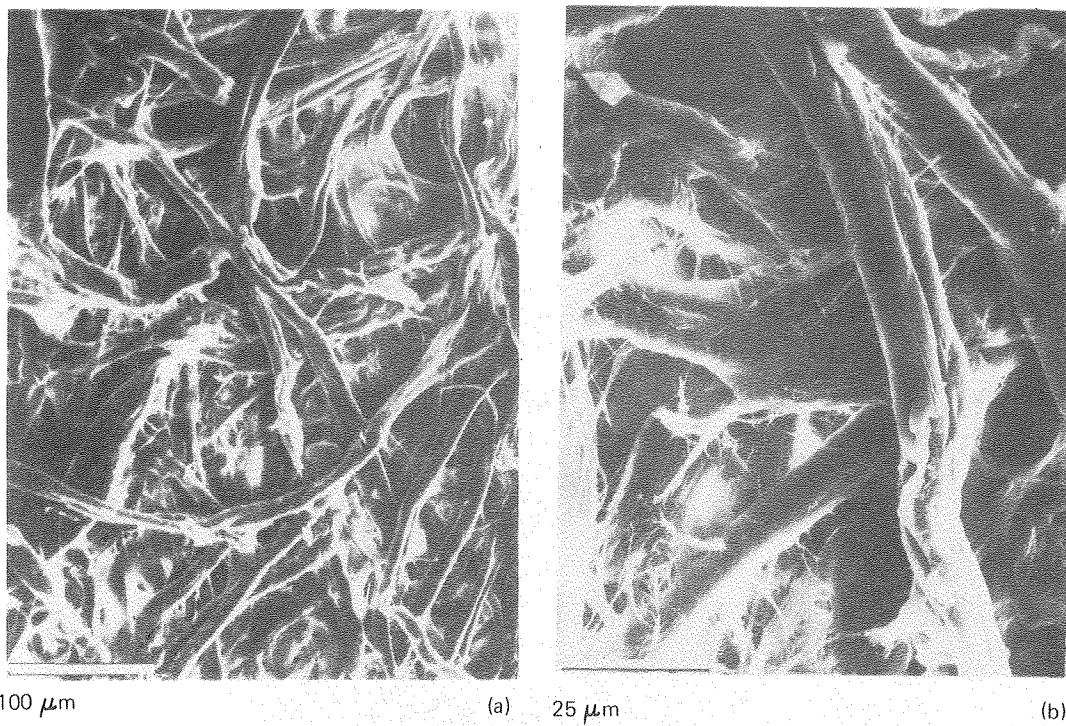
XBB 804-5021

Figure 49.   (a,b) Cellulose before treatment
(c) After treatment with $ZnCl_2$-CH_3OH, 250°C, 1 hr

25 μm   (a)   25 μm   (b)
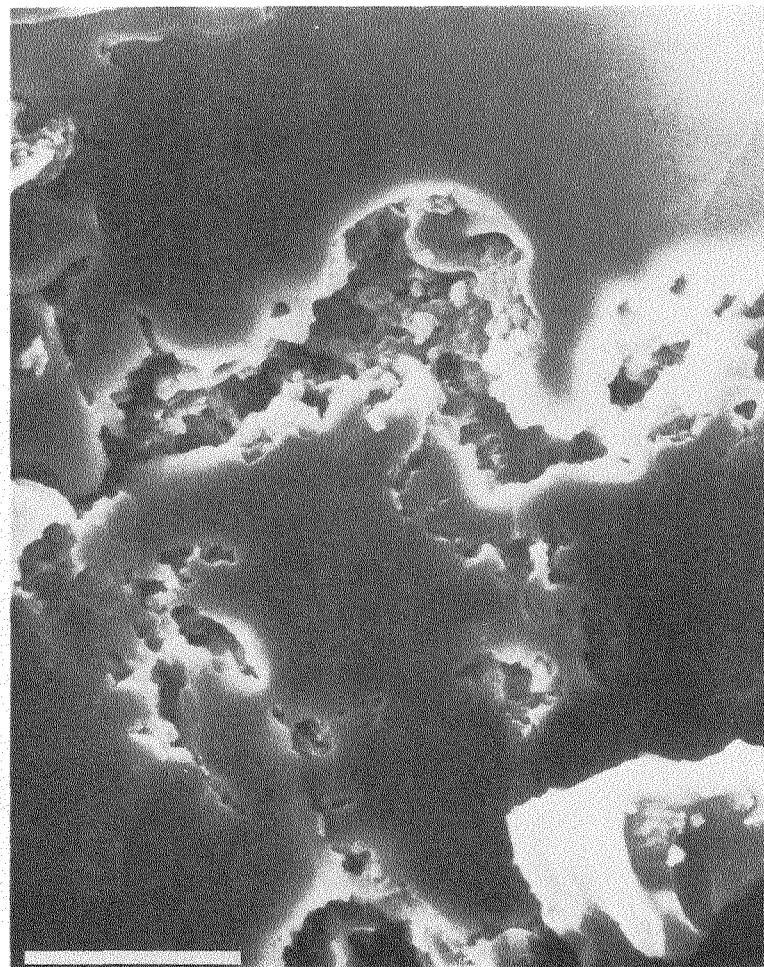
Figure 50. Effect of 1-hr treatment at 250°C on cellulose (a) $ZnCl_2$-CH_3OH
    (b) $ZnCl_2$-H_2O

pyridine-extracted, the aqueous-melt product, (Figure 51b), shows a rough, shallow, pitted surface of the unconverted materials. By contrast, the extraction residue from the $ZnCl_2$-CH_3OH treatment, (Figure 51a), shows a compact lava-like structure of mixed mineral and organic material.

Wood chips, as shown in Figure 52a, comprise a highly consolidated tubular fibers, around 30 μm in diamter, which appears to be cemented into a compact texture of low permeability. At higher magnification, Figure 52b shows rectangular dome-like structures within the fibers probably bordered pits connecting longitudinal tracheids with a dual function of conduction and support.

The effect of zinc chloride on wood chips is shown in the additional photomicrographs. First, Figures 53a and b show wood chips subjected to only heatup (up to 250°C), with only 11% solubilization; these show initial distortion and spreading apart of the fibers, with peeling and transverse weakening. Noncrylstalline hemicellulose and lignin, located in the outer regions of the wood fibers (M11) may well be susceptible to zinc chloride attack, and their removal would tend to explain the fiber configuration that is seen here. As reaction proceeds at 250°C, the fibrous structure disintegrates almost completely (Figure 53c).

The same product from heatup only, after pyridine extraction shows retension of the bulk structure with more radical disrupture of the individual fibers. For one-hour
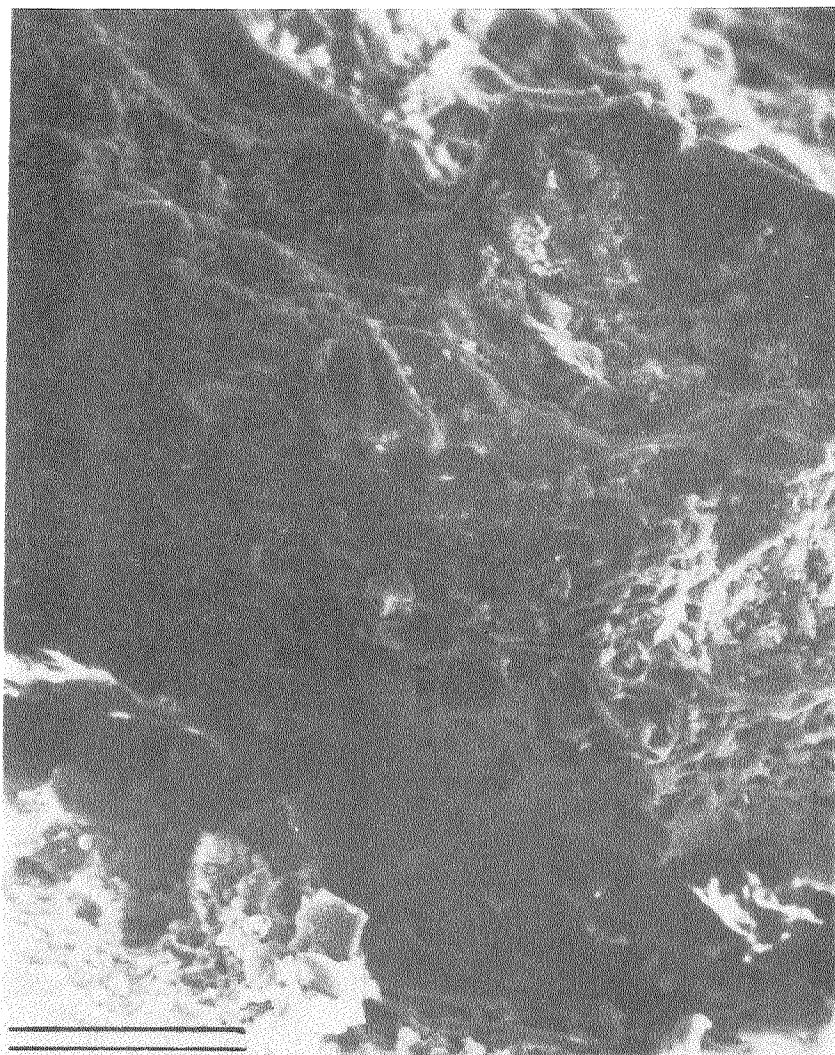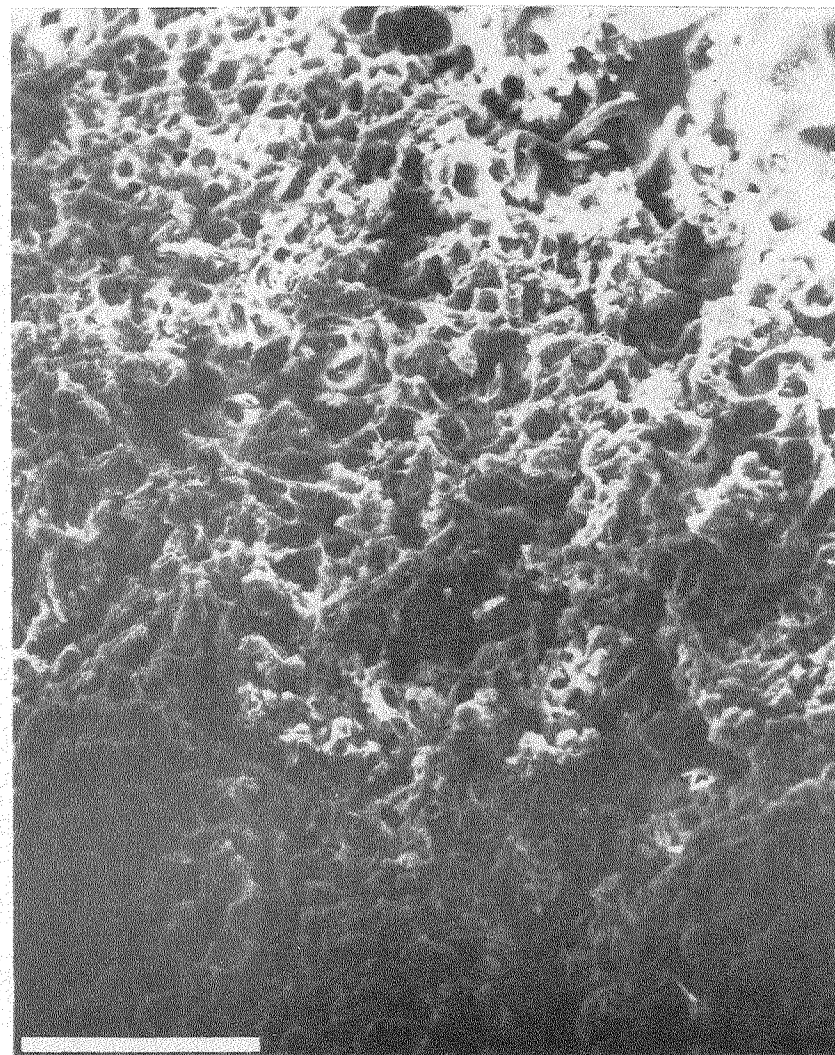
100 μm   (a)   100 μm   (b)

XBB 804-5020

Figure 51. Cellulose residue from treatment (250°C, 1 hr) and pyridine extraction

(a) $ZnCl_2$-CH_3OH (b) $ZnCl_2$-H_2O
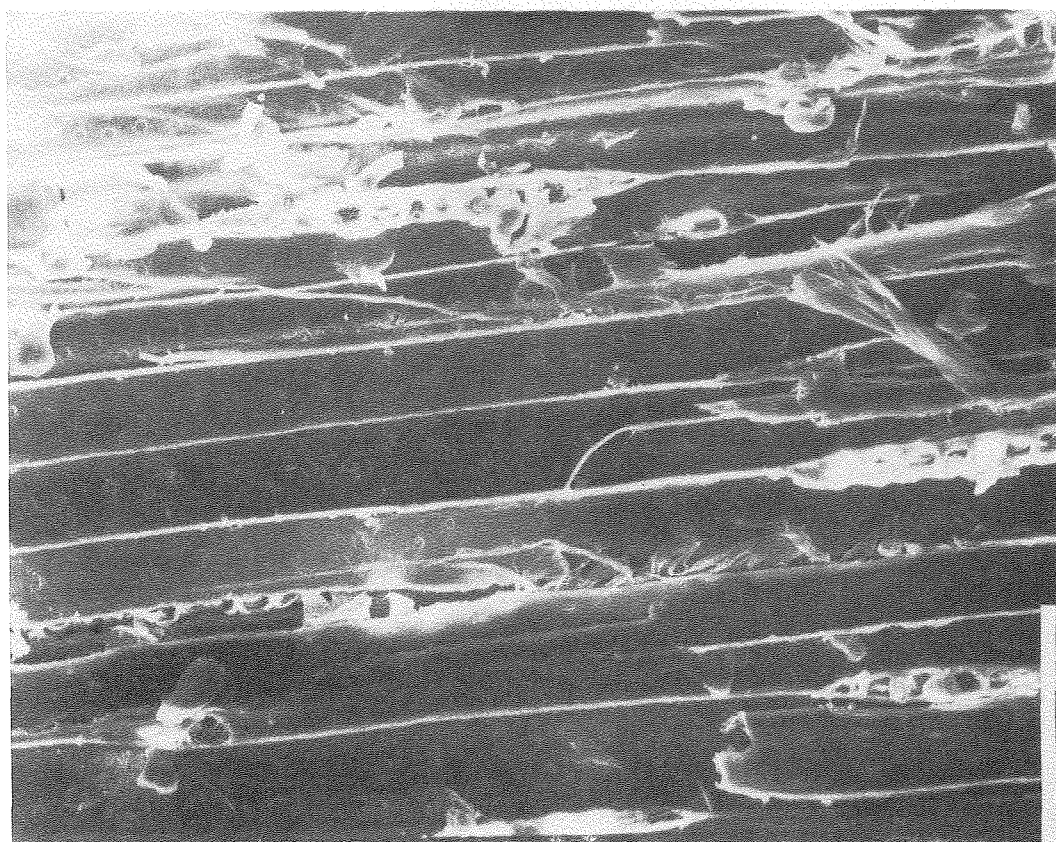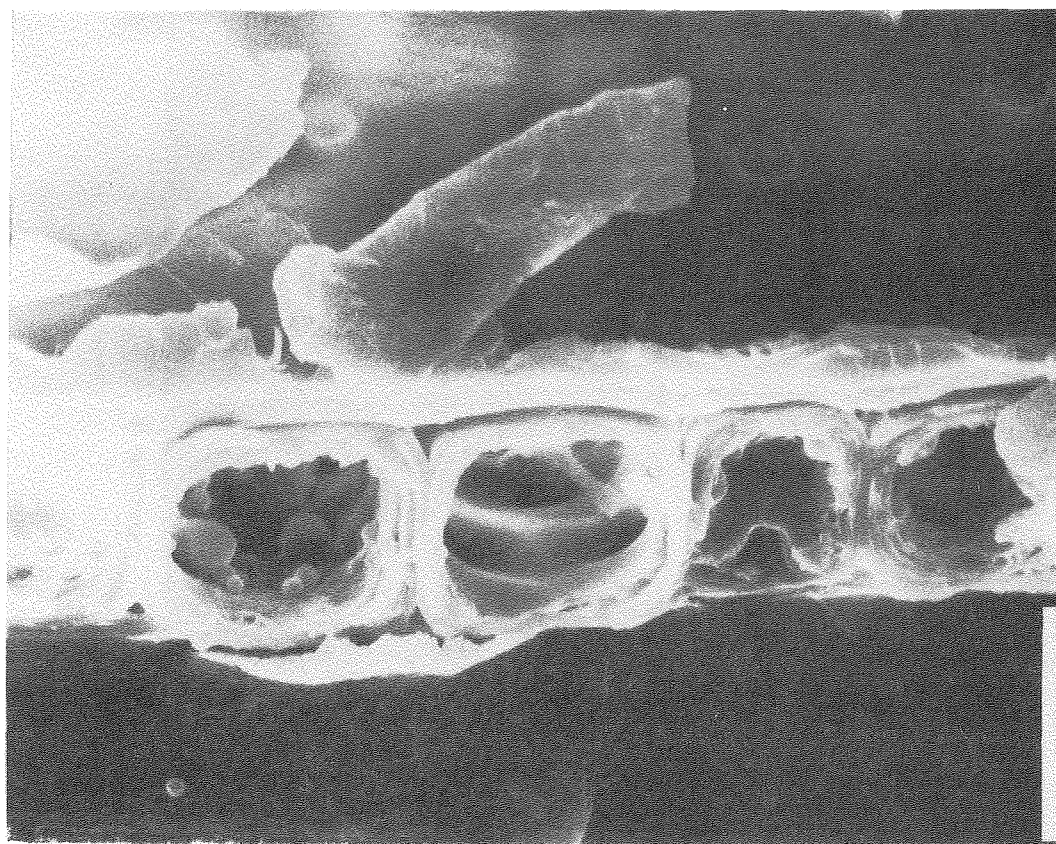
(a)   25 μm   (b)

Figure 52a,b. Untreated wood chips

100 μm   (a)   25 μm   (b)

100 μm   (c)

XBB 804-5022
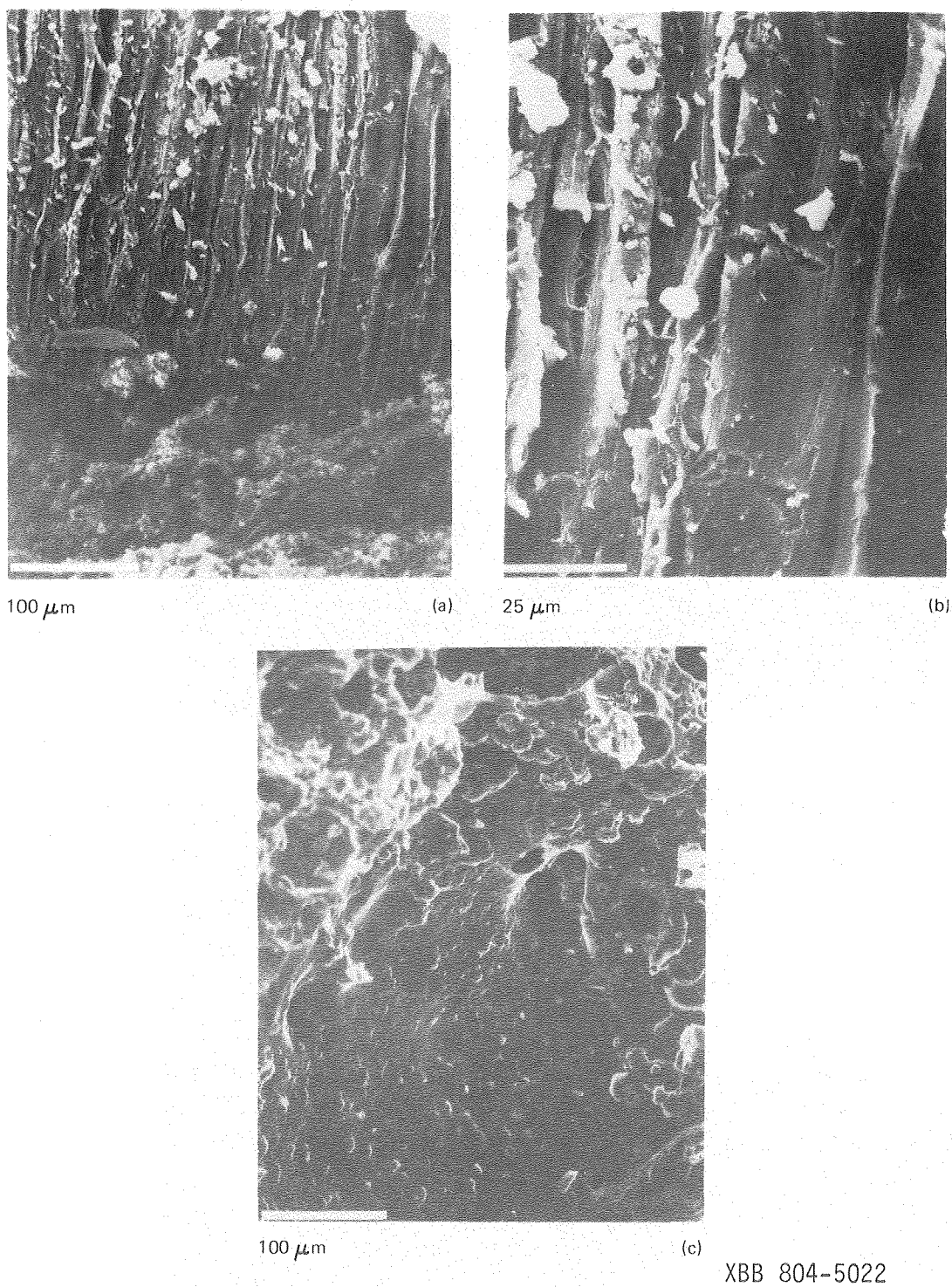
Figure 53. Wood chips after treatment with $ZnCl_2$-CH_3OH at 250°C
(a,b) Heatup only   (c) 1 hr reaction time

treatment at 250°C, followed by pyridine extraction which removes nearly all the organic content, the mainly mineral residue (or "ash") respresents another complete change in appearance (Figure 54c).

The effect of lower-temperature treatment, at 200°C, was compared with the relatively successful treatment at 250°C which has just been described. Even at 200°C, great physical and chemical change occur (Figure 55a), even with only 6% solubilization. The original structure has been fragmented extensively. Extraction with pyridine again shows the disarranged remains of the initial fibrous structure (Figure 56a). The effects are qualitatively similar to those with heatup to 250°C, althouth the product has a different appearance. The extensive deformation in both cases shows that a relatively large amount of chemical reaction has occured, even though it has not resulted in much pyridine-soluble product.

Gel-Permeation Chromatography

GPC analysis has been used to characterize the reaction products more fully, and gain clearer insight into the mechanisms of wood liquefaction. The effect of reaction variables on the molecular-weight distribution was investigated for various product fractions listed in Table 56.

Figure 57 shows the molecular-weight distribution in oils, asphaltenes, and preasphaltenes produced in one hour of treatment at 250°C. As expected, molecular size decreases
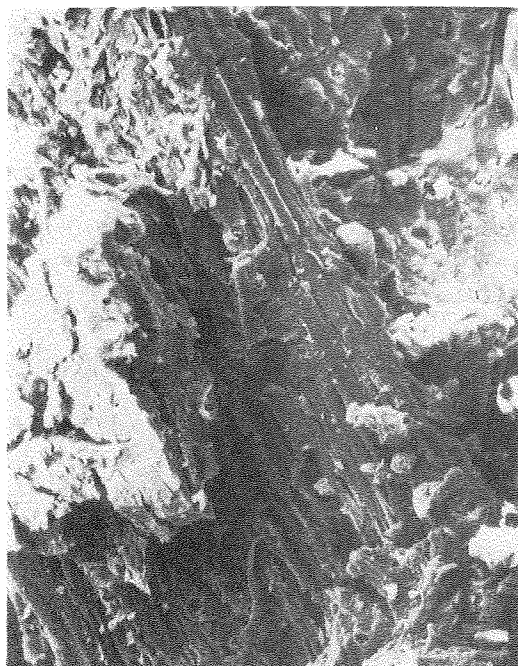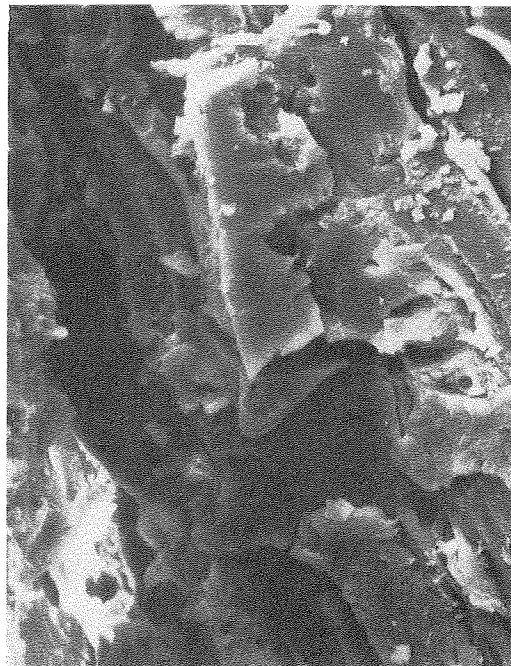
100 μm   (a)   25 μm   (b)
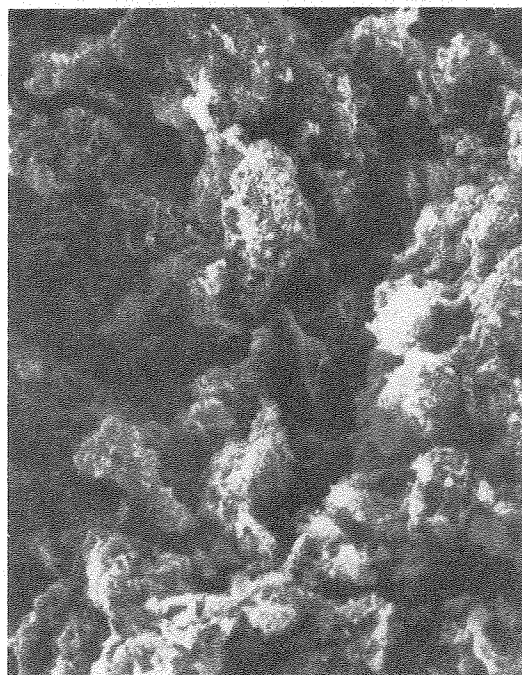
25 μm   (c)

XBB 804-5023

Figure 54. $ZnCl_2$-CH_3OH treatment (250°C) of wood after pyridine extraction (a,b) heatup only (c) 1 hour reaction time
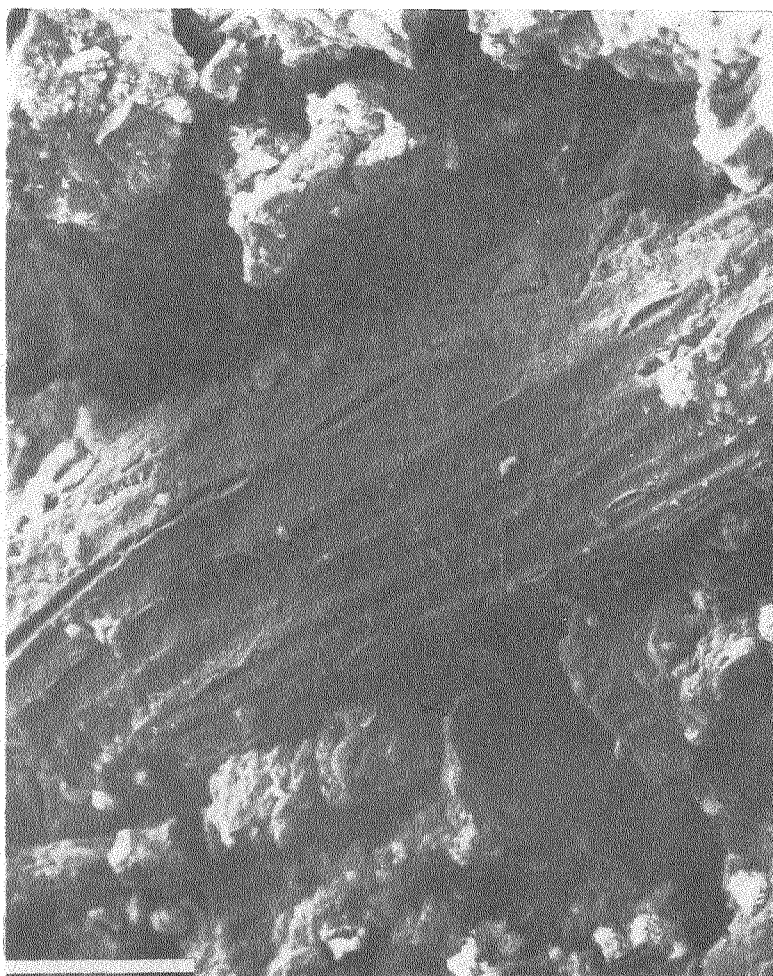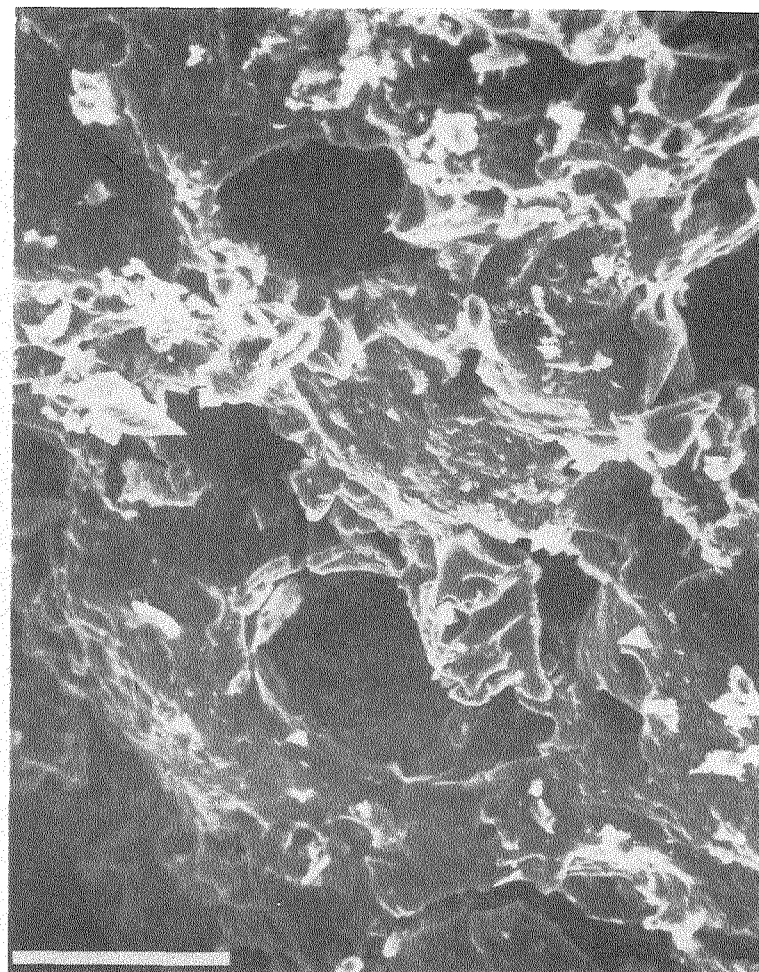
100 μm   (a)   100 μm   (b)

XBB 804-5026

Figure 55. Effect of temperature on $ZnCl_2$-CH_3OH treatment of wood for 1 hr at
       (a) 200°C   (b) 250°C

50 μm (a) 100 μm (b)
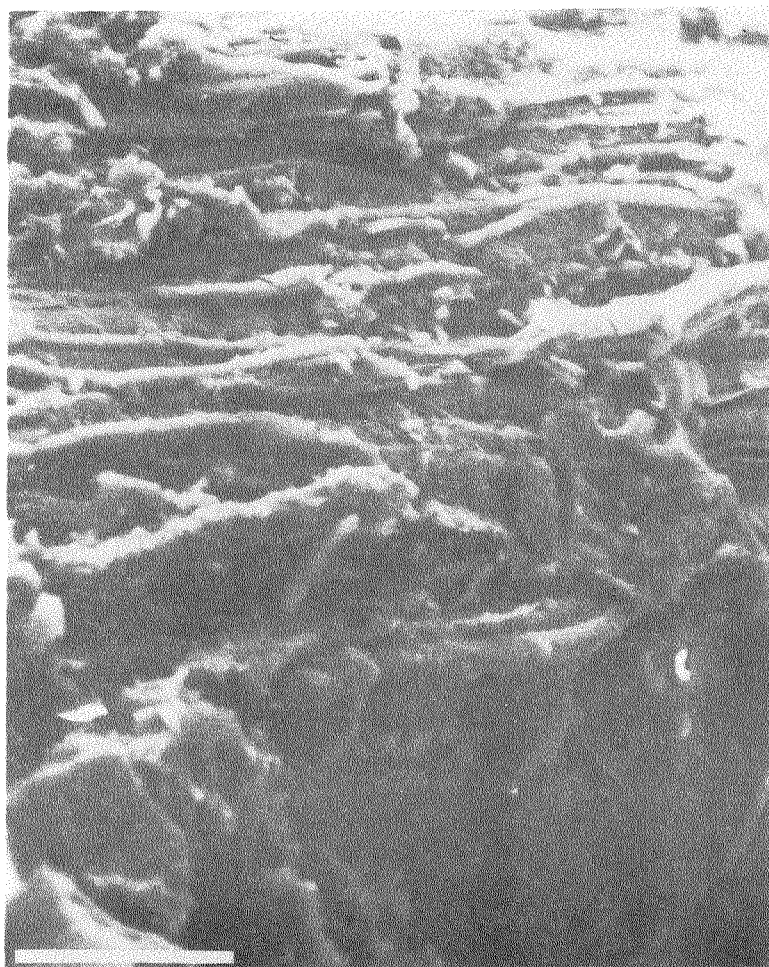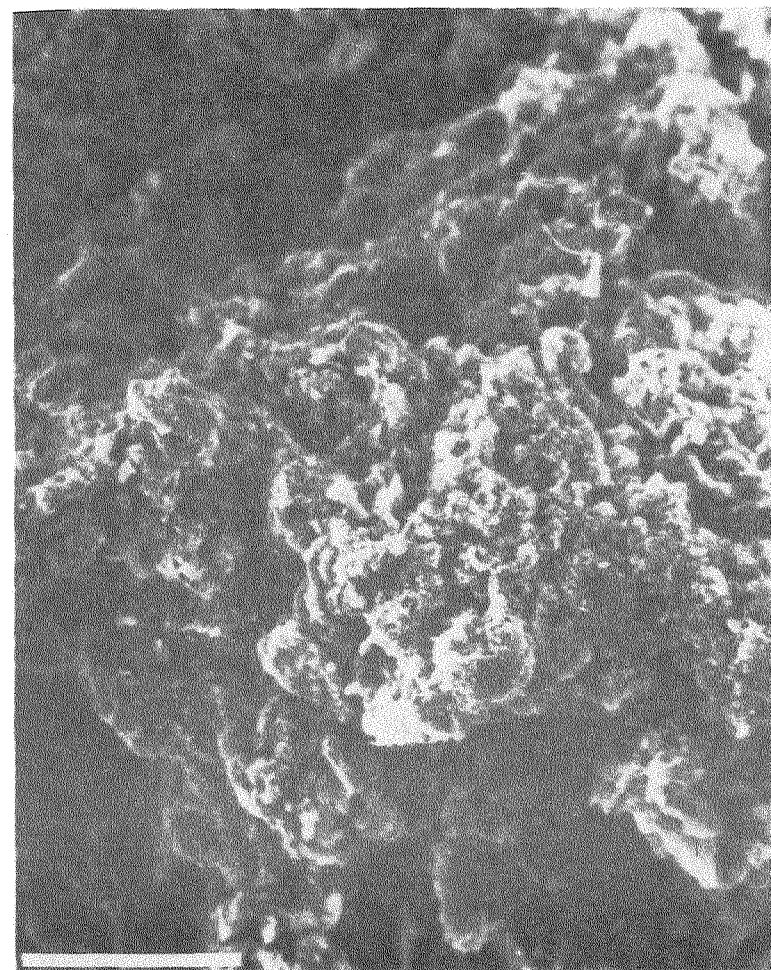
Figure 56. Wood residue after $ZnCl_2$-CH_3OH treatment (1 hr) and pyridine extraction
(a) 200°C   (b) 250°C

192

Table 56. Treatment Conditions and Extraction Yields for Wood Samples Examined by Gel-Permeation Chromotography (250 gm $ZnCl_2$, 50 gm CH_3OH; 800 psig H_2)

Run No.	Temp. ($^\circ$C)	Time (min)	Recovered Solids, daf. Basis, %		
			Oils	Asphaltenes	Preasphaltenes
22	225	60	12	9	33
28	250	0	0	0	11
21	250	60	31	17	52
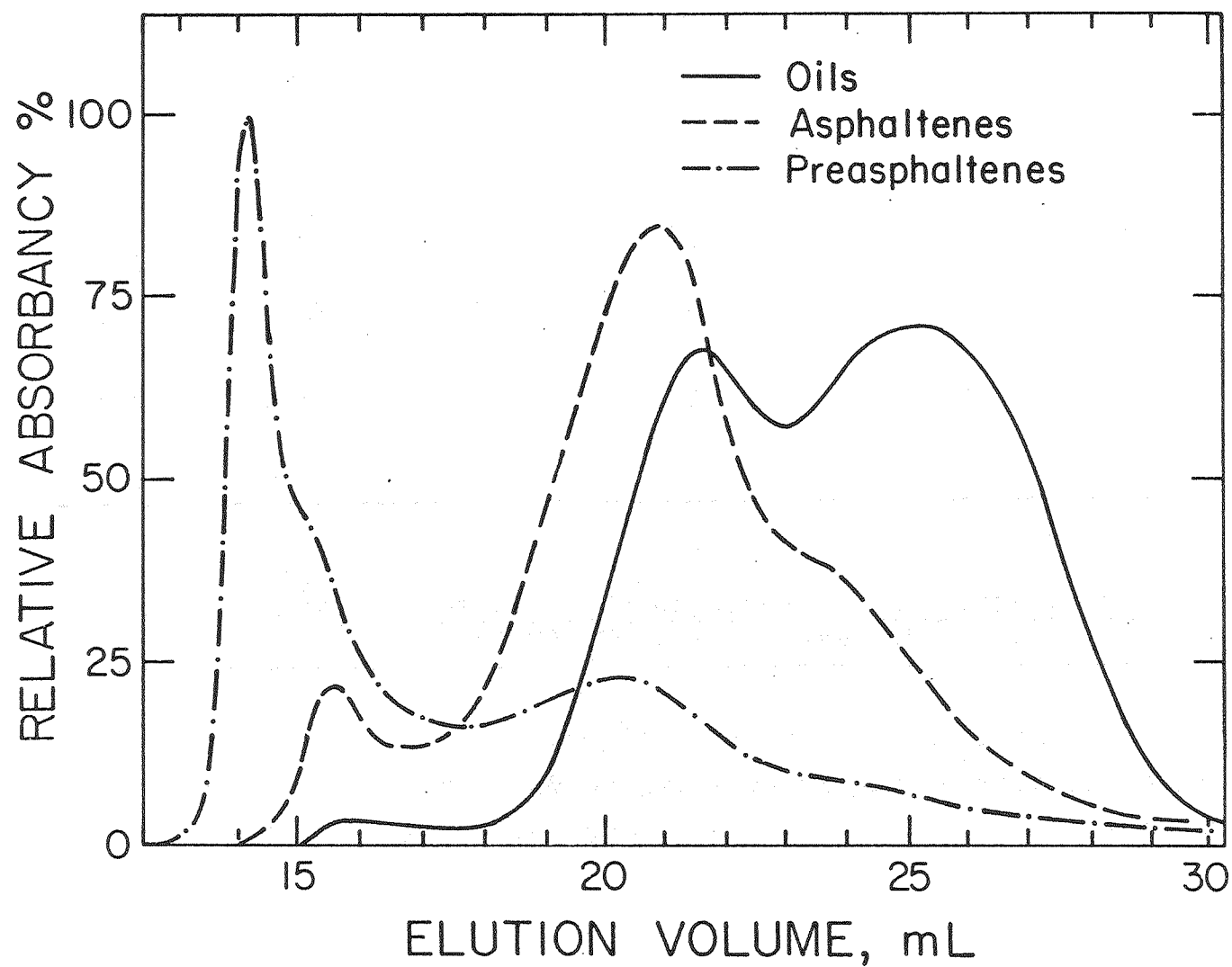
Figure 57. Elution of various reaction products from a gel-permeation column.

XBL 804-635

in the order preasphaltenes>asphaltenes>oils.

Paradoxically, more stringent reaction conditions serve to increase the average molecular weight of the preasphaltenes, as their yield improves (Figure 58). With heatup only, the preasphaltenes are composed predominantly of low-molecular-weight components, with a relatively low melting point (Run 28, Table 57). The explanation is that during wood solubilization, different chemical bond types are cleaved at different extents of reaction, with the weakest bonds being opened the earliest. Disappearance of the low-molecular-weight products at higher reaction times can be ascribed most probably to further hydrogenation (rendering them transparent to the UV detector), and/or subsequent conversion to asphaltenes and oils. Because of the low yield of Run 28, the molecular weight distribution of asphaltenes and oils could not be studied.

The effect of reaction temperature on the molecular weight distribution of the preasphaltenes is shown in Figure 59. Reaction at lower temperature (225°C) also gives lower molecular weight components, again reflecting the lower extent of reaction. However, no significant difference was observed in either the oils or asphaltenes, between the 225° and 250°C runs.

Melting Point Determination

The melting points of representative product fractions were determined, as shown in Table 57. Asphaltenes and
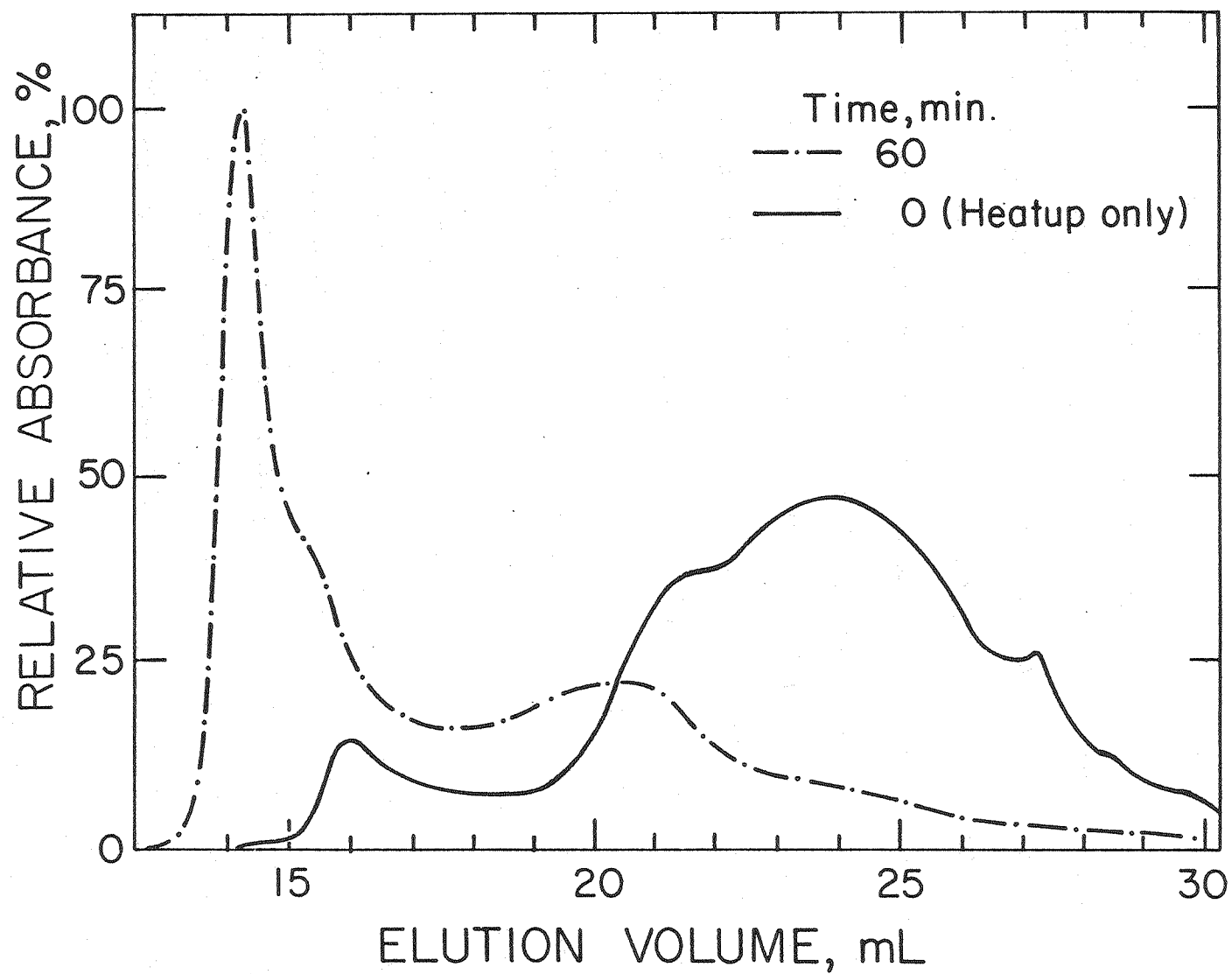
Figure 58 . Effect of reaction time on elution of   XBL 804-634
preasphaltenes from a gel-permeation column.

Table 57. Melting points of the various extracts.

(250 gm $ZnCl_2$, 50 gm CH_3OH.)

Run No.	Substrate*	Temp. (°C)	H_2 Press. (psig)	Time (min)	Cumulative Pyridine Extractibles, %	Melting Points (°C)		
						Oils	Asphaltenes	Preasphaltenes
11	Cellulose	250	500	60	92	85-106	152-181	over 400
20	Lignin	250	500	60	85	83-130	109-152	264+[S]
21	Wood flour	250	800	60	99	98-153[T]	258+[S]	over 400
24	Wood chips	250	800	60	98	82-129	229+[T]	over 400
25	Wood chips	250	500	60	93	92-136	227+[T]	127+[S]
26	Wood chips	250	200	60	99	81-112	252+[T]	over 400
28	Wood chips	250	800	0	11	——	——	103-158
29[++]	Wood chips	225	500	60	16	——	108-137	147-[S]
30[+]	Wood chips	225	500	60	46	86-116	168-276[T]	over 400
32	Wood flour	225	200	60	26	——	164-241[T]	over 400

S: A small percentage of sample melts leaving behind a solid residue. T: Tarry residue.
*: Amounts used are given in Table 8. +: 25 gm CH_3OH used.   ++: 75 gm CH_3OH used.
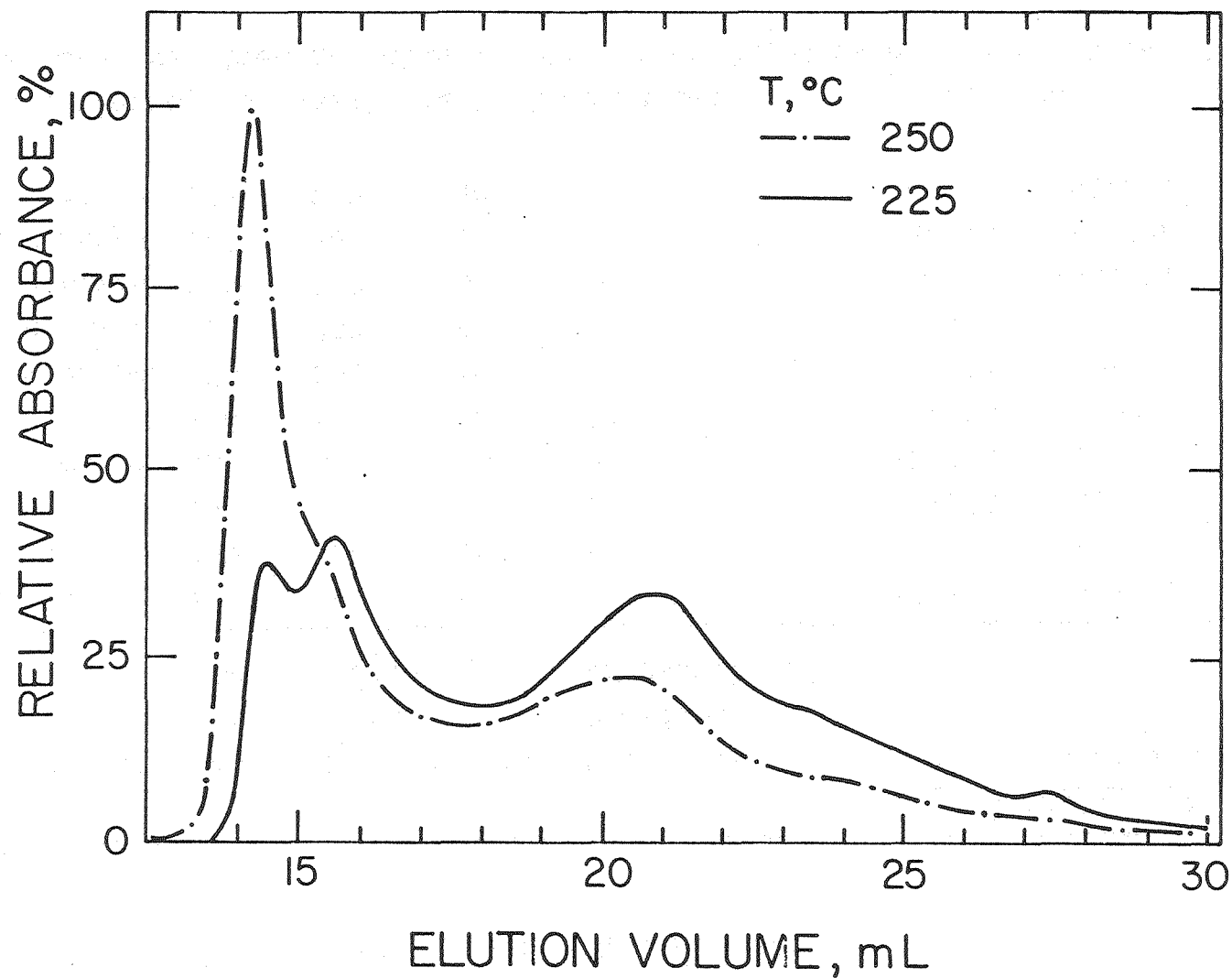
Figure 59 . Effect of temperature on elution of preasphaltenes from a gel-
permeation column.

XBL 804- 636

preasphaltenes derived from lignin showed lower melting points than those derived from cellulose. No significant difference was observed between wood flour and wood chips. While hydrogen pressure and reaction temperature have no significant effect on the melting points, reaction time had a marked effect. Mere heatup produced preasphaltenes with a melting-point range resembling that of asphaltenes, in general agreement with the gel-permeation chromatograph of the preasphaltenes from Run 28 as discussed above. Low methanol loading produces higher-melting products.

DISCUSSION

Reaction between a solid and a liquid depends greatly on the effectiveness of contact between them. Hence the ability of the zinc chloride-methanol melt to penetrate the pores of wood particles to extract the reaction products, as shown by scanning electron micrography, plays a major role in the biomass liquefaction runs. The superiority of methanol over water in achieving penetration of the wood structure may be due to, first, its lower viscosity, and second, its greater organic character and consequent compatibility with wood.

The scanning electron micrographs show that certain parts of the wood fibers are weaker than others and hence more easily solubilized. Swelling of the fibers, cutting them into fragmented units, peeling of the topmost layers constitute the first stages in wood solubilization. Having both hemicellulose and lignin on the outer layers and equally

sandwiched between blocks of cellulose molecules can explain the scraping and peeling of outermost layers and cutting of the fibers into fragmented units, cbserved under low-yield conditions.

Investigation of the low-conversion regime is needed to throw more light on the conversion mechanism. Short contact time (0-15 min.) at low temperatures (200°-225°C) will prove useful.

CHAPTER V

SUMMARY AND CONCLUSIONS

COAL

This investigation has provided new data on the re-
activity of coal at pre-pyrolysis temperatures. A very high
conversion of coal to oils has been achieved. This has re-
sulted partly from the addition of finely powdered metals,
especially metallic zinc, it not being known whether they
dissolve or remain in suspension. Reasonable correlation
has been found between the yield of oils and the H/C ratio
of the melt-treated coal, reflecting the fact that consider-
able hydrogenation is required to form the oils.

Operating at higher temperatures gives improved yields,
oils reaching a maximum at 325°C. Nearly complete conversion
of coal to extractible products is achieved in 30-minute
reaction time at temperatures of 275° to 300°C; this conver-
sion tends to fall off at 325°C or above.

A staged progression of two or more reaction tempera-
tures in series has been found to increase both the overall
conversion and the yield of oils. Our results show that
initial treatment at 275°C is beneficial, preferable to pre-
treatment only at 250°C, and equivalent to pretreatment at
both 250° and 275°C. Comparing a run at 275°C with one at
300°C, or with a staged run at 275°/300°C, there is no incen-
tive to operate at 300°C. Operation at 300°C, instead of
275°C slightly increases methanol incorporation and slightly
reduces the H/C ratio. Increasing the temperature to 325°C
after an initial stage at a lower temperature, brings about
a substantial product improvement, including a 54% yield of

oils.

It is also important to note that the preasphaltenes ob-
tained at 325°C are considerably different from those obtain-
ed at either 275° or 300°C. The higher-temperature preasphal-
tenes begin to melt at 200°C, and nearly 30% have melted by
400°C; whereas the lower-temperature preasphaltenes do not
melt below 400°C. In GPC studies, the higher-temperature
preasphaltenes show a lower average molecular weight with
fewer aromatic fused rings. SEM studies show that a complete
structural change has taken place in the 325°C treatment.

Increasing the reaction temperature to 340°C results in
degeneration of the oils, and further lowers the melting
point of the preasphaltenes. The former is highly undesir-
able and indicates the need after treatment at 325°C, for a
phase separation (not yet perfected) before undertaking any
higher-temperature treatment. The latter is of great signi-
ficance, since it demonstrates that still higher temperatures
(or longer residence time at 340°C) could further convert
preasphaltenes to low-melting-point components.

The effect of reaction time was studied at both 275°C
(between 0 and 45 minutes) and 325°C (between 0 and 30 min-
utes). At 275°C, all product fractions increase with reac-
tion time; the most rapid increase is observed in the first
15 minutes. At 325°C, the yield of oils increases at a
fast rate for the first 15 minutes after which a moderate in-
crease is observed. The H/C ratio of the melt-treated coal
increases with reaction time, the bulk of the increase oc-

curring in the second 15 minutes. Staged operation involving 20 minutes at 275°C and 20 minutes at 325°C, a combination not actually tried, may give the best result.

The high conversions obtained consume a considerable part of the batch charge of hydrogen to the reactor. Maintaining a high hydrogen partial pressure throughout the reaction is shown to be beneficial, in terms of high yields of oils and increased H/C ratio of the products. High hydrogen concentration was maintained by recharging fresh hydrogen one or more times during the reaction.

Methanol loading between 35 to 65 gm, for a zinc chloride loading of 250 gm had no significant effect on product distribution. A particle-size change from -30 +60 mesh to -60 to +100 mesh did not affect either coal solubilization or product H/C ratio, confirming that intraparticle diffusion does not restrict reaction rate under these operating conditions.

Zinc oxide in combination with metallic zinc appeared to show beneficial effects on coal conversion. However, when used alone (2.5% of the melt), it reduced the catalytic activity of zinc chloride. All the inorganic salts investigated increased the yield of preasphaltenes, and had little effect on the yield of oils and asphaltenes.

Of the complexants studied, urea and malonic acid showed high levels of incorporation and resulted in a reduction in coal conversion, whereas hexyl mercaptan and bipyridine increased the yield of oils. Although added wetting agents were highly incorporated, they did improve the yield of oils.

Acetonitrile, added as a trial co-solvent with methanol, strongly reduced the catalytic activity of zinc chloride.

In a study of alternate inorganic catalytic systems, the antimony chloride-methanol system proved to have high catalytic activity even at low temperatures. At 225^OC, 75% conversion to pyridine-soluble materials was obtained, compared to only 40% with zinc chloride. Its catalytic activity diminishes when used in small amounts with zinc chloride. Antimony chloride is difficult to separate from the reaction products, and was strongly corrosive to stainless-steel reactor internals.

As was previously known, very low conversions are obtained in phosphoric acid treatment, and it was thought desirable to examine whether such treatment produces a refractory char. When the phosphoric acid-treated coal was reacted in $ZnCl_2$-CH_3OH at 275^OC, nearly complete conversion occurred, showing that the coal had not been irreparably damaged.

Calcium chloride, investigated as a possible diluent for zinc chloride, strongly reduced the catalytic activity when used in massive amounts. The higher methanol content needed to form a melt, and the possible increased formation of tetrachlorozinc anions may both have contributed to this result.

BIOMASS

The zinc chloride-methanol catalytic system has been shown to be active in the solubilization of wood. The major wood constituents, cellulose and lignin, showed high relativity

and this effect was substantiated in later runs on wood flour and wood chips. Irrespective of their particle size, both forms of wood showed the same high levels of conversion. On a dry, ash-free basis, a carbon recovery of 79% was obtained with a charge of cellulose, and a 90% recovery for both wood flour and wood chips.

Wood solubilization is highly temperature-dependent, starting with less than 10% conversion at $200^{\circ}C$ and approaching complete conversion at $250^{\circ}C$. Methanol incorporation increased with temperature, and decreased with hydrogen pressure leading to an incorporation of 0.17 gram of retained methanol per gram of wood-derived organic producted in reactions at $250^{\circ}C$ with 500 psig of hydrogen.

Reaction is fast at $250^{\circ}C$ with nearly 80% conversion in the first 25 minutes, and near complete conversion in 60 minutes. The H/C ratio of the MTW depends somewhat on hydrogen pressure; a large increase occuring between 200 and 500 psig at $250^{\circ}C$.

Maximum catalytic activity of zinc chloride is observed with roughly 0.85 mole methanol per mole of zinc chloride, or 40 grams per 250 grams. At maximum catalytic activity, methanol incorporation reaches a maximum, whereas the H/C ratio of the product is at a minimum.

Under treatment, wood changes markedly in form before solubilization begins. At low solubilization, the bulk of the wood is converted to preasphaltenes, with oils and asphaltenes being formed as the reaction increases. Oxygen removal correlates well with solubilization. Two forms of ox-

ygen functionality are kinetically distinct, the first form being easily removed whereas the second is more resistant to attack.

SEM studies show that swelling and fragmenting of the fibers are the first effects in conversion. Methanol is more effective than water in enabling the catalyst to penetrate the solid substrate.

Comparing wood and coal, we find wood to be more reactive.

REFERENCES

A1   A.L. Austin, B. Rubin, Lawrence Livermore Laboratory Report UCLL-51221 (May 30, 1972).

A2   J.A. Alich, F.A. Schooley, R.K. Ernest, K.A. Miller, B.M. Louks, T.C. Veblen, J.G. Witwer, and R.H. Hamilton, Symp. on Fuels and Energy from Renewable Resources. 174th ACS Meeting, Chicago. (Aug. 1977).

A3   A. Attar and F. Dupius, On the Distribution of Sulfur Groups in Coal, Prep. Div. Fuel Chem., ACS, 23, (2), 44 (1978).

A4   J. Alich, R.E. Inman, and K. Ernest, An Evaluation of the Use of Agricultural Residues as an Energy Feedstock Menlo Park, Calif.: S.R.I. (July 1976). NTIS PB-260, 763. Also, S.R.I. Crop, Forestry and Manure Residue Inventory-Continental United States (June 1976), S.R.I. Project 5093.

A5   J.A. Alich, and R.E. Inman. Effective Utilization of Solar Energy to Produce Clean Fuels. Final Report. Menlo Park, CA: S.R.I., Project 2643, (June 1974).

A6   V.A. Avilov, O.N. Eremenko, O.N. Efimov, A.G. Ovcharenko, P.S. Chekrii, and M.L. Khidekel, 2nd All-Union Conf. on Liquid-Phase Catalytic Reactions, Izv. Nauka Kazakh SSR. Alam-Ata, 147 (1966).

A7   V.A. Avilov, M.L. Khidekel, O.N. Efimov, A.G. Ovcharenko, and P.S. Chekrii. U.S. Patent 3,755,194 (1973); Brit. Pat. 262,855 (1972); Can. Pat. 943, 132 (1972).

B1   L. Blom, L. Edelhausen and D.W. Van Krevelen, Fuel, 36, 135 (1957).

B2   B.M. Benjamin, V.F. Raaben, P.H. Maupin, L.L. Brown, and
     C.J. Collins, Fuel, 57, 269 (1978).

B3   D.M. Bodily, Stanford Res Inst., Coal Chemistry Workshop,
     1, Session 1, Paper 5. Menlo Park, CA. (1976).

B4   D.M. Bodily, S.H. Lee, and W.H. Wiser, Preprints, Div. of
     Fuel Chem., A.C.S., 20 (3), 7 (1975).

B5   British Petroleum, Ltd., Gas Making and Natural Gas,
     London (1972).

B6   M. Boudart, J.A. Cusumano, and R.B. Levy, New Catalytic
     Materials for the Liquefaction of Coal prepared by Cata-
     lytica Assocs. for EPRI (Oct. 1975).

B7   D.M. Bodily, Preprints, Div. of Fuel Chem., A.C.S., 16
     (2), 124 (1972).

B8   Bechtel Corp. Fuels from Municipal Refuse for Utilities-
     Technology Assessment. Prepared for EPRI: NTIS PB-242,
     413 (March 1975).

B9   W.R. Benson, Biomass Potential from Agricultural Produc-
     tion in Conference Proceedings, Biomass-a cash crop for
     the future? Midwest Research Inst. and Battelle
     Columbus Labs, 85-110 (March 1977).

B10 B.L. Browing, The Chemistry of Wood Interscience, N.Y.
     (1963).

B11 A.S. Berenblyum, V.A. Grinberg, M.L. Khidekel, and V.V.
     Tsodikov, Izv. Akad. Nauk U.S.S.R. Ser. Khim, 3, 696
     (1973).

B12 F.B. Boucher, Pyrolysis of Industrial Wastes for Oil and
     Activated Carbon Recovery EPA-600/2-77-091 (May 1977).

C1   Chem. & Engr. News, (Aug. 27, 1979).

C2 Coal Processing-Gasification, Liquefaction, Desulfuriza-
    tion. A Bibliography. U.S. A.E.C. (1974).

C3 B.P. Curran, R.T. Struck, and E. Gorin, Ind. Eng. Chem.,
    Proc. Des. Dev., 6 (2), 167 (1967).

C4 W.G. Courtney, Ann. N.Y. Acad. Sci. 200, 717 (1972).

C5 F.A. Cotton & G. Wilkinson. Advanced Inorganic Chemis-
    try, 3rd Edition, John Wiley & Sons (1972).

C6 G.P. Curran, R.T. Struck and G. Everrett, Ind. Eng. Chem.
    Proc. Des. Dev., 6, 166 (1967).

D1 N.C. Deno, B.A. Greigger, and S.G. Stroud, Fuel, 57, 455
    (1978).

D2 N.C. Deno, B.A. Greigger, L.S. Messer, M.D. Meyer, and
    S.G. Stroud, Tetrahedron Lett., 1703 (1977).

D3 N.C. Deno, E.J. Jedziniak, L.S. Messer, M.D. Meyer, S.G.
    Stroud, and E.S. Tomezsko, Tetrahedron, 33, 2503 (1977).

D4 T.T. Derencsenyi and T. Vermeulen, Lawrence Berkeley Lab-
    oratory Report LBL-3265 (1975).

D5 C. Doree and L. Hall, J. Soc. Chem. Ind. 43, 257 T (1924).

D6 T.T. Derencsenyi and T. Vermeulen, Lawrence Berkeley Lab-
    oratory Report LBL-9777 (Sept. 1979).

E1 G. Eglinton and M.J. Murphy, eds., Organic Geochemistry,
    Springer Verlag, (1969).

E2 EPRI ER-746-SR, Biofuels: A Survey (June 1978).

E3 O.N. Efimov, M.L. Khidekel, V.A. Avilov, P.S. Chekrii,
    O.N. Eremenko, and A.G. Ovcharenko, Zh. Obshch. Khim., 38
    (12), 2668-2677 (1968).

E4 O.N. Efimov, O.N. Eremenko, A.G. Ovcharenko, M.L. Khid-
    ekel, and P.S. Chekrii, Izv. Akad. Nauk U.S.S.R. Ser.
    Khim. 4, 855 (1969).

E5 V.H. Emmons, and W. Tautz, Z. anorg. allg. chem. 388
    245-256 (1972).

F1 L.E. Furlong, E. Effron, L.W. Vernon, and E.L. Wilson,
    Coal Liquefaction by the Exxon Donor Solvent Process,
    presented at Am. Inst. Chem. Eng. Natl. Meeting, Los
    Angeles (Nov. 1975).

F2 K. Freudenberg and A.C. Neish, Constitution and Biosyn-
    thesis of Lignin, Springer-Verlag, (1968).

G1 H. Gan, S.P. Nandi, and P.L. Walker, Jr., Fuel, 51,
    272 (1972).

G2 P.H. Given, Preprints, Div. of Fuel Chem., A.C.S. 20
    (1), 66 (1975).

G3 D.W. Goheen, Advances in Chem. Ser. A.C.S., 59, 205
    (1966).

G4 H.V. Gaal, H. Cuppers and A. Ent, J. Chem. Soc. Chem.
    Comm., 1694 (1970).

H1 R. Hayatsu, R.E. Winans, R.G. Scott, L.P. Moore and M.H.
    Studier, Fuel, 57, 541 (1978).

H2 J.L. Huston, R.G. Scott and M.H. Studier, Fuel, 55, 281
    (1976).

H3 L.A. Heredy and M.B. Neuworth, Fuel, 41, 221 (1962).

H4 L.A. Heredy, A.E. Kostyo and M.B. Neuworth, Fuel, 43,
    414 (1964).

H5 L.A. Heredy, A.E. Kostyo and M.B. Neuworth, Fuel, 44,
    125 (1965).

H6 H.C. Hottel and J.B. Howard, New Energy Technology, M.I.T. Press, (1974).

H7 B. Hlavica, Palivai a Topeni 11, 150, (1929); via Chem. Abstr., 24, 4914 (1930).

H8 W. Hodek and L. Kuehn, Compend-Dtsch Ges Mineraleelwiss. Kohlechem, 76-7 (1), 384 (1976); via Chem. Abstr. 87, 204094g (1977).

H9 R.R. Holten and T. Vermeulen, Lawrence Berkeley Laboratory, Report LBL-5948 (1977).

H10 F. Hershkowitz and E.A. Grens, Lawrence Berkeley Laboratory, Berkeley, report in preparation.

H11 K. Howlett & A. Gamache, Silviculture Biomass Farms; Vol. IV, Forest and Mill Residues as a Potential Source of Biomass, Georgia Pacific Corp., Mitre Corp., Techn. Rept. 7347, Vol. 4, (May 1977).

H12 N. Holy, T. Nalesnik, and S. McClanahan, Fuel, 56, 47 (1977).

H13 R. Hayatsu, R.G. Scott, L.P. Moore, and M.H. Studier, Nature, 261, 77 (1976).

H14 R. Hayatsu, R.G. Scott, L.P. Moore, and M.H. Studier, Nature, 257, 378 (1975).

I1 Institute of Gas Technology, Sumposium Papers-Clean Fuels from Coal. Chicago, (Sept. 1973).

I2 R.E. Inman, Silviculture Biomass Farms; Vol. 1 Summary, McLean, Va.: Mitre Corp. Technical Report 7347, Vol. 1 (May 1977).

I3 Intertechnology/Solar Corp. The Photosynthesis Energy Factory: Analysis, Synthesis and Demonstration. Warren-

town, Va. (June 1977).

J1   L. Jurasek, A.I.Ch E. 72nd Annual Meeting, San Francisco,
      (Nov. 1979).

J2   W.R. Jackson, F.P. Larkins, M. Marshall, D. Rash, and
      N. White, Fuel, 58, 281 (1979).

J3   B.R. James, and L.D. Markham, Inorg. Chem., 13, 97
      (1974).

J4   B.R. James, Homogeneous Catalysis, John Wiley & Sons,
      N.Y. (1973).

K1   N. Kanda, H. Itoh, S. Yokoyama, and K. Ouchi, Fuel, 57,
      676 (1978).

K2   W. Kawa, Preprints, Div. of Fuel Chem., A.C.S., 14, (4)
      Part 1, 19 (1970).

K3   D.L. Klauss, and S. Ghosh, Fuel Gas from Organic Wastes
      Chem. Tech. 3 (11), 689, (1973).

L1   H.H. Lowry, ed., Chemistry of Coal Utilization, Suppl.
      Vol., John Wiley & Sons, (1963).

L2   A. Lachman, U.S. Patents, 1, 826,787 (Oct. 13, 1932).
      2,035,607 (March 31, 1935), 2,042,718 (June 2, 1936).

L3   E.S. Lipinsky, System Study of Fuels from Sugar Cane,
      Sweet Sorghum, and Sugar Beets, Vol. 11, Agricultural Con-
      siderations. Battelle, Columbus Laboratories BMI-1957,
      Vol. 2. (Dec. 1976).

L4   E.S. Lipinsky, System Study of Fuels from Sugar Cane,
      Sweet Sorghum and Sugar Beets; Vol. IV, Corn Agricul-
      ture, Battelle, Columbus Laboratory, BMI-1957A, Vol. 4
      (March 1977).

L5 A. Lindblad, Ing. Ventenskaps Akad, Handl. 107, 7
    (1931).

L6 J.W. Larsen, ed., Organic Chemistry of Coal A.C.S.
    Symp. Ser., 71, Washington, D.C., (1978).

L7 Y.Z. Lai, F. Shafizadeh, and C.R. McIntyre, A.C.S.
    Symp. Ser. 48, 257 (1977).

M1 F.R. Mayo, J.G. Huntington and N.A. Kirshen, Chemistry of
    Coal Liquefaction A.C.S. Symp. Ser. 71 (1978).

M2 G.M. Makh, Zh. Prikl. Khim., Leningr, 10,457 (1939).

M3 D.K. Mukherjee, and P.B. Chowdhury, Fuel, 55, 4 (1976).

M4 O.P. Mahajan, A. Tomita, J.R. Nelson and P.L. Walker,
    Jr. Fuel, 56, 33 (1977).

M5 D.P. Mobley, Ph.D. Thesis, Dept. of Chem. Eng., Univ. of
    California, Berkeley, (June 1980).

M6 E.O. Mariani, The Eucalyptus Fuel Plantation as a New
    Source of Energy. Beverly Hills, CA. Marelco Inc.,
    (1976).

M7 E.L. Muetterties, and F.J. Hiresekorn, J. Am. Chem. Soc.
    96, 1920 (1974).

M8 L. Metrico, and S. Pellizza, Med. Lav. 65, 174 (1974).

M9 J.B. McLean, and T. Vermeulen, Lawrence Berkeley Labor-
    atory Report LBL-6858 (Dec. 1977).

M10 J. Maienschein, Ph.D. Thesis, Dept. of Chem. Eng., Univ.
    of California, Berkeley, in preparation.

M11 R.G. MacDonald, ed., The Pulping of Wood Vol. 1, 2nd
    Edition, McGraw Hill Book Co. (1969).

M12 M.V. McCabe, and M. Orchin, Fuel, 55, 266 (1976).

M13 D.J. Medeiros, and E.E. Petersen, Lawrence Berkeley
    Laboratory Report LBL-4439 (Dec. 1975).

N1 National Coal Board Mining Dept., Control of Harmful
    Dust in Coal Mines, London (1973).

O1 W.J. Oswald, and C.G. Goljeke Biological Transformation
    of Solar Energy Adv. in Appl. Microbio. Vol. 2, 223-
    262 (March 1960).

P1 A. Pines and D.E. Wemmer, Stanford Research Institute
    Coal Chemistry Workshop, 1, Session IV, Paper 18, Menlo
    Park, (1976).

P2 M. Pell, W.A. Parker, J.T. Maskew, C.W. Zielke and R.T.
    Struck, Zinc Halide Technical Progress Report, CONOCO
    Coal Dev. Co., NTIS PC 11/MFA01 (Feb. 1, 1977-Jan. 31,
    1978).

P3 Project Western Coal: Conversion of Coal into Liquids-
    Final Rept. Res. and Dev. Rept. No. 18, prepared by the
    Univ. of Utah for the Office of Coal Research (May 1970).

P4 D.H. Page, Wood and Fiber 7, 246-248, (1976).

P5 K.W. Pilz, Min Eng. 24, 81 (1972).

P6 R.H. Perry, and C.H. Chilton, ed., Chemical Engineers'
    Handbook 5th Edition, McGraw Hill Book Co., (1973).

P7 G.R. Pastor, J.M. Angelovich and H.F. Silver, Ind. Eng.
    Chem.-Process Des. Dev. 9,609 (1970).

P8 R.B. Peel, J.S.V. Diaz and C.A. Luengo, Fuel 58 299
    (1979).

R1 F.W. Richardson, Oil from Coal, Chem. Techn. Rev. #53,
    Noyes Data Corp., Park Ridge (1975).

R2 V.F. Raaben, unpublished observation, for example, di-carboxylic acids through adipic acid were observed.

R3 I.B. Rapoport, and A. Khudyakova, Khimiya tverd. Topl. 7, 246 (1937); via Chem Abstr. 31, 1583[2] (1937).

R4 J.M. Radovich, P.G. Risser, T.G. Shannon, C.F. Pomeroy, S.S. Sofer, and C.M. Sliepcevivh, EPRI Rept. AF-974 TPS 77-716, (Jan. 1979).

S1 Shell, The National Energy Outlook, 1980-1990 (March 1973).

S2 J.E. Schiller, Anal. Chem. 49 (14), 2292 (1977).

S3 J.L. Shultz, T. Kessler, R.A. Friedel, and A.G. Sharkey, Jr. Fuel 51 242 (1972).

S4 J.W. Smith, Fuel 45, 233 (1966).

S5 J. Shinn and T. Vermeulen, Lawrence Berkeley Laboratory Report LBL-9372, Berkeley (1979).

S6 B.K. Schmid and D.M. Jackson, Recycle SRC Processing for Liquid and Solid Fuels, Proceedings: 4th Annual Int. Conf. on Coal Gasification, Liquefaction and Conversion to Electricity, Pittsburgh (1977).

S7 B.K. Schmid, and D.M. Jackson, The SRC II Process; Pro-ceedings: 3rd Annual Int. Symp. on Gasification and Liquefaction, Pittsburgh (1976).

S8 F.B. Sellers, U.S. Patent, 2,753,296 (July 3, 1956).

S9 W.P. Scarrah, Ph.D. Thesis, Dept. of Chem. Engr., Montana State Univ., Bozeman, MT (June 1973).

S10 R.T. Struck, W.E. Clark, P.J. Dudt, W.A. Rosenhoover, C.W. Zielke and E. Gorin, Ind. Eng. Chem.-Proc. Des.

Dev., 8, 546 (1969).

S11 R.P. Skowronski and H.L. Recht, Fuel, 57, 705 (1978).

S12 S.S. Salim, Ph.D. Thesis, Dept. of Chem. Eng., Univ of California, Berkeley (June 1980).

S13 M. Seth, R. Djafar, G. Yu and S. Ergun Catalytic Liquefaction of Biomass Prepared for Thermochemical Conversion Contractors' Meeting, Folla, Missouri, (Nov. 1979).

S14 A. Streitwieser and C.H. Heathcock, Introduction to Org. Chem. Macmillan Publishing Co., Inc. (1976).

S15 A.M. Sullivan Coal Age 83, 62 (1978).

T1 G. Tingey, and J.R. Morrey, Coal Structure and Reactivity, Battelle Energy Program Report, Pacific Northwest Laboratory, Richland, Washington (1973).

T2 N.D. Taylor, and A.T. Bell, Lawrence Berkeley Laboratory, Report LBL-7807, Berkeley (April 1978).

U1 U.S. Dept. of Agric., Forestry Service, The Feasibility of Utilizing Forest Residues for Energy and Chemicals. Report to NSF-RANN, (March 1976).

V1 K.B. Vaissel'berg, Khimiga tverd. Topl. 8, 232 (1937); Via Chem. Abstr. 32, 1428^9 (1938).

V2 M.E. Yol'pin J. Am Chem. Soc. 97, 3366 (1975).

W1 D.D. Whitehurst, M. Farcasiu, and T.O. Mitchell, The Nature and Origin of Asphaltenes in Processed Coal, Mobil Research and Dev. Corp., Princeton, EPRI AF 252 (Feb. 1976).

W2 D.D. Whitehurst, Properties and Liquefaction Behavior of Western Coals in Synthetic Recycle Solvents, Presented at

EPRI Contractors Conference, Palo Alto (May 1979).

W3 D.D. Whitehurst, *A Primer on the Chemistry and Constitution of Coal A.C.S. Symp. Ser. 71* (1978).

W4 C.Y. Wen, and S. Tone, *Coal Conversion Reaction Engineering*, West Virginia Univ., (1978).

W5 R.E. Wood, and W.H. Wiser, *Ind. Eng. Chem. Proc. Des. Dev. 15* (1), 144 (1976).

W6 S. Weller, *Catalysis*, 4, 518, Reinhold, N.Y., (1956).

W7 C.H. Wright, and D.E. Severson, *Am. Chem. Soc. Div. Fuel Chem. Preprints* 16, (2), 68 (1972).

W8 O. Weisser, and S. Landa, *Sulfide Catalysts-Their Properties and Applications*, Pergamon Press (1973).

W9 K. Walter, H.F. Feldmann, and R.W. Hiteshue, *A.C.S. Div. of Fuel Chem. Preprints 14* (4), 19 (1970).

W10 R. Willstatter, and L. Kalb, *Ber 55*, 2637 (1922).

W11 W.H. Wiser, *Stanford Research Institute, Coal Chemistry Workshop II* Menlo Park (March 1978).

W12 D.E. Wemmer, Lawrence Berkeley Laboratory Report, LBL-8042, (August 1978).

W13 M.M. Wald, U.S. Patent 3,543,665, (Nov. 24, 1970).

W14 R.E. Winans, R. Hayatsu, J.L. Huston, R.G. Scott, L.P. Moore, and M.H. Studier, *ERDA Div. Physical Chem. Res.-Fuel Chemistry Research.* Washington, D.C. (May 1977).

W15 R.E. Winans, R. Hayatsu, R.G. Scott, L.P. Moore, and M.H. Studier, Stanford Research Institute Coal Chemistry Workshop I, Session III, Paper 13. Menlo Park (1976).

W16 D.D. Whitehurst, T.O. Mitchell and M. Farcasiu. *The*

<u>Nature and Origin of Asphaltenes in Processed Coals</u>,
EPFI paper AF-480. Palo Alto (July 1977).

Y1 Y.K. Yen, D.E. Furlani, and S.W. Weller, <u>Ind. Eng. Chem.-</u>
<u>Prod. Res. Dev.</u> 15, (1), 24 (1976).

Z1 C.W. Zielke, R.T. Struck, J.M. Evans, C.P. Costanza, and
E. Gorin, <u>Ind. Eng. Chem. Proc. Des. Dev.</u> <u>5</u> (2), 151
(1966).

Z2 C.W. Zielke, R.T. Struck, J.M. Evans, C.P. Costanza, and
E. Gorin, <u>Ind. Eng. Chem. Proc. Des. Dev.</u> <u>5</u> (2), 158
(1966).

Z3 C.W. Zielke, R.T. Struck, and E. Gorin, <u>Ind. Eng. Chem.</u>
<u>Proc. Des. Dev.</u>, <u>8</u> (4), 552 (1969).

Z4 C.W. Zielke, W.A. Parker, M. Pell, and R.T. Struck,
<u>ERDA Rept.</u> FE-1743-33 (Feb. 1977).

Z5 C.W. Zielke, E.B. Klunder, J.T. Maskew, and R.T. Struck,
<u>Continuous Hydroliquefaction of Sub-bituminous Coal in</u>
<u>Molten ZnCl$_2$</u> Presented at the Am. Inst. of Chem. Engs.
Natl. Meeting, Philadelphia (1978).

Z6 C.W. Zielke, <u>Preprints, Div. of Fuel Chem., Amer. Chem.</u>
<u>Soc.</u>, <u>19</u> (2) 124 (1972).

Z7 P. Zwietering, and D.W. Van Krevelen, <u>Fuel</u>, <u>33</u>, 331 (1954).

APPENDIX A

PRESSURE VARIATION WITH TIME DATA OBTAINED IN COAL STUDIES

Tables 34 to 37 show the effect of phosphoric acid, antimony chloride, wetting agents, and complexants on the pressure variation with time.

Table 34. Effect of phosphoric acid on pressure variation
with time

(250 gm $ZnCl_2$, 50 gm Coal, 35 gm CH_3OH; 275°C, 800 psig

H_2, 30 min.)

Run No.	Substrate (gm)	P_{max} (psig)	P_{final} (psig)	$P_{max}-P_{H_2}$ (psi)	$P_{max}-P_{final}$ (psi)
49[+]	Coal (50)	1190	1190	690	0
55	PTC (34)*	910	890	110	20
43	Coal (50)	1050	740	250	310

+ 15 gm C_2H_5OH added, 500 psig H_2.

* PTC — Phosphoric acid treated coal (obtained from Run 49)

Table 35. Effect of antimony chloride on pressure variation with time

(250 gm $ZnCl_2$, 50 gm Coal; 275°C, 30 min.)

Run No.	Catalyst*	Solvent	P_{H_2} (psig)	P_{max} (psig)	P_{final} (psig)	$P_{max} - P_{H_2}$ (psi)	$P_{max} - P_{final}$ (psi)
5	$ZnCl_2$	CH_3OH	500	610	510	110	100
37[++]	$SbCl_3$	CH_3OH	800	1200	950	400	250
39	$ZnCl_2$ $SbCl_3^2$	CH_3OH	500	680	470	180	210
40[+]	$SbCl_3$ $ZnCl_2^3$	none	800	760	630	-40	130

* Amounts used are given in Table 7.

+ Reaction at 200°C, 60 min.; ++ Reaction at 225°C, 60 min.

Table 36. Effect of wetting agents on pressure variation
with time

(250 gm $ZnCl_2$, 50 gm Coal, 35 gm CH_3OH;

275°C, 800 psig H_2, 30 min.)

Run No.	Wetting Agent**	P_{max} (psig)	P_{final} (psig)	$P_{max} - P_{H_2}$ (psi)	$P_{max} - P_{final}$ (psi)
43	none	1050	740	250	310
33	Oleic acid	1050	790	250	260
42	DPTS*	1050	750	250	300

* DPTS— Dodecyl para-toluene sulfonate

** Amounts used are given in Table 7.

Table 37. Effect of complexants on pressure variation with time

(250 gm $ZnCl_2$, 50 gm Coal; 275°C, 30 min.)

Run No.	Complexants*	CH_3OH Loading (gm)	H_2 Pressure (psig)	P_{max} (psig)	P_{final} (psig)	$P_{max} - P_{H_2}$ (psi)	$P_{max} - P_{final}$ (psi)
38	none	35	800	1110	790	310	320
35	Urea	35	800	1100	830	300	270
34	Malonic acid	35	800	1140	820	340	320
41	Hexyl mercaptan	35	800	1110	740	310	370
5	none	25	500	610	510	110	100
46	Bipyridyl	25	500	690	540	190	150
56	Sodium ferrocyanide	25	500	800	610	300	190

*   Amounts used are given in Table 7.

APPENDIX B

PRESSURE VARIATION WITH TIME DATA OBTAINED IN BIOMASS STUDIES

Tables 50 to 54 show the effect of reaction temperature, time, methanol loading, hydrogen pressure, and various wood components on pressure variation with time.

Table 50.   Effect of Reaction Temperature on Pressure
Variation with Time

Run No.	Temp. ($^{\circ}$C)	P_{H_2} (psig)	P_{Max} (psig)	P_{Final} (psig)	$P_{Max}-P_{H_2}$ (psi)	$P_{Max}-P_{Final}$ (psi)
23	200	800	1000	940	200	60
22	225	800	1090	920	290	170
21	250	800	1180	850	380	330

Table 51: Effect of Reaction Time on Pressure
Variation with Time

Run No.	Time (min)	P_{H_2} (psig)	P_{Max} (psig)	P_{Final} (psig)	$P_{Max}-P_{H_2}$ (psi)	$P_{Max}-P_{Final}$ (psi)
28	0	800	1100	1100	300	0
27	30	800	1100	905	300	195
24	60	800	1130	840	330	290

Table 52: Effect of Methanol Loading on Pressure Variation with Time

Run No.	Methanol Loading (gm)	P_{H_2} (psig)	P_{Max} (psig)	P_{Final} (psig)	$P_{Max}-P_{H_2}$ (psi)	$P_{Max}-P_{Final}$ (psi)
30	25	500	640	560	140	80
31	50	500	760	670	260	90
29	75	500	930	840	430	90

Table 53. Effect of Hydrogen Pressure on Pressure
Variation with Time

Run No.	Temp. ($^\circ$C)	P_{H_2} (psig)	P_{Max} (psig)	P_{Final} (psig)	$P_{Max}-P_{H_2}$ (psi)	$P_{Max}-P_{Final}$ (psi)
26	250	200	540	420	340	120
25	250	500	955	680	455	275
24	250	800	1130	840	330	290
32	225	200	520	470	320	50
22	225	800	1090	920	290	170

Table 54: Pressure Variation with Time Data Illustration the Effect of $ZnCl_2$-CH_3OH Solubilization of Wood and Its Constituents

Run No.	Substrate	P_{H_2} (psig)	P_{Max} (psig)	P_{Final} (psig)	$P_{Max}-P_{H_2}$ (psi)	$P_{Max}-P_{Final}$ (psi)
11	Cellulose	500	810	635	310	175
20	Lignin	500	830	550	330	280
21	Wood flour	800	1180	850	380	330
24	Wood chips	800	1130	850	330	290

APPENDIX C. ROSTER OF EXPERIMENTS

Run No.	Temp. °C	Pres. psig	Time min	MeOH g	Zn g	Other Additives	H/C	N/C	$\frac{O+S}{C}$	Solv. Incor	Hex Soly %	Tol Soly %	Pyr Soly %	Corr Pyr %
Untreated							.976	.014	.255					
2	275	500	30	25	4	$CaCl_2$,20	1.018	.010	.069	.095	38.5	46.5	85	84
3						";ZnO,5	.964	.011	.062	.17	36.7	46.9	83.6	80.8
4					Sn,7	"	1.044	.009	.161	.084	36	39.4	75.4	73.4
5					--	"	.893	.114	.102	.11	31	58	89	88
6					--	";Mo,6	.888	.009		.130	31.8	54.0	85.8	83.9
7					--	";Al,2	.737	.011	.027	.205	41.9	43.0	84.9	81.8
8		800	30	1		-	.99	.01	.07	.047	31.4	42.9	74.3	73.1
9					4	$CaCl_2$,11; ZnO,2	1.16		.07	.04	36.4	45.3	81.7	80.5
10	275	500	30	25	-	",20;Fe,1	.99	.01	.08	.09	38.9	43.6	73.6	71.7
11*	250	500	60	50		Cellulose,17	1.02	.004	.066	.312	38.2	55.9	94.1	92.3
12	250/200	500/20 O_2	90	H_2O,25	1	-	1.017	.012	.21	0	7.5	12.1	19.6	19.6
13	275	500	30	25	-	$CaCl_2$,20;Ni,1	.91	.014		.17	30.0	38.9	68.9	64
14						" ; Co,1	.94	.010		.14	31.5	38.8	70	66
15						" ; Mn,1	.95	.011		.14	29.4	36.7	66.2	61
16		800				Fe,10;"	1.17	.010	.11	.025	18.1	40.9	72.7	72
18*	250	500	60	H_2O,25		Cellulose,17	.73	0	.174		0	.6	14.1	14.1
19	275	500	30	13		MeCN,12	.90	.014	.140	.074	0	13.3	56.3	53.1
20*	250	500	60	50		Lignin,50	.99	.004	.012	.156	19.3	37.5	87.2	85.2
21*	250	800				Woodflr,20	1.06	.006	0	.174	28.3	44	92	91
22*	225	800				"	.96	.002	.09	.135	11.7	20.4	53.8	48
23*	200	800				"	.86	.001	.20		0	0.2	5.5	5.5
24*	250	800				Woodchp,20	.91	.0	.027	.10	33.9	46.7	94.2	93.8
25*	250	500				"	.98	.0	.039	.108	33.7	44.1	94.0	93.4
26*	250	200				"	.75	.001	.040	.322	36.9	49.4	99.5	99.3
27*	250	800	30	50		"	1.01	.001	.025	.113	30.3	45.4	85.3	84
28*	250	800	0	50		"	.87	.001	.18		0.1	0.4	10.6	10.6
29*	225	500	60	75		"	.93	.004	.10		3.1	7.8	15.7	15.7
30*				25		"	.93	.002	.113	.108	15.2	22.2	51.0	45.7
31*				50		"	.84	.005	.019	.238	10.6	21.8	64.6	56.2
32*	225	200	60	50		"	.73	.002	.076	.29	9.4	14.5	42.3	36
33	275	800	30	35		Oleic,7.5	.65	.01	.095	.69	26	39	100	70
34						Malonic,2.6 $FeCl_2$,4;$NiCl_2$,5	1.02	.012	.212	.15	25.0	35.4	95.5	94.8
35						$FeCl_2$,4;$NiCl_2$,5 Urea,5	.62	.011	.103	.55	12	22	73	55
36				45		$FeCl_2$,4;$NiCl_2$,5 ZnS,7	1.00	.008	.045	.23	32	46	91	89
37				25		$SbCl_3$,228 no $ZnCl_2$	1.32	.007	.027		8	14	75	75
38				35		$FeCl_2$,4;$NiCl_2$,5	1.02	.01	.06	.123	26.5	39	100	100
39				25		$SbCl_3$,25	.86	.01	.09	.150	14.9	28.9	92.4	91
40	200	800	60	0		$ZnCl_2$,91 $SbCl_3$,153	.95	.01		.045	1.0	3.1	29.8	26.6
41	275	800	30	35		$FeCl_2$,4;$NiCl_2$,5 $C_6H_{13}SH$,1.5	1.03	.009	.089	.14	26.4	39.9	99.9	99.9
42						$C_7H_7SO_3C_{12}H_{25}$,1	1.01	.009	.075	.158	27.3	39.5	100	100
43						none	1.01	.01	.025	.116	22.3	37.0	100	100
44					4		1.03	.01	.04	.118	29.6	45.5	100	100
45	275	800	30	65		$ZnCl_2$, 79 $CaCl_2$,158	.60	.01	.24	.44	3.4	5.4	20.8	17
46	275	500	30	25		Bipyridyl,2	.89	.01	.07	.174	18.7	30.9	93.6	92.5
47						$Zn(CN)_2$,5	1.01	.01	.09	.12	18.2	30.7	94.8	94

Run No.	Temp. °C	Pres. psig	Time min	MeOH g	Zn g	Other Additives	H/C	N/C	O+S/C	Solv. Incor	Hex Soly	Tol Soly	Pyr Soly	Corr Pyr
48	275	CO,200	60	EtOH,75 H2O,75		ZnCl2,50 FeCl2,50	1.02	.01	.19	.75	3.7	5.7	16.1	8
49	275	500	30	EtOH,15 H2O,15		H3PO4,135 ZnCl2,35	.88	.01	.16	.11	5.4	8.0	31.7	24.2
50		800		25		ZnO,7	.97	.01	.08	.146	17.2	28.9	71.8	67.7
51		800		35	8		1.15	.01	.06	.05	31.9	47.1	100	100
52		500		25	-	AgCl,3	.91	.01	.06	.17	15.3	27.9	100	100
53						CuCl2,6	.83	.01	.03	.20	15.5	27.3	100	100
54	300						.88	.01	.04	.16	16.7	30.9	91.9	91
55#	275	800	30	35		#49 prod,34	.86	.01	.07	.17	14.3	29.4	98.3	98
56	275	500	30	25		Na4Fe(CN)6,5	.93	.01	.09	.146	16.0	28.5	82.8	80
57						NH4Cl,5;ZnO,4	.98	.01	.09	.15	16.7	29.6	98.6	98.4
58		CO,300 H2,300				FeCl3,7;FeCl2,5	.85	.012	.068	.22	15.3	27.3	76.9	71.8
59		500				none	.96	.009	.07	.20	22.2	34.1	100	100
60	(275 / 325 / 275	800 / 500 / 800	30 / 30 / 30	28 / / +14	6 / / more coal,50)		1.06	.011	.07		12.1	20.3	66.0	
61	275	500	30	25	8	DPTS(p81)1.4	1.02	.009	.09	.13	23.5	35.2	99	98
62	"	"			-	NH4Cl,5;ZnO,4	.98	.010	.09	.14	19.4	31.2	82.7	80
63	275	(800 / 800 / 800	15 / 15 / 15)	35	8	--	1.09	.010	.05	.09	35.5	50.4	98.0	98.?
64	275	500	30	25	-	fine grind	.96	.011	.06	.09	14.9	27.9	84.0	82
65						GaCl3,2.5	.80	.011	.06	.21	14.0	25.7	91	89
66						ZnI2,7.5	.89	.010	.07	.18	14.0	27.3	99.8	97
67	(275 / 300 / 325	800 / 800 / 800	15 / 15 / 15)	35	8	--	1.11	.008	.011		51.3	65.4	100	100
68	(275 / 300	800 / 800	15 / 15)				1.11	.009	.02	.06	37.7	50.3	99.3	99
69	(275 / 300 / 325	800 / no / reprn.	15 / 15 / 15)				1.10	.010	.021		45.9	56.4	100	100
70	275	800	15				1.00	.009	.04	.15	30.7	44.5	99	99
71			0				.94	.010	.14	.13	9	17	59	55
72	325	800	30				1.08	.003	.02		45.6	59.8	97.2	
73	(275 / 300 / 325	800 / 800 / 800	15 / 15 / 30)				1.19	.007	.03		54	64	100	100
74	(275 / 300 / 325 / 340	800 / 800 / 800 / 800	15 / 15 / 15 / 15)				1.13	.007	.09		50.8	60.0	100	100
75	275	800	30	35		NiCl2,5 FeCl2,4	.99	.009	.044	.181	30	45	100	100
76	(275 / 300 / 325	800 / 800 / 800	15 / 15 / 0)	35	8	--	1.1	.010	.040	.046	37	55	100	100
77	300	800	30	35	8		1.04	.010	.021	.088	33	50	100	100
78	(250 / 275 / 300 / 325	800 / no repr. / 800 / no repr.	10 / 10 / 10 / 10)	35	8		1.06	.008	.025	.014	39.6	55.1	99.7	99
79	(same as run 78)			35	-		1.09	.008	.06	.056	26.9	36.5	100	100
80	(same as run 78)			35	8	MeSalic,5	1.09	.009		.063	33.8	47.4	100	100
81	(same as run 78)			35	8	--	1.20	.008	.113		39.0	51.6	100	100
82	(275 / 300	800 / 800	15 / 30)	35	8	--	1.10	.009	.049	.05	34.5	52.4	98.9	98.1
83	(same as run 78)					NiCl2,5 (NH4)6Mo7O24,5)	1.19 .010			.041	31.0	43.3	96.6	96.0
86	(same as run 78)			50	8	--	1.25	.008	.04		41	53	100	100
87*	250	80	60	50	-	Peat,20	1.2	.01	.19		41	55	88	88
88*						Lignite,50	.88	.01	.24	.20	12	19	41	30
89*						" 20	.80	.01		.29	29	40	83	78